Hard Processes in Particles and Nuclei

by

Muhammad Nzar

Department of Physics
Quaid-e-Azam University
Islamabad, Pakistan

1995

This work is submitted as a dissertation
in partial fulfilment of
the requirements for the degree of

DOCTOR OF PHILOSOPHY

in

PHYSICS

Department of Physics
Quaid-e-Azam University
Islamabad, Pakistan

Certificate

Certified that the work contained in this dissertation was carried out by Mr. Muhammad Nzar under my supervision.

(Prof. Dr. Pervez A. Hoodbhoy)
Department of Physics
Quaid-i-Azam University
Islamabad, Pakistan.

Submitted through:

(Prof. Dr. Kamaluddin Ahmed)
Chairman
Department of Physics
Quaid-i-Azam University
Islamabad, Pakistan.

TO MY LOVING MOTHER

Acknowledgements

All praise be to Almighty Allah, the most benevolent and merciful, the creator of the universe, Who enabled me to complete this dissertation.

First and the foremost, I would like to express my immense gratitude to my supervisor, Professor Pervez A. Hoodbhoy, for introducing the subject and for his invaluable suggestions, comments and professional criticism which played an important role in completing this research work. Without his encouragement and guidance, it would have been almost impossible for me to complete this work.

I would like to thank all the members of the Nuclear/Particle group, i.e., Rafia Ali, Hafsa Khan and Muhammad Ali Yusuf who all made it a stimulating and enjoyable activity. My thanks are also due to Amjad Hussain Gilani (one of my group fellows) who taught me Latex and helped me in typing my Ph.D. thesis. I would also like to thank Professors R.L. Jaffe and Xiangdong Ji from the Centre for Theoretical Physics at MIT, USA, for useful discussions during their respective visits to Islamabad. I am thankful to Professor Ahmed Ali as well as the Pakistan Atomic Energy Commission and the World Laboratory for financially supporting this research work.

Finally, my deepest sense of gratitude goes to my family, especially to my mother whose kindness, love, and encouragement enabled me to complete this work.

(MUHAMMAD NZAR)

Abstract

This thesis concerns hard processes i.e., reactions in which the large transfer of momentum to quarks and gluons allows for the application of perturbative QCD. Three problems, described below, were tackled.

The first research problem relates to deep inelastic scattering of leptons from a $J \geq 1$ target. There exists a leading twist structure function $\Delta(x, Q^2)$ which can be measured in deep inelastic scattering from polarized targets with spin ≥ 1, and which is a measure of the polarized gluon distribution in the target. I have estimated $\Delta(x, Q^2)$ for the deuteron, assuming a model for the deuteron which contains a $\Delta - \Delta$ isobar component, and in which the virtual photon interacts with each isobar independently. Although the predicted transverse asymmetry cross section is small, the results could be tested in view of a proposed experiment to measure $\Delta(x, Q^2)$.

The second research problem considered in this thesis relates to nuclear gluon shadowing. I have investigated the possibility of studying the nuclear gluon distribution by looking at large transverse momentum jets in deep inelastic lepton-nucleus scattering. Provided that a colliding beam of leptons and nuclei, rather than a fixed nuclear target, can be arranged, a clean measurement of gluon shadowing appears possible.

The third, and final, research problem concerns quark fragmentation into specific baryons. Fragmentation of partons produced in a high-energy process into definite hadronic states is a problem in QCD of considerable current interest. I have used a simple quark-diquark model for nucleon and Λ structure to calculate leading twist light-cone fragmentation functions for a quark to inclusively decay into P or Λ. The parameters of the model are determined by fitting to the known deep inelastic structure functions of the nucleon. The calculated fragmentation functions are in remarkable agreement with those extracted from partially inclusive $e - P$ and e^+e^- experiments at high energies. Predictions are made, using no additional parameters, for a longitudinally and transversely polarized quark to fragment into P or Λ.

Contents

List of publications

1. **Effect of quark antisymmetrization on the binding energy of nuclear matter,**
   Phys. Rev. **C42**, 1778 (1990),
   M. Nzar, P. Hoodbhoy.

2. **Estimation of the double helicity–flip deuteron structure function,**
   Phys. Rev. **D45**, 2264 (1992),
   M. Nzar, P. Hoodbhoy.

3. **Measuring nuclear gluon shadowing through three–jet production in electron–nucleus collisions,**
   J. Phys. **G18**, 1911 (1992),
   M. Nzar, P. Hoodbhoy.

4. **Quark fragmentation functions in a diquark model for proton and Λ hyperon production,**
   Phys. Rev. **D51**, 32 (1995),
   M. Nzar, P. Hoodbhoy.

Note: The thesis is based on publications 2, 3, and 4 listed above.

Chapter 1

Introduction

1.1 General survey

In the late sixties, studies on the classification of hadrons, hadron mass spectra, and hadronic interactions strongly suggested that hadrons were made of quarks, the fundamental building blocks. In order to obtain experimental information on quarks, the insides of hadrons (e.g., protons) were probed by bombarding them with a beam of structureless particles (e.g., leptons). This method of studying the structure of target particles was essentially the same as the one used a long time ago by Geiger, Marsden, and Rutherford in unravelling the structure of atoms. For the study of the hadronic structure much higher energies and larger momentum transfers are needed to obtain the higher resolution. The first series of such experiments to probe the structure of the proton was initiated in the 1960's at Stanford Linear Accelerator Centre (SLAC) and the process was called deep inelastic electron-proton scattering.

The deep inelastic scattering experiments were based on the following consideration: electron-nucleon scattering proceeds through the electromagnetic interaction which has well known properties. Therefore e-N scattering experiments

are an ideal tool with which to investigate the internal structure of the nucleon, its charge and current distribution. The SLAC-MIT team of scientists performed inelastic electron proton scattering with incident electron enegies between 7 and 17 GeV. In the reaction $e + P \longrightarrow e' + X$, they only counted the number of outgoing electrons e' at 6^o and 10^o angles, leaving the debris X unobserved. Such cross sections are termed "inclusive". To their surprise, the experimenters observed hundreds of times more counts at these angles than expected. In elastic scattering $e + P \longrightarrow e' + P'$, the outgoing particles are the same as the incoming ones, and the cross section falls off very fast as a function of the scattering angle due to the finite size of the nucleon. The original experimental result indicated that in high energy inelastic scattering, the incoming electrons occasionally hit hard point-like constitutents inside the proton, just as in Rutherford's experiment the incident α-particle was sometimes scattered by the atomic nucleus.

To elaborate a little more on this point, consider the elementary process

$$e + P \longrightarrow e' + X, \tag{1.1}$$

as depicted in Fig. 1.1. The four-momenta of the incoming and outgoing electrons are labelled by k^μ and k'^μ and the four-momentum of the target proton by p^μ. In a deep inelastic process like (1.1), where a large amount of energy and momentum has been transferred to the target, the proton breaks up into hadrons X. The four-momentum transfer from the electron to the target is

$$q = k - k'.$$

Now the central point is the following. In an inelastic process like this, there should be two independent variables, the energy loss $(E_e - E'_e)$ and the three momentum transfer $\mathbf{q}$ on which the inclusive scattering cross section should depend. Instead, it was found that the cross section depends, to a good degree, only on one variable $x = Q^2/2M\nu$, where $Q^2 = -q^2$, and $\nu = (E_e - E'_e)$ in the laboratory frame. This is the signature of an elastic scattering of the electron from a free,

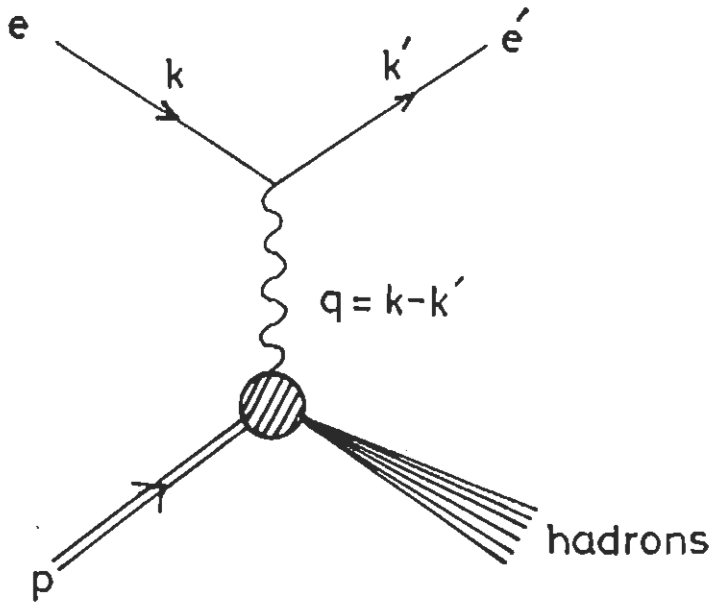

Figure 1.1: Feynman diagram for deep inelastic electron proton scattering.

pointlike constituent that is carrying a fraction x of the four-momentum of the proton. This is called "Bjorken scaling" [1] because the measured cross section. at Q^2 and ν, is the same as the cross section at Q'^2 and ν', provided the variables are scaled as

$$\frac{\nu}{\nu'} = \frac{Q^2}{Q'^2}. \tag{1.2}$$

It is this observation of scaling in the original experiment that implied the existence of the point-like constituents of the nucleon, called partons. The experiment also pointed to what is called "asymptotic freedom" – that for large Q^2, the partons seem to be moving freely of each other, i.e., interact only weakly with each other. Thus Bjorken scaling implies that the constituents of the nucleon look almost free and pointlike when observed with high spatial resolution. Hence, if one accepts the parton idea, the dynamics governing the parton system should have the property that the interaction between partons becomes weaker at short distances. The partons were later identified with quarks since experimentally it was suggested that their quantum numbers such as charges and spin were the same as those of the quarks fulfilling the SU(3) symmetry postulated by Gell-

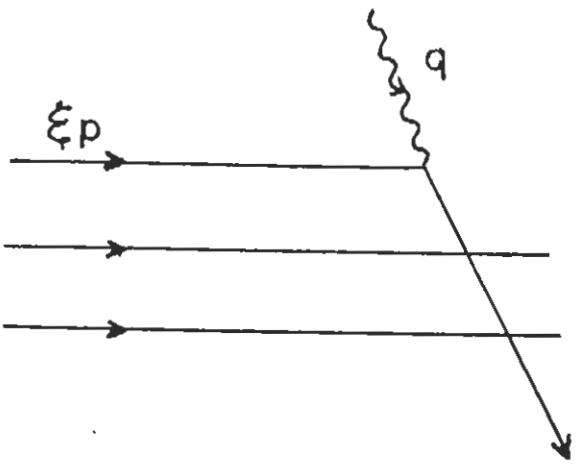

Figure 1.2: The scattering of a parton in the nucleon via a virtual photon absorption.

Mann and Zweig. It was then natural to look for a theory of strong interaction that waned in strength at shorter distances.

To appreciate the significance of the scaling variable $x = Q^2/2M\nu$, assume that the proton is made up of point-like constituents, each having a mass m, and carrying a fraction ξp of its momentum (see Fig. 1.2). A constituent absorbs the virtual photon of momentum q and gets scattered elastically. In practice, since it is part of a bound system, and interacts with other constituents, its momentum would be smeared to some extent, and the encounter is "quasielastic". Ignoring such effects, the four momentum of the struck parton is $(\xi p + q)$, and

$$\begin{aligned} (\xi p + q)^2 &= m^2, \\ \Rightarrow \xi &= \frac{Q^2}{2p.q}. \end{aligned}$$

This is a Lorentz invariant quantity, and may be evaluated in any frame. In the laboratory frame, $p.q = M\nu$, and we see that

$$\frac{Q^2}{2p.q} = \frac{Q^2}{2M\nu} = x.$$

When the conditions Q^2 and $M\nu >> M^2$ are met, the process is called deep inelastic, and x may be identified with the fractional four-momentum ξ. In Fig.

1.2, the struck constituent cannot get loose by itself, unlike in nuclear physics where a nucleon, as a constituent of a nucleus, may be knocked out. The free partons are never seen in isolation. Hence the underlying theory, in addition to being asymptotically free, must be confining the constituents.

The above qualitative picture was confirmed, substantially extended and made more detailed in similar and other relevant hard processes (i.e., processes with large momenta transferred from leptons (or photons) to hadrons, or from one group of hadrons to another group of hadrons.): neutrino-nucleon scattering, e^+e^- annihilation into hadrons, and production of massive lepton pairs or particles with large transverse momenta in hadronic collisions. The parton model, with its assumption of limited parton transverse momenta, did not follow, however, from the updated quantum field theory models, and therefore it was not completely satisfactory from a theoretical point of view.

This problem was solved, and great success was achieved through the fruitful development of gauge field theories. In this way, a theory of strong interactinos was constructed, quantum chromodynamics (QCD), which gave a theoretically self consistent description of strong interactions of hadrons at small distances agreeing with experiment.

The main hypothesis underlying QCD is that a quark of any flavour has a three-fold degree of freedom, besides the usual coordinates and spin, i.e., each quark has a so called "colour" (hence the name chromodynamics), and the quark wavefunction has the colour index $i = 1, 2, 3$. The physical hadron states are colourless. The necessity of colour stems from data on the spectroscopy of low lying baryonic states, on the decays $\pi^0 \longrightarrow 2\gamma$, $\eta \longrightarrow 2\gamma$, as well as other evidence. One of the most clear arguments in favour of this hypothesis is the experimentally observed value of the cross section of e^+e^- annihilation into hadrons.

It is assumed in QCD that the quanta mediating the interaction are 8 coloured massless vector mesons (gluons), and that the quark-gluon interaction

is described by a gauge invariant theory, like quantum electrodynamics(QED). There is a very important difference between QCD and QED. In QED, the gauge transformations are elements of the abelian group U(1), having a single generator, the electric charge, while in QCD three colours exist and the gauge transformations are elements of the non-abelian group $SU(3)_c$, having 8 generators coupled to 8 gluon fields. A consequence of the gauge invariance of QCD is the direct self-interaction of the gluons (besides the interaction via quark pairs). Because of the gluonic self-interaction, the small distance behaviour of the effective coupling constant in QCD is quite unlike that in QED. It is well known that in QED the effective charge squared, $\alpha(r) = e^2(r)/4\pi\hbar c$, increases at small distances. In other words, the physical charge determined at very large distances becomes infinitely small for any given value of the bare charge, defined for $r \longrightarrow 0$ (This phenomenon is the so-called "zero physical charge" of QED.). In QCD, on the other hand, the effective strong coupling constant squared $\alpha_S(r) = g_S^2(r)/4\pi\hbar c$, has a logarithmic fall-off for $r \longrightarrow 0$, $\alpha_S(r) \sim [ln(\frac{1}{r})]^{-1}$, so that the interaction is switched off in the asymptotic limit and the theory goes over into a free particle theory (asymptotic freedom). Thus QCD provides qualitative grounds for the parton model, and vice versa, the experimental evidence in favour of the parton model confirms QCD in its first rough approximation. It should be emphasized that unlike theories with a Yukawa-type interaction (e.g., QED) the small distance behaviour of QCD is self-consistent. Though the strong interaction constant $\alpha_S(r)$ decreases with rise of the momentum transfer $Q \sim \hbar/r$, its fall-off is rather slow. That is why in QCD at large Q, corrections appear to the predictions of the parton model and, in particular, some deviations arise from the expected scale invariant behaviour of deep inelastic cross sections. These corrections are calculated in the framework of QCD and can, in principle, be used for an experimental test of the theory. When applied to deep inelastic processes, QCD not only confirms the results of the parton model and makes them more precise, but it also predicts new qualitative phenomenon relevant to the quark-gluon interaction. The most

manifest effect among them is production of gluon jets and the corresponding rise of the transverse momenta of hadrons in hard processes. In the quark-parton model, one might expect, for instance, that a quark-antiquark pair produced in e^+e^- annihilation into hadrons, would create two hadronic jets with large longitudinal (w.r.t the jet axis in the c.m.s.) hadronic momenta and small transverse momenta. The angular distribution of the jet in e^+e^- annihilation was predicted unambiguously, and its experimental observation was the greatest success of the quark parton model. In QCD, besides the quark jets, gluonic jets must also be produced owing to the large angle hard gluon emission by the quarks. In e^+e^- experiments, this effect was revealed as three-jet events with definite properties. Such events have indeed been found at the e^+e^- colliding beam storage ring PETRA. The observation of these events can be considered as an experimental proof of the existence of gluons and thereby as a convincing confirmation of QCD. Also the momentum distribution of the quarks inside the proton forces us to the conclusion that a substantial fraction of the proton's momentum is carried by neutral partons, not by quarks. These are the gluons of QCD.

The fall-off of the effective charge at small distances is intimately related in QCD to the rise of the charge at large distances, so the interaction in QCD becomes strong at $r \sim 1fm$. The rise of $\alpha_S(r)$ with r is necessary both to explain the properties of the low energy (as well as at high energies and low momentum transfers) strong interactions of hadrons, and to solve principle problem of QCD - to understand why the physical hadrons are colourless and why coloured objects are confined (the confinement problem). At present, the problem of the large distance behaviour is still awaiting its solution in QCD. This is why it is impossible at present to examine consistently the transitions of quarks and gluons into physical hadrons. In place of such a consideration one has to substitute a phenomenological description, introducing experimentally determined probabilities of hadron fragmentation into quarks (gluons) and vice versa. Performing this program, one has to find those physical characteristics of hard processes which

would be free of ambiguities due to large distances. The desired characteristics may indeed be found e.g. the hadronic jets mentioned above, the cross section of e^+e^- annihilation into hadrons, etc.

As QCD is asymptotically free theory, this means that in the high energy limit the running coupling constant of QCD becomes small, small enough for perturbative calculations. However, for decreasing energies the coupling constant grows, until finally perturbation theory breaks down, somewhere in the region 0.5–5 GeV. As a consequence of this, the study of QCD has split into two directions. On the one hand there have been successful calculations of all kinds of high energy observables, which have been confirmed by experiment. The area of perturbative QCD is quite well understood and unchallenged as yet. On the other hand the study of non-perturbative QCD has seen less progress. Specifically the problem of hadronic structure is still poorly understood.

One part of the hadron structure problem deals with the question how a hadron is built up out of quarks. On the purely theoretical side attemps have been made to solve the non-perturbative problem with lattice gauge theories. On the phenomenological side we have some important clues, coming from the combination of models and experiments. Firstly there is the constituent quark model which can give a reasonable prediction of various static hadronic properties. Secondly we have the Bag model and the Skyrme model that are quite successful in reproducing mass-spectra for hadrons. Thirdly the parton model, together with the technique of the operator product expansion (OPE), can explain the near scaling behaviour of the structure functions of deep inelastic scattering of leptons off hadrons.

The other part of the hadronic structure problem deals with the question how a quark transforms itself into hadrons, the so called fragmentation or hadronization. It is an experimental fact that no free quark has ever been detected - only hadrons are seen. One says that the quarks are confined within

the hadrons. On the other hand according to theoretical models like the parton model, a high energy electron can knock a quark out of a hadron through the exchange of a virtual photon. It follows that this quark somehow has to transform itself into hadrons which are subsequently observed. Often the ejected quark then manifests itself as a jet of hadrons, coming out of the interaction region. This process is the analogue of the hadronic structure problem mentioned above.

1.2 Brief description of Ph.D. research work

One of the most challenging problems in theoretical high energy physics is to compute the bound-state structure of the proton and other hadrons from QCD. The goal is to not only calculate the spectrum of hadron masses from first principles, but also to derive the momentum and spin distributions of the quarks and gluons which control high energy hadron interactions. These distributions first need to be extracted from the data using theoretical models.

In this thesis I shall be concerned with the hadronic structure problem in connection with hard processes (deep inelastic lepton-hadron scattering and hadronization process.). Hard processes have been of tremendous importance in uncovering the structure of matter at the deepest level. Hard reactions are more suited than soft reactions for this because of the dramatic weakening of the strength of the interaction between quarks at large energies. This means that in the high energy limit the running coupling constant of QCD becomes small enough for perturbative calculations. Hard processes that I have investigated during my Ph.D. research work include the following:

1.2.1 Deep inelastic scattering of leptons from polarized targets

The first research problem considered here relates to deep inelastic scattering of leptons from a $J \geq 1$ target [2]. Using leptons to probe hadrons has been the most popular way of uncovering deep hadronic structure. Spin adds an important extra dimension to the problem and has been the subject of many investigations for spin-half objects like the nucleon. It was pointed out by Jaffe and Manohar [3] that there exists a leading twist structure function (given the name $\Delta(x, Q^2)$ by them) in QCD which can be measured in deep inelastic scattering from polarized targets with spin ≥ 1. The structure function measures the polarized gluon distribution in the target and vanishes for a state with spin less than one. The only stable targets with spin ≥ 1 are nuclei. $\Delta(x, Q^2)$ vanishes identically for a nucleus made up of protons, neutrons and pions regardless of Fermi motion or binding corrections in the approximation in which the nucleons or pions scatter the virtual photon independently. It is therefore an unambiguous probe of that part of the gluonic content of a nucleus which cannot be identified with any of the constituent neutrons, protons, or virtual pions. For this reason, $\Delta(x, Q^2)$ would be very interesting to measure. I have estimated the gluonic hadron structure function $\Delta(x, Q^2)$ for the deuteron. We assume a model for the deuteron which contains a $\Delta - \Delta$ isobar component, and in which the virtual photon interacts with each isobar independently. First we estimate, using the MIT bag model, $\Delta(x, Q^2)$ for a $\Delta(1232)$ particle. Then, using the convolution model, we estimate $\Delta(x, Q^2)$ for a deuteron in the $\Delta - \Delta$ configuration. The nucleons, having spin less than one, do not contribute to $\Delta(x, Q^2)$. It is expected that a proposed experiment at the DESY e-p collider HERA, using an internal gas jet polarized deuteron target, will be able to measure various structure functions, including $\Delta(x, Q^2)$.

1.2.2 Jet physics and measurement of nuclear gluon shadowing

The second problem considered in this thesis relates to nuclear gluon shadowing [4]. It is not easy to measure the contribution of gluons in deep inelastic scattering processes because the virtual photon has no direct coupling with gluons, and must perforce interact through a mechanism such as the box diagram. The contribution of this must be added on to the usual tree level $\gamma^* - q$ diagram, and this makes isolation of the gluon component very difficult. In principle the gluon contribution to deep inelastic scattering from a hadron target can be measured by classifying events according to the final state. Whereas $\gamma^* - q$ scattering leads to single jet events, $\gamma^* - g$ scattering leads to two back-to-back jets in the center of mass system in the lowest order.

This process has been the basis of a proposal for measuring the gluon content of a polarized proton by measuring the large transverse momentum jets [5]. Unfortunately, as pointed out by Manohar [6], this is not experimentally feasible for protons at rest in the laboratory. The problem is that, in the laboratory frame, for transverse momentum of order Q the angle θ between the jets, $\sin\theta \sim M/Q$, becomes small for large Q. For smaller values of the transverse momentum, $\sin\theta \sim M/k_\perp$. This too does not lead to a satisfactory situation because only events with $k_\perp \gg \langle k_\perp \rangle_{intrinsic}$ ought to be considered in order to avoid contamination with the proton's intrinsic transverse momentum. Thus, for a target at rest, two-jet events are difficult to separate from the dominant one-jet events.

A possible way out has been suggested by Manohar [6], who considers an experimental situation in which both the electron and the polarized proton are highly relativistic in the laboratory frame, an arrangement which may be possible at colliders such as HERA. The kinematics for this process suggest that the three

jets (the third being the proton debris) will be distinguishable, provided that the opening angle between any two jets exceeds a certain minimum value δ, and the transverse-jet momentum fraction is large enough,

$$\lambda^2 \geq (1 - cos\delta)\frac{E_{min}^2/E_P^2}{2x(x + E_l/E_P)}$$

Here $\lambda^2 = k_\perp^2/Q^2$, E_l is the lepton energy, E_P is the proton energy, and E_{min} is the minimum energy of a jet which should be large compared to Λ_{QCD}. It additionally obeys the restriction $E_{min} \leq (\xi - x)E_P$, where ξ is the longitudinal momentum fraction carried by the struck gluon. The requirement that perturbative QCD hold, $Q^2 \geq Q_{min}^2$, translates into the condition that $x \geq x_{min}$ for measureable 3-jet events, where $x_{min} = Q_{min}^2/4E_P E_l$.

In this thesis the discussion of Ref.[6] has been adapted for the purpose of measuring the unpolarized gluon distribution in a hadron. I have calculated the 3-jet contribution to $F_1(x)$ (spin averaged structure function of the target) arising from a gluon distribution $g(\xi)$. Nuclear gluons at small x are of particular interest since, for $x \leq \frac{1}{2MR}$ (M is the nucleon mass and R is the nuclear radius), partons are no longer confined to individual nucleons. Instead, they extend over the entire nucleus in the longitudinal direction as a consequence of which they undergo recombination. This nuclear effect leads to an altered (or shadowed) gluon distribution. To observe this would be very interesting. I have investigated the possibility of studying the nuclear gluon distribution by looking at large transverse momentum jets in deep inelastic lepton-nucleus scattering. As a result of the calculations it was found that the 3-jet contribution to $F_1(x)$ of the target has a measureable value if the energy of the target is sufficiently high. Also, 3-jet events could discriminate between different nuclear gluon distributions. It thus appears that a clean measurement of gluon shadowing is possible, provided that a colliding beam of leptons and nuclei, rather than a fixed nuclear target, can be arranged.

1.2.3 Fragmentation of quarks into baryons

The third, and final, research problem contained in this thesis concerns quark fragmentation into specific baryons [7]. Fragmentation of partons produced in a high-energy process into definite hadronic states is a problem in QCD of considerable current interest. Parton fragmentation, in a sense, is dual to the process of uncovering hadron structure using high momentum probes. This duality has recently been emphasized by Jaffe and Ji [8]. These authors have made a detailed exploration of the spin, chirality, and twist structures of fragmentation using the fact that parton fragmentation functions can be expressed in QCD as matrix elements of quark and gluon field operators at light-cone separations. Indeed, a one-to-one correspondence between fragmentation functions and parton distribution functions can be established. While this is a useful step towards understanding the nature of the hadronization process, it certainly does not solve the problem – the calculation of distribution functions belongs to the realm of non-perturbative QCD and therefore can only be modeled. Fragmentation functions are even harder to model theoretically, and existing models using strings and shower algorithms etc.[9] are complicated and involve many parameters.

I have used a simple quark-diquark model for nucleon and Λ structure to calculate leading twist light-cone fragmentation functions for a quark to inclusively decay into P or Λ. The parameters of the model are determined by fitting to the known deep inelastic structure functions of the nucleon. When evolved from the initial to the final Q^2 scale, the calculated fragmentation functions are in remarkable agreement (for $z > 0.4$) with those extracted from partially inclusive $e - P$ and e^+e^- experiments at high energies. Predictions are made, using no additional parameters, for a longitudinally or transversely polarized quark to fragment into P or Λ.

References

[1] J.D. Bjorken, Phys. Rev. **179**, 1547 (1969).
R.P. Feynman, Phys. Rev. Lett. **23**, 1415 (1969).

[2] M. Nzar and P. Hoodbhoy, Phys. Rev. **D45**, 2264 (1992).

[3] R.L. Jaffe and A. Manohar, Phys. Lett. **B223**, 218 (1989).

[4] M. Nzar and P. Hoodbhoy, J. Phys. **G18**, 1911 (1992).

[5] R.D. Carlitz, J.C. Collins and A.H. Mueller, Phys. Lett. **B214**, 224 (1988).

[6] A.V. Manohar, Phys. Lett. **B255**, 579 (1991).

[7] M. Nzar and P. Hoodbhoy, Phys. Rev. **D51**, 32 (1995).

[8] R.L. Jaffe and X. Ji, Phys. Rev. Lett. **71**, 2547 (1993).
X. Ji, Phys. Rev. **D49**, 114 (1994).

[9] See, for example, V.D. Barger and R.J.N. Phillips, Collider Physics, (Addison-Wesley, Reading, MA, 1987).

Chapter 2

Estimation of the double helicity-flip deuteron structure function

2.1 Introduction

It is of fundamental interest in hadron physics to measure the contribution of gluons in deep inelastic scattering processes. This is not easily done because the virtual photon has no direct coupling with gluons, and must perforce interact through a mechanism such as the box diagram. The contribution of this must be added on to the usual tree level $\gamma^* - q$ diagram, and this makes isolation of the gluon component very difficult. Fortunately, as pointed out by Jaffe and Manohar [1], favourable experimental circumstances can sometimes be arranged in which the gluons alone contribute. More precisely, one needs a polarized hadron target with spin $J \geq 1$. The signature for the gluonic contribution is the presence of a double helicity flip Compton amplitude. In the language of the operator product expansion (OPE), there exists a tower of gluon operators

$G_{\mu\mu_1} \overrightarrow{D}_{\mu_3} \cdots \overrightarrow{D}_{\mu_3} G_{\nu\mu_2}$, with coefficient functions of order $\alpha_s(Q^2)$ obtained from the box graph, that contributes for targets with spin $J \geq 1$ and gives rise to the double helicity flip structure function $\Delta(x, Q^2)$. Anomalous dimensions of these operators have also been calculated [2]. These operators have vanishing matrix elements in any state with spin less than one.

$\Delta(x, Q^2)$ can be measured by scattering an unpolarized electron beam from a target aligned perpendicular to the beam (Actually any direction not exactly parallel to the beam will do, but perpendicular is best.). The only stable targets with spin $J \geq 1$ are nuclei. $\Delta(x, Q^2)$ vanishes identically for a nucleus made up of protons, neutrons and pions regardless of Fermi motion or binding corrections in the approximation in which the nucleons or pions scatter the photon independently. It is therefore an unambiguous probe of that part of the gluonic content of a nucleus which cannot be identified with any of the constituent neutrons, protons, or virtual pions. For this reason, $\Delta(x, Q^2)$ would be very interesting to measure. In addition to $\Delta(x, Q^2)$, there also exist other interesting (but quark dominated) structure functions for spin $J \geq 1$ [3]. It is expected that a proposed experiment at the DESY e-P collider HERA, using an internal gas jet polarized deuteron target, will be able to measure these various structure functions, including $\Delta(x, Q^2)$ [4].

$\Delta(x, Q^2)$ has a direct parton level interpretation. Consider the target in an infinite momentum frame with its spin aligned along the $\hat{x}$ direction, which is perpendicular to its momentum. Define $g_{\hat{x}}(x, Q^2)$, $g_{\hat{y}}(x, Q^2)$ to be the probability (per unit x) to find a gluon carrying fraction x of the target's momentum and linearly polarized along the $\hat{x}$, $\hat{y}$ direction respectively. Let

$$a(x, Q^2) = g_{\hat{x}}(x, Q^2) - g_{\hat{y}}(x, Q^2). \tag{2.1}$$

Then in terms of $a(x, Q^2)$, the $\Delta(x, Q^2)$ structure function is,

$$\Delta(x, Q^2) = \frac{\alpha_s(Q^2)}{2\pi} Tr Q^2 x^2 \int_x^1 \frac{dy}{y^3} a(y, Q^2). \tag{2.2}$$

Where Q is the quark charge matrix, $Q = diag\left(\frac{2}{3},\ -\frac{1}{3},\ -\frac{1}{3}\right)$ for u, d, s quarks. The integral in Eq. (2.2) reflects the non-local character of the box graph and occurs for all gluon operators in deep inelastic scattering. Eq. (2.2) is easier to interpret if it is written as,

$$\Delta(x,Q^2) = \frac{\alpha_s(Q^2)}{2\pi} Tr Q^2 \int_0^1 dy\, dz\, \delta(x-yz)\, z^2\, a(y,Q^2), \tag{2.3}$$

which can be viewed as the convolution of the transverse aligned gluon distribution $a(y,Q^2)$ with a "splitting function" $\frac{\alpha_s(Q^2)}{2\pi} Tr Q^2 Z^2$ from the box graph, subject to the kinematic constraint $x = yz$. Experimentally $\Delta(x,Q^2)$ is measureable through the ϕ dependence of the cross section, $d\sigma \propto \Delta(x,Q^2)\cos 2\phi$. Here ϕ is the azimuthal angle between the plane formed by the beam and the alignment axis, and the plane formed by the beam and the scattered electron as shown in Fig. 2.1.

In this chapter, we first discuss the kinematics of the double helicity-flip contribution to deep inelastic scattering. Next we present the operator product expansion and project out the operators which contribute to double helicity-flip. Then the parton model interpretation of our results is developed. The presentation for the case of a spin -3/2 target is made but it applies without modification to a spin-1 target as well. If the target has spin-2 or greater, there is more than one double helicity-flip Compton amplitude and changes are necessary, though the basic idea is unchanged. Next, using the MIT bag model, the $\Delta(x,Q^2)$ structure function for a spin-3/2 Δ particle is estimated. This provides a guide to the magnitude of $\Delta(x,Q^2)$ that might be found in an experiment. Using the convolution model, we estimate $\Delta(x,Q^2)$ for a deuteron in the $\Delta-\Delta$ configuration. Nucleons have spin less than one and so do not contribute to the $\Delta(x,Q^2)$ structure function of a deuteron. By way of comparison, we also estimate the spin-averaged structure function $F_1^{\Delta}(x)$ for a Δ particle using the MIT bag model. The convolution model is used to estimate $F_{1\Delta}^{D}(x)$ for the deuteron, which measures the quark distribution in the $\Delta-\Delta$ configuration of the deuteron. Finally, we compare

$\Delta_D(x, Q^2)$ with $F_{1\Delta}^D(x)$ and close with a discussion of results.

2.2 Kinematics

In this section the inelastic scattering of an electron (or muon) of initial four momentum k^μ, and final four momentum $k'^\mu = k^\mu - q^\mu$, from a target of four momentum P^μ will be studied. We work in the rest frame of the target, $P^\mu = (M, \vec{0})$, and orient the virtual photon along the $\hat{z}$-direction, $q^\mu = (q^0, 0, 0, q^3)$. The azimuthal angle of the final lepton with respect to the x-axis (which is the alignment axis of the target) in the xy-plane is ϕ (Fig. 2.1). As usual, we define

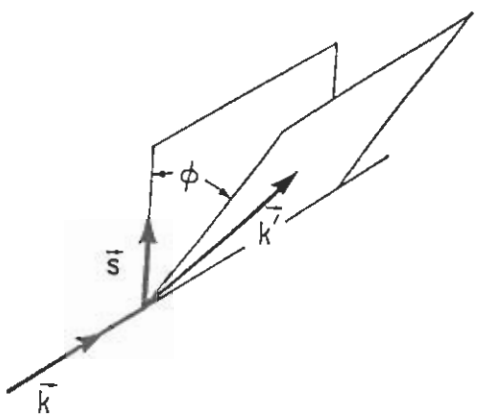

Figure 2.1: Definition of the azimuthal scattering angle ϕ.

$Q^2 \equiv -q^2 = (q^3)^2 - (q^0)^2$, $\nu = p.q = Mq^0$, and $q^3 = -\sqrt{\kappa} q^0$, where $\kappa = 1 + \frac{M^2 Q^2}{\nu^2}$.

The cross-section for inelastic lepton scattering from a polarized spin 3/2 target is proportional to the imaginary part of the amplitude for forward virtual

Figure 2.2: $\gamma_h + target_H \rightarrow \gamma_{h'} + target_{H'}$

Compton scattering,

$$\begin{aligned} W_{\mu\nu}(H', H) &= \frac{1}{4\pi} \int d^4x e^{iq\cdot x} \langle PH' | [J_\mu(x), J_\nu(0)] | PH \rangle \\ &= \frac{1}{2\pi} Im\, T_{\mu\nu}(H', H), \end{aligned} \tag{2.4}$$

where,

$$T_{\mu\nu}(H', H) = i \int d^4x e^{iq\cdot x} \langle PH' | T(J_\mu(x) J_\nu(0)) | PH \rangle \tag{2.5}$$

If we were only interested in targets polarized along $\hat{z}$, we could set $H = H'$. However, targets polarized perpendicular to the incident photon are linear superpositions of states polarized along $\hat{z}$ and terms with $H \neq H'$ occur.

$W^{\mu\nu}$ can be related to the imaginary part of helicity amplitudes for virtual Compton scattering. We choose the $\hat{z}$-axis (the direction of the virtual photon) to quantize the angular momentum of the target and photon. We call the initial and final photon spin components along $\hat{z}$ as h and h' and the initial and final target spin components as H and H'. The helicity amplitude for forward Compton scattering (see Fig. 2.2) is denoted by $T(h, H; h', H')$.

Angular momentum conservation along the $\hat{z}$-axis implies that

$$h + H = h' + H'$$

Reflecting in the plane of the scattering does not change any of the momenta, but reverses all the spins. Thus parity invariance implies that,

$$T(h, H; h', H') = T(-h, -H; -h', -H')$$

Time reversal exchanges initial and final states, and reverses the directions of momenta and spin. Since the helicity of the photons and the target is defined as the component of spin along the direction of motion of the photon, helicity does not change sign under time-reversal. Thus time-reversal invariance implies that,

$$T(h, H; h', H') = T(h', H'; h, H)$$

The helicity amplitudes can be computed in terms of $T_{\mu\nu}$ using

$$T(h, H; h', H') = \epsilon^{*\mu}_{h'} \epsilon^{\nu}_{h} T_{\mu\nu}(H, H') \tag{2.6}$$

where ϵ^{μ}_{h} are photon polarization vectors,

$$\begin{aligned} \epsilon^{\mu}_{\pm} &= \mp \frac{1}{\sqrt{2}}(0, 1, \pm i, 0) \\ \epsilon_0 &= \frac{1}{\sqrt{Q^2}}(q^3, 0, 0, q^0) \end{aligned} \tag{2.7}$$

Now define $A(h, H; h', H')$ as,

$$A(h, H; h', H') = \epsilon^{\mu}_{h} \epsilon^{*\nu}_{h'} W_{\mu\nu}(H, H'). \tag{2.8}$$

This is $1/2\pi$ times the imaginary part of the forward Compton helicity amplitude $T(h, H; h', H')$. We are interested only in the double helicity-flip amplitudes $A(+, -1/2, -, 3/2)$ and $A(-, 1/2; +, -3/2)$ (for a spin 3/2 target). These are equal by parity invariance. Thus we define,

$$\begin{aligned} \Delta(x, Q^2) &\equiv A(+, -1/2; -, 3/2) \\ &= \epsilon^{\mu}_{+} \epsilon^{*\nu}_{-} W_{\mu\nu}(-1/2, 3/2) \end{aligned} \tag{2.9}$$

Next we calculate the contribution of $\Delta(x, Q^2)$ to deep inelastic scattering from a target polarized transverse to the photon beam. We work in the Bjorken limit

where the virtual photon is nearly parallel to the incident electron so that the target may be regarded as polarized perpendicular to the incident electron beam. The target is polarized along the x-axis and its state is expanded in the z basis as,

$$\left|\frac{3}{2}\right\rangle_x = \frac{1}{2\sqrt{2}}\left[\left|\frac{3}{2}\right\rangle + \sqrt{3}\left|\frac{1}{2}\right\rangle + \sqrt{3}\left|-\frac{1}{2}\right\rangle + \left|-\frac{3}{2}\right\rangle\right]. \tag{2.10}$$

If the scattering cross section is measured as a function of the usual variables, $x = Q^2/2\nu$, $y = \nu/ME$, and the azimuthal angle ϕ then in the scaling limit ($Q^2, \nu \to \infty, x$ fixed) [2],

$$\frac{d\sigma}{dxdyd\phi} = \frac{e^4 ME}{4\pi^2 Q^4}\left[xy^2 F_1(x,Q^2) + (1-y)F_2(x,Q^2) - \frac{x(1-y)}{2}\Delta(x,Q^2)\cos 2\phi\right]. \tag{2.11}$$

Here $F_1(x,Q^2)$ and $F_2(x,Q^2)$ are the usual spin averaged structure functions of the target. In Eq. (2.11), we have dropped both higher twist structure functions and kinematic corrections which vanish like powers of M_N^2/Q^2 in the Bjorken limit.

2.3 Operator product expansion and parton model

We now proceed to analyze deep inelastic scattering using an operator product expansion for the time ordered product of two currents.

$$\mathcal{T}_{\mu\nu}(q) \equiv i\int d^4x e^{iq\cdot x} T\left(j_\mu(x) j_\nu(0)\right). \tag{2.12}$$

Next project out the operators which contribute to double helicity-flip

$$\frac{1}{2}\mathcal{T}_{\mu\nu}(q) = \cdots + \sum_{n=2,4,\cdots} \frac{2^n q^{\mu_1}\cdots q^{\mu_n}}{(Q^2)^n} C_n(Q^2) O_{\mu\nu\mu_1\cdots\mu_n}, \tag{2.13}$$

where

$$C_n(Q^2) = \frac{\alpha_s(Q^2)}{2\pi} Tr Q^2 \frac{2}{n+2}, \tag{2.14}$$

and

$$O_{\mu\nu\mu_1\cdots\mu_n} \equiv \frac{1}{2}\left(\frac{i}{2}\right)^{n-2} \mathcal{S}\left\{G^a_{\mu\mu_1}\overleftrightarrow{D}_{\mu_2}\cdots\overleftrightarrow{D}_{\mu_n} G^a_{\nu\mu_2}\right\}. \tag{2.15}$$

In Eq. (2.15) $G^a_{\mu\nu}$ is the gluon field strength, $\mathcal{S}$ symmetrizes and removes traces in the indices $\mu_1 \cdots \mu_n$, and $O_{\mu\nu\mu_1\cdots\mu_n}$ is understood to be renormalized at a scale Q^2.

The terms omitted from Eq. (2.13) are the standard ones which do not contribute to the double helicity-flip Compton amplitude. The reason the operator defined in Eq. (2.15) can generate a double helicity-flip is its antisymmetry in $\mu \leftrightarrow \mu_1$ and $\nu \leftrightarrow \mu_2$. All of the other gluon operators appearing in the expansion of $T(J_\mu(x)J_\nu(0))$ have a contracted Lorentz index on each gluon field strength-tensor. For example $O^\alpha_{\alpha\mu_1\cdots\mu_n}$ is the standard gluon operator contributing to $F_1(x)$ and $F_2(x)$ at $O(\alpha_s)$ and cannot generate a double helicity flip structure. To proceed, take the matrix element of $O_{\mu\nu\mu_1\cdots\mu_n}$ in a spin 3/2 target,

$$\begin{aligned}\langle PH'|O_{\mu\nu\mu_1\cdots\mu_n}|PH\rangle &= \frac{1}{2}\mathcal{S}\left\{\left[\left(p_\mu \bar{u}_{\mu_1}(H') - p_{\mu_1}\bar{u}_\mu(H')\right)\left(p_\nu \bar{u}_{\mu_2}(H) - p_{\mu_2}\bar{u}_\nu(H)\right)\right.\right. \\ &+ \left.\left.(\mu \leftrightarrow \nu)\right] p_{\mu_3}\cdots p_{\mu_n}\right\} A_n(Q^2)\cdots \qquad (2.16)\end{aligned}$$

$u^\mu(PH)$ are Rarita-Schwinger spinors describing the spin orientation of the spin 3/2 target and are given by,

$$u^\mu(PH) = C^{1\ \frac{1}{2}\ \frac{3}{2}}_{\lambda\ \lambda'\ H} E^\mu(P\lambda)u(P\lambda'). \qquad (2.17)$$

In the target rest frame the polarization vectors $E^\mu(\lambda)$ are,

$$\begin{aligned}E^\mu(\pm) &= \epsilon^\mu_\pm \\ E^\mu(0) &= (0,0,0,1), \qquad (2.18)\end{aligned}$$

and $u(\lambda')$ are Dirac spinors. Consequently,

$$\begin{aligned}u^\mu(3/2) &= E^\mu(+)u(1/2) \\ u^\mu(1/2) &= \sqrt{\frac{1}{3}}E^\mu(+)u(-1/2) + \sqrt{\frac{2}{3}}E^\mu(0)u(1/2) \\ u^\mu(-1/2) &= \sqrt{\frac{1}{3}}E^\mu(-)u(1/2) + \sqrt{\frac{2}{3}}E^\mu(0)u(-1/2) \\ u^\mu(-3/2) &= E^\mu(-)u(-1/2). \qquad (2.19)\end{aligned}$$

In Eq. (2.16), the omitted terms (traces) are lower twist. We project out the double helicity-flip amplitude by contracting $\mathcal{T}_{\mu\nu}$ with $\epsilon_+^{*\mu}\epsilon_-^{\nu}$:

$$\begin{aligned}\frac{1}{2}T(-,3/2;+,-1/2) &= \sum_{n=2,4,\cdots}\left(\frac{2p\cdot q}{Q^2}\right)^n C_n(Q^2)A_n(Q^2) \\ &= \sum_{n=2,4,\cdots}\omega^n C_n(Q^2)A_n(Q^2) \\ &= \frac{\alpha_s(Q^2)}{2\pi}TrQ^2\sum_{n=2,4,\cdots}\left(\frac{1}{x}\right)^n\frac{2}{n+2}A_n(Q^2), \quad (2.20)\end{aligned}$$

where we have substituted for $C_n(Q^2)$ from Eq. (2.14). Now we relate this expansion to $\Delta(x, Q^2)$.

The operator product expansion allows us to compute $T(\omega) \equiv T\left(-,\frac{3}{2};+,-\frac{1}{2}\right)$ as a power series in ω about $\omega = 0$ in QCD. The radius of convergence of the power series is $|\omega| = 1$, since that is the location of the first singularity in the complex ω plane. This is precisely where the physical region begins.

Thus $T(\omega)$ can be computed near $\omega = 0$, but not in the physical region $1 \leq |\omega| \leq \infty$. To understand this better, it is useful to use light-cone coordinates,

$$q^{\pm} = \frac{1}{\sqrt{2}}\left(q^0 \pm q^3\right)$$

Because $Q^2 = 2q^+q^-$, therefore the deep inelastic limit (x fixed, $Q^2 \to \infty$) is the same as the limit q^+ fixed, $q^- \to \infty$. Clearly,

$$x = \frac{1}{\omega} = \frac{q^+}{p^+}.$$

Thus deep inelastic scattering is not a short distance process - it probes the structure of the hadron along the light-cone. However, if we look at the unphysical region and let $\omega \to 0$, then $q^+ \to \infty$ (and we already have $q^- \to \infty$). The expansion of the scattering amplitude around $\omega = 0$ is a short distance expansion, which is why one can compute it in QCD.

We can relate $T(\omega)$ in the unphysical region to its value in the physical region using contour integration. We can write $T(\omega)$ as

$$T(\omega) = \frac{1}{2\pi i}\oint_{|\omega'|=\gamma<1} d\omega' \frac{T(\omega')}{\omega' - \omega}$$

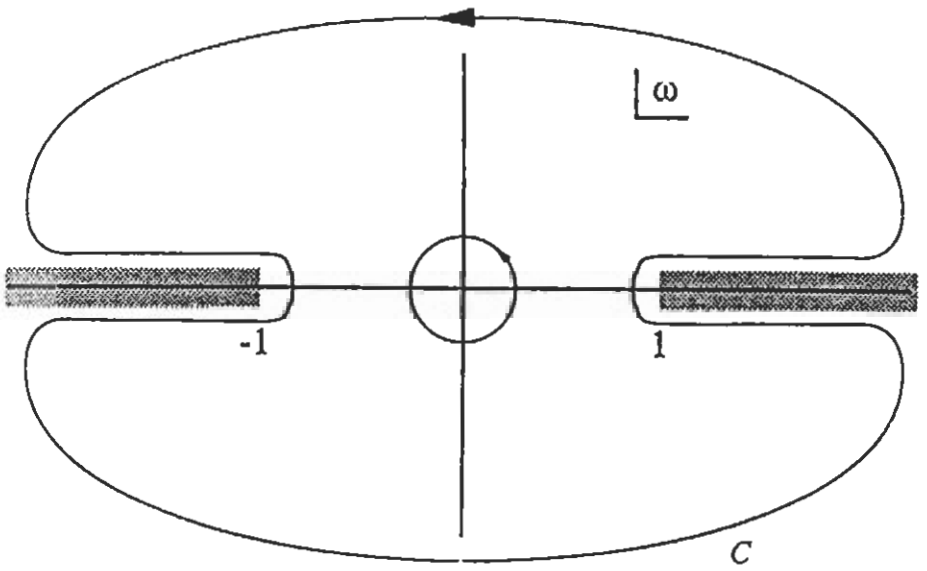

Figure 2.3: The contours used to derive the moment sum rules.

over a circle in the complex ω plane around the origin, as shown in Fig. 2.3. The contour of integration can then be deformed to the contour C. This gives

$$T(\omega) = \frac{1}{2\pi i} \oint_C d\omega' \frac{T(\omega')}{\omega - \omega'}$$

We now have to assume that the contour at infinity does not contribute to the integral, and can be neglected. In that case, only the discontinuities across the cuts contribute to the integral over contour C.

$$\begin{aligned} T(\omega) &= \frac{1}{2\pi i}\left[\int_1^\infty \frac{d\omega'}{\omega' - \omega} T(\omega' + i\epsilon) + \int_{-\infty}^{-1} \frac{d\omega'}{\omega' - \omega} T(\omega' + i\epsilon)\right. \\ &\quad \left. + \int_{-1}^{-\infty} \frac{d\omega'}{\omega' - \omega} T(\omega' - i\epsilon) + \int_\infty^1 \frac{d\omega'}{\omega' - \omega} T(\omega' - i\epsilon)\right]. \end{aligned}$$

Putting $\omega' = -\omega'$ in the second and third terms gives,

$$\begin{aligned} T(\omega) &= \frac{1}{2\pi i}\left[\int_1^\infty \frac{d\omega'}{\omega' - \omega} T(\omega' + i\epsilon) - \int_1^\infty \frac{d\omega'}{\omega' + \omega} T(-\omega' + i\epsilon)\right. \\ &\quad \left. + \int_1^\infty \frac{d\omega'}{\omega' + \omega} T(-\omega' - i\epsilon) - \int_1^\infty \frac{d\omega'}{\omega' - \omega} T(\omega' - i\epsilon)\right]. \end{aligned}$$

Now use the Schwartz reflection theorem which states that if F(z) is a complex function which is real and analytic on the real axis, then $F(z^*) = F^*(z)$. In consequence,

$$\begin{aligned} T(\omega) &= \frac{1}{2\pi i}\left[\int_1^\infty \frac{d\omega'}{\omega'-\omega}\left(T(\omega'+i\epsilon)-T^*(\omega'+i\epsilon)\right)\right. \\ &\quad \left.+\int_1^\infty \frac{d\omega'}{\omega'+\omega}\left(T(\omega'+i\epsilon)-T^*(\omega'+i\epsilon)\right)\right]. \end{aligned}$$

In the above we have used $T(-\omega') = T(\omega')$, which is clear from Eq. (2.20). Continuing,

$$\begin{aligned} T(\omega) &= \frac{1}{2\pi i}\int_1^\infty d\omega'\left(\frac{1}{\omega'-\omega}+\frac{1}{\omega'+\omega}\right)2i\,ImT(\omega') \\ &= \frac{2}{\pi}\int_1^\infty \frac{\omega'\,d\omega'}{\omega'^2-\omega^2}\,ImT(\omega') \\ &= 4\int_1^\infty \frac{\omega'\,d\omega'}{\omega'^2-\omega^2}\,A(\omega') \\ &= 4\int_1^\infty \frac{d\omega'}{\omega'}\left[1+\left(\frac{\omega^2}{\omega'^2}\right)+\left(\frac{\omega^2}{\omega'^2}\right)^2+\cdots\right]A(\omega'). \end{aligned}$$

where we have used Eqs. (2.4), (2.6) and (2.9), and $\omega < 1$. Recall that $A(\omega') \equiv A(+,-1/2;-,3/2)$. Now put $\omega' = 1/x'$ and $\omega = 1/x$ to get, finally,

$$T(x,Q^2) = 4\int_0^1 \frac{dx'}{x'}\left[1+\left(\frac{x'^2}{x^2}\right)+\left(\frac{x'^2}{x^2}\right)^2+\cdots\right]\Delta(x',Q^2).$$

In the unphysical region $|x| > 1$, the Taylor expansion of $T(x,Q^2)$ in $1/x^2$ is guaranteed to converge (T is analytic for $|x| > 1$). Comparing this expansion with Eq. (2.20), we obtain

$$M_n(\Delta) = \frac{\alpha_s(Q^2)}{2\pi} Tr\mathcal{Q}^2 \frac{A_n(Q^2)}{n+2}, \tag{2.21}$$

where $n = 2,4,6,\cdots$ The nth moment of Δ, $M_n(\Delta)$, is defined by

$$M_n(\Delta) = \int_0^1 dx x^{n-1}\Delta(x,Q^2). \tag{2.22}$$

Now to cast Eq. (2.21) in a more familiar form, we define inverse Mellin transforms,

$$A_n(Q^2) = \int_0^1 dy y^{n-1} a(y,Q^2) \tag{2.23}$$

and use the obvious identity,

$$\frac{1}{n+2} = \int_0^1 dz z^{n-1} z^2.$$

Eq. (2.21) becomes,

$$\begin{aligned} M_n(\Delta) &= \frac{\alpha_s(Q^2)}{2\pi} Tr\mathcal{Q}^2 \int_0^1 dy \int_0^1 dz (yz)^{n-1} z^2 a(y) \\ &= \frac{\alpha_s(Q^2)}{2\pi} Tr\mathcal{Q}^2 \int_0^1 dx \delta(x-yz) \int_0^1 dy \int_0^1 dz (yz)^{n-1} z^2 a(y) \\ &= \frac{\alpha_s(Q^2)}{2\pi} Tr\mathcal{Q}^2 \int_0^1 dx \int_0^1 dy \int_0^1 dz \frac{1}{y} \delta\left(\frac{x}{y} - z\right) (yz)^{n-1} z^2 a(y) \\ &= \frac{\alpha_s(Q^2)}{2\pi} Tr\mathcal{Q}^2 \int_0^1 dx x^{n-1} x^2 \int_x^1 \frac{dy}{y^3} a(y) \end{aligned}$$

Comparing the above equation with Eq. (2.22) we obtain,

$$\Delta(x, Q^2) = \frac{\alpha_s(Q^2)}{2\pi} Tr\mathcal{Q}^2 x^2 \int_x^1 \frac{dy}{y^3} a(y, Q^2) \tag{2.24}$$

Generally the inverse Mellin transform of the tower of twist-2 operator matrix elements is identified with a parton probability distribution in the parton model version of perturbative QCD. To make this connection for $a(x, Q^2)$, we contract Eq. (2.16) with $\epsilon_+^{*\mu}\epsilon_-^{\nu}$,

$$\begin{aligned} &\epsilon_+^{*\mu} \langle PH' | O_{\mu\nu\mu_1\cdots\mu_n} | PH \rangle \epsilon_-^{\nu} \\ &= \frac{1}{2} [\epsilon^*(+) \cdot \bar{u}(H') \epsilon(-) \cdot u(H) + \epsilon(-) \cdot \bar{u}(H') \epsilon^*(+) \cdot u(H)] p_{\mu_1} \cdots p_{\mu_n} A_n(Q^2) \end{aligned}$$

Polarizing the target along the x-direction, i.e., $H = H' = H_x = 3/2$, and using Eqs. (2.7), (2.10), and (2.19), we obtain,

$$\epsilon_+^{*\mu} \langle PH_x = 3/2 | O_{\mu\nu\mu_1\cdots\mu_n} | PH_x = 3/2 \rangle \epsilon_-^{\nu} = \frac{1}{4} p_{\mu_1} p_{\mu_2} \cdots p_{\mu_n} A_n(Q^2).$$

Which implies that,

$$A_n(Q^2) = \frac{4}{(p^+)^n} \epsilon_+^{*\mu} \langle PH_x = 3/2 | O_{\mu\nu++\cdots} | PH_x = 3/2 \rangle \epsilon_-^{\nu}. \tag{2.25}$$

In the above we have set $\mu_1 = \mu_2 = \cdots = \mu_n = +$ on both sides. Now using light-cone gauge $A^+ = 0$, Eq. (2.15) becomes,

$$O_{\mu\nu++\cdots} = \frac{1}{2} \left(\frac{i}{2}\right)^{n-2} S \left\{ G_{\mu+}^a \left(\overleftrightarrow{\partial}_+\right)^{n-2} G_{\nu+}^a \right\}$$

and Eq. (2.24) becomes,

$$A_n(Q^2) = -\frac{1}{(p^+)^n}\left(\frac{i}{2}\right)^{n-2}\left\langle PH_x = 3/2\left|G^a_{L+}\left(\overleftarrow{\partial}_+\right)^{n-2}G^a_{L+}\right|PH_x = 3/2\right\rangle, \tag{2.26}$$

where,

$$\begin{aligned} G^a_{L+} &= G^a_{x+} - iG^a_{y+} \\ G^a_{x+} &= -\partial_+ A^a_x \\ &= -\frac{1}{\sqrt{2}}\left[\partial_0 A^a_x + \partial_z A^a_x\right] \\ &= -\frac{1}{\sqrt{2}}\left[E^a_x + B^a_y\right] \end{aligned} \tag{2.27}$$

Recall here that in the light cone gauge $A^a_+ = 0$ *and* $A^a_0 = -A^a_z$. Similarly,

$$\begin{aligned} G^a_{y+} &= -\partial_+ A^a_y \\ &= -\frac{1}{\sqrt{2}}\left[\partial_0 A^a_y + \partial_z A^a_y\right] \\ &= -\frac{1}{\sqrt{2}}\left[E^a_y - B^a_x\right] \end{aligned} \tag{2.28}$$

But equally well, we can contract Eq. (2.16) with $\epsilon^{*\mu}_- \epsilon^\nu_+$ and then we would get,

$$A_n(Q^2) = -\frac{1}{(p^+)^n}\left(\frac{i}{2}\right)^{n-2}\left\langle PH_x = 3/2\left|G^a_{R+}\left(\overleftarrow{\partial}_+\right)^{n-2}G^a_{R+}\right|PH_x = 3/2\right\rangle \tag{2.29}$$

where,

$$G^a_{R+} = G^a_{x+} + iG^a_{y+}$$

Taking the average gives,

$$\begin{aligned} A_n(Q^2) = -\frac{1}{(p^+)^n}\left(\frac{i}{2}\right)^{n-2} \quad & \left\langle PH_x = 3/2\left|G^a_{L+}\left(\overleftarrow{\partial}_+\right)^{n-2}G^a_{L+}\right.\right. \\ & \left.\left. + G^a_{R+}\left(\overleftarrow{\partial}_+\right)^{n-2}G^a_{R+}\right|PH_x = 3/2\right\rangle. \end{aligned}$$

This then becomes,

$$\begin{aligned} A_n(Q^2) = \frac{1}{(p^+)^n}\left(\frac{i}{2}\right)^{n-2} \quad & \left\langle PH_x = 3/2\left|G^a_{y+}\left(\overleftarrow{\partial}_+\right)^{n-2}G^a_{y+}\right.\right. \\ & \left.\left. + G^a_{x+}\left(\overleftarrow{\partial}_+\right)^{n-2}G^a_{x+}\right|PH_x = 3/2\right\rangle. \end{aligned} \tag{2.30}$$

Now comparing Eqs. (2.23) and (2.30), we have

$$\int_0^1 dz z^{n-1} a(z) = \frac{1}{(p^+)^n}\left(\frac{i}{2}\right)^{n-2} \quad \left\langle PH_x = 3/2 \left| G^a_{y+}\left(\overleftrightarrow{\partial}_+\right)^{n-2} G^a_{y+} \right.\right.$$
$$\left. \left. -G^a_{x+}\left(\overleftrightarrow{\partial}_+\right)^{n-2} G^a_{x+} \right| PH_x = 3/2 \right\rangle \quad (2.31)$$

We want an expression for $a(z)$ which yields Eq. (2.31). If we had started out the OPE with $T(J_\mu(x)J_\nu(0))$ instead of $T(J_\mu(x/2)J_\nu(-x/2))$, we would have ended up with

$$\int_0^1 dz z^{n-1} a(z) = \frac{i^{n-2}}{(p^+)^n} \quad \left\langle PH_x = 3/2 \left| G^a_{y+}\left(\vec{\partial}_+\right)^{n-2} G^a_{y+} \right.\right.$$
$$\left. \left. -G^a_{x+}\left(\vec{\partial}_+\right)^{n-2} G^a_{x+} \right| PH_x = 3/2 \right\rangle \quad (2.32)$$

Motivated by the usual form encountered in quark distributions, we guess that

$$za(z) = \frac{1}{2p^+}\int \frac{d\xi^-}{2\pi} \quad e^{-izp^+\xi^-} \left\langle PH_x = 3/2 \left| G^a_{y+}(\xi^-) G^a_{y+}(0) \right.\right.$$
$$\left. \left. -G^a_{y+}(0) G^a_{y+}(\xi^-) \right| PH_x = 3/2 \right\rangle - (y \to x) \quad (2.33)$$

Now,

$$\int_0^1 dz z a(z) z^{n-2} = \int_{-\infty}^{+\infty} dz z^{n-1} a(z)$$

where it has been assumed that, since $a(z)$ has a probabilistic interpretation, it vanishes for $z > 1$ and $z < 0$.

$$\int_0^1 dz z^{n-1} a(z) = \int_{-\infty}^{+\infty} dz z^{n-1} a(z)$$

$$= \frac{1}{2p^+}\int_{-\infty}^{+\infty} dz z^{n-2} \int_{-\infty}^{+\infty} \frac{d\xi^-}{2\pi} e^{-izp^+\xi^-}$$
$$\left\langle G^a_{y+}(\xi^-) G^a_{y+}(0) + G^a_{y+}(0) G^a_{y+}(\xi^-) \right\rangle - (y \to x)$$

$$= \frac{1}{2p^+}\int_{-\infty}^{+\infty} \frac{d\xi^-}{2\pi}\left(\frac{i}{p^+}\right)^{n-2}\left(\frac{\partial}{\partial \xi^-}\right)^{n-2} \int_{-\infty}^{+\infty} dz z^{n-2} e^{-izp^+\xi^-}$$
$$\left\langle G^a_{y+}(\xi^-) G^a_{y+}(0) + G^a_{y+}(0) G^a_{y+}(\xi^-) \right\rangle - (y \to x)$$

$$= \frac{1}{2p^+}\left(\frac{i}{p^+}\right)^{n-2}\int_{-\infty}^{+\infty} d\xi^- \left(\frac{\partial}{\partial\xi^-}\right)^{n-2}\delta(p^+\xi^-)$$
$$\left\langle G^a_{y+}(\xi^-)G^a_{y+}(0) + G^a_{y+}(0)G^a_{y+}(\xi^-)\right\rangle - (y\to x)$$

$$= \frac{(i)^{n-2}}{2(p^+)^n}\int_{-\infty}^{+\infty} d\xi^-\delta(\xi^-)$$
$$\left\langle \left(\partial_+^{n-2}G^a_{y+}(\xi^-)\right)G^a_{y+}(0) + G^a_{y+}(0)\partial_+^{n-2}G^a_{y+}(\xi^-)\right\rangle - (y\to x)$$

$$= \frac{(i)^{n-2}}{(p^+)^n}\left\langle G^a_{y+}(0)\left(\vec{\partial}_+\right)^{n-2}G^a_{y+}(0) - G^a_{x+}(0)\left(\vec{\partial}_+\right)^{n-2}G^a_{x+}(0)\right\rangle$$

which is the same as Eq. (2.32) and thus confirms the correctness of the guess. Using Eqs. (2.27) and (2.28) in Eq. (2.33), we have

$$\begin{aligned} za(z) &= \frac{1}{p^+}\int_{-\infty}^{+\infty}\frac{d\xi^-}{2\pi}e^{-izp^+\xi^-}\left\langle PH_x = 3/2\right|\left(E^a_y(\xi^-) - B^a_x(\xi^-)\right)\left(E^a_y(0) - B^a_x(0)\right) \\ &\quad -\left(E^a_x(\xi^-) + B^a_y(\xi^-)\right)\left(E^a_x(0) + B^a_y(0)\right)\left|\, PH_x = 3/2\right\rangle \\ &= g_{\hat{x}}(z) - g_{\hat{y}}(z) \end{aligned} \tag{2.34}$$

2.4 Estimation of $\Delta(x, Q^2)$ for the Δ^{++}

As can be seen from Eq. (2.24), we can easily calculate $\Delta(x, Q^2)$ by first calculating $a(y)$ as given by Eq. (2.34). Evaluation of the matrix element indicated in Eq. (2.34) requires a definite model for the hadronic state. The MIT bag model [5,6] is perhaps adequate – at least as a first estimate.

A Δ^{++} aligned in the $\hat{x}$-direction with $H_x = 3/2$ is represented in the bag model by three u quarks (assumed massless), all in the lowest mode of the bag cavity (in the $S_{\frac{1}{2}}$ orbital), and spin along the$\hat{x}$-direction. Since they have the same mass, the color electric field

$$\mathbf{E}^a = \sum_{i=1}^{3}\mathbf{E}^a_{(i)}$$

is proportional to $\sum_{i=1}^{3} \lambda^a_{(i)}$. This annihilates the color singlet hadron state. The color magnetic field

$$\mathbf{B}^a = \sum_{i=1}^{3} \mathbf{B}^a_{(i)}, \tag{2.35}$$

produced by the color current of S state quarks is obtained from the solution of

$$\nabla \times \mathbf{B}^a_{(i)} = \mathbf{J}^a_{(i)},$$

subject to the bag boundary conditions. Explicitly the solution is [7],

$$\mathbf{B}^a_{(i)}(r) = g\lambda^a_{(i)} \left[\sigma_i f(r) + \hat{\mathbf{r}}(\sigma_{(i)} \cdot \hat{\mathbf{r}})h(r)\right] \tag{2.36}$$

where $f(r)$ and $h(r)$ are elementary functions given by

$$f(r) = \frac{\omega^2}{16\pi(X-1)\sin^2 X}\left[\frac{\sin 2\omega r}{2(\omega r)^3} - \frac{\cos 2\omega r}{2(\omega r)^2} - \frac{\sin 2X}{2X^3} + \frac{\cos 2X}{X^2}\right] \tag{2.37}$$

and,

$$h(r) = \frac{\omega^2}{16\pi(X-1)\sin^2 X}\left[\frac{2+\cos 2\omega r}{2(\omega r)^2} - 3/2\frac{\sin 2\omega r}{(\omega r)}\right]. \tag{2.38}$$

Here $X = \omega R$ is the bag constant, R is the bag radius, and ω is the energy of the quark in the lowest mode of the bag cavity.

One must take into account that the expectation value in Eq. (2.34) must be taken in a state normalized according to

$$\langle P_\Delta H_\Delta | P_\Delta H_\Delta \rangle = (2\pi)^3 2P^0_\Delta \delta^3(0). \tag{2.39}$$

However a bag state is normalized to unity. Changing normalization to the bag state ($P_\Delta = 0$) Eq. (2.34) becomes,

$$ya(y) = \frac{2M_\Delta V}{P^+_\Delta} \int_{-\infty}^{+\infty} \frac{d\xi^-}{2\pi} e^{-iyp^+\xi^-} \left\langle H_x = 3/2 \left| B^a_x(\xi^-)B^a_x(0) - B^a_y(\xi^-)B^a_y(0) \right| H_x = 3/2 \right\rangle.$$

Using translational invariance, and $\frac{1}{V}\int d^3r = 1$ gives,

$$
\begin{aligned}
ya(y) &= \frac{2M_\Delta}{P_\Delta^+}\int_{-\infty}^{+\infty}\frac{d\xi^-}{2\pi}d^3re^{-iyp_\Delta^+\xi^-} \\
&\quad \left\langle H_x=3/2\left|B_x^a(\xi^-+\mathbf{r})B_x^a(\mathbf{r})-B_y^a(\xi^-+\mathbf{r})B_y^a(\mathbf{r})\right|H_x=3/2\right\rangle \\
&= \frac{4}{M_\Delta}\int d^3k\delta\left(y-\frac{k^+}{P_\Delta^+}\right)\left\langle H_x=3/2\left|B_x^{a2}(\mathbf{k})-B_y^{a2}(\mathbf{k})\right|H_x=3/2\right\rangle .
\end{aligned}
\tag{2.40}
$$

Where $\mathbf{B}^a(\mathbf{k})$ is the Fourier transform of Eq. (2.36) i.e.,

$$
\begin{aligned}
\mathbf{B}^a(\mathbf{k}) &= \frac{1}{(2\pi)^{3/2}}\int d^3re^{i\mathbf{k}\cdot\mathbf{r}}\mathbf{B}^a(\mathbf{r}) \\
&= g\lambda^a\left[\sigma F(k)+\hat{\mathbf{k}}(\sigma\cdot\hat{\mathbf{k}})H(k)\right]
\end{aligned}
\tag{2.41}
$$

with

$$
F(k) = \sqrt{\frac{2}{\pi}}\int_0^R drr^2\left[j_0(kr)f(r)+\frac{1}{3}h(r)\left(j_0(kr)+j_2(kr)\right)\right] \tag{2.42}
$$

$$
H(k) = -\sqrt{\frac{2}{\pi}}\int_0^R drr^2j_2(kr)h(r). \tag{2.43}
$$

Since $k^+=\frac{k^0+k^3}{\sqrt{2}}$, it is necessary to specify the gluon energy k^0 which occurs in Eq. (2.40). The $\mathbf{B}$ field in Eq. (2.40) has been obtained semiclassically but in terms of first order perturbation theory it corresponds to the field of a $l=1$ transverse electric (TE) gluon [8] in the lowest cavity mode.

Using Eq. (2.35) in Eq. (2.40), we have

$$
\begin{aligned}
ya(y) &= \frac{4}{M_\Delta}\sum_a\sum_{i,j=1}^3\int d^3k\delta\left(y-\frac{k^0+k^3}{M_\Delta}\right) \\
&\quad \left\langle H_x=3/2\left|B_{(i)x}^a(k)B_{(j)x}^a(k)-B_{(i)y}^a(k)B_{(j)y}^a(k)\right|H_x=3/2\right\rangle
\end{aligned}
\tag{2.44}
$$

where $B_{(i)x}^a$ is the x-component of the a color magnetic field due to quark i. Now,

$$
\begin{aligned}
B_{(i)x}^a(k)B_{(j)x}^a(k) &= g^2\lambda_{(i)}^a\lambda_{(j)}^a\left[F^2(k)\sigma_{(i)x}\sigma_{(j)x}+H^2(k)(\hat{\mathbf{k}})_x(\hat{\mathbf{k}})_x(\sigma_{(i)}\cdot\hat{\mathbf{k}})(\sigma_{(j)}\cdot\hat{\mathbf{k}})\right. \\
&\quad \left.+F(k)H(k)(\hat{\mathbf{k}})_x\left(\sigma_{(i)x}(\sigma_{(j)}\cdot\hat{\mathbf{k}})+(\sigma_{(i)}\cdot\hat{\mathbf{k}})\sigma_{(j)x}\right)\right]
\end{aligned}
$$

where we have used Eq. (2.41). Thus Eq. (2.44) becomes

$$
ya(y) = 8\pi g^2\sum_a\sum_{ij}\left\langle\lambda_{(i)}^a\lambda_{(j)}^a\right\rangle\left\langle\sigma_{(i)x}\sigma_{(j)x}-\sigma_{(i)y}\sigma_{(j)y}\right\rangle
$$

$$\int_{k_{min}}^{\infty} dk\, k \left[F(k) + \frac{1}{2} H(k) \left(1 - \frac{k_{min}^2}{k^2} \right) \right]^2 \tag{2.45}$$

where $k_{min} = |M_\Delta y - k^0|$

For i=j,

$$\sigma_{(i)x}\sigma_{(j)x} - \sigma_{(i)y}\sigma_{(j)y} = \sigma_{(i)x}^2 - \sigma_{(i)y}^2 = 0$$

Then with the Δ^{++}–particle with its spin along the positive x-axis, for $i \neq j$, $\sigma_{(i)x} = 1$, $\sigma_{(i)y} = 0$, and thus $\sigma_{(i)y}\sigma_{(j)y} = 0$. Therefore,

$$\sum_{ij} \left(\sigma_{(i)x}\sigma_{(j)x} - \sigma_{(i)y}\sigma_{(j)y} \right) = 2 \sum_{i<j} \left(\sigma_{(i)x}\sigma_{(j)x} - \sigma_{(i)y}\sigma_{(j)y} \right) = 6$$

and,

$$\sum_{a} \lambda_{(i)}^a \lambda_{(j)}^a = -\frac{8}{3}$$

for $i \neq j$.

Using these expectation values in Eq. (2.45), we arrive at the final expression for $a_\Delta(y)$,

$$y a_\Delta(y) = -128\pi g^2 \int_{k_{min}}^{\infty} dk\, k \left[F(k) + \frac{1}{2} H(k) \left(1 - \frac{k_{min}^2}{k^2} \right) \right]^2 \tag{2.46}$$

Now to find the value of g we use the fact that in the bag model the Δ^{++}–proton mass difference arises solely from the color–magnetostatic energy, which is given by an integral quadratic in the color magnetic fields:

$$E_n = -\sum_a \sum_{i<j} \int_{bag} d^3 r \mathbf{B}_i^a(\mathbf{r}) \cdot \mathbf{B}_j^a(\mathbf{r})$$

Evaluating these integrals for the proton and Δ^{++} we find,

$$M_\Delta - M_p = 64\pi g^2 \int_0^{\infty} dk k^2 \left[F^2(k) + \frac{2}{3} F(k) H(k) + \frac{1}{3} H^2(k) \right] \tag{2.47}$$

Numerical estimation of $a_\Delta(z)$ in Eq. (2.46) requires that various bag parameters be specified. For s quarks $\omega R = 2.04$, and $k^0 R = 2.75$ for the lowest energy gluon mode[8]. The bag radius $R = 1.1$ fm. The $\Delta - N$ mass splitting formula Eq. (2.44) then determines $\alpha_s = g^2/4\pi \approx 2.2$. Once we have calculated $a_\Delta(y)$ we

can calculate $\Delta_\Delta(x,Q^2)$ using Eq. (2.34). $xa_\Delta(x)$ and $x\Delta_\Delta(x)$ have been plotted in Fig. 2.4. We can easily reproduce the first moment of $\Delta_\Delta(x,Q^2)$ given by Sather[2],

$$\int_0^1 dx x\Delta_\Delta(x,Q^2) = -0.012\alpha_s. \tag{2.48}$$

This is a check on our calculations.

2.5 Estimation of $\Delta(x,Q^2)$ for the deuteron

Consider now the scattering of leptons off a deuteron. If the deuteron is merely a bound state of two nucleons then $\Delta(x,Q^2)$ is identically zero; it is impossible for a spin $\frac{1}{2}$ object to flip its spin by two units (scattering from two nucleons, i.e., final state interactions, could flip the deuteron spin by two units and hence contribute to $\Delta(x,Q^2)$. However this is a higher twist effect which vanishes in the Bjorken limit.). However, the transient existence of $J \geq 1$ nucleon resonances can change this conclusion. Working in this conventional baryon picture, the deuteron state can be expressed as

$$|D\rangle = |NN) + \epsilon\,|\Delta\Delta\rangle + \cdots \tag{2.49}$$

As an isospin zero object, the deuteron has no Δ-N component; the Δ's must come in pairs. Estimates for ϵ^2, the total $\Delta - \Delta$ component, range from 0.01 to 0.03 [9-13]. Spectator experiments have sought to measure this component by knocking out one Δ and detecting the other by its subsequent decay into a nucleon and pion. The validity of the two step model illustrated in Fig. 2.5 is assumed; i.e., the incident virtual photon interacts with only one of the Δ's. The experiment is totally inclusive. However, we parenthetically observe that if the observation of the spectator Δ was experimentally possible, it would be very interesting to study the isospin dependence of the struck Δ's $\Delta(x, Q^2)$.

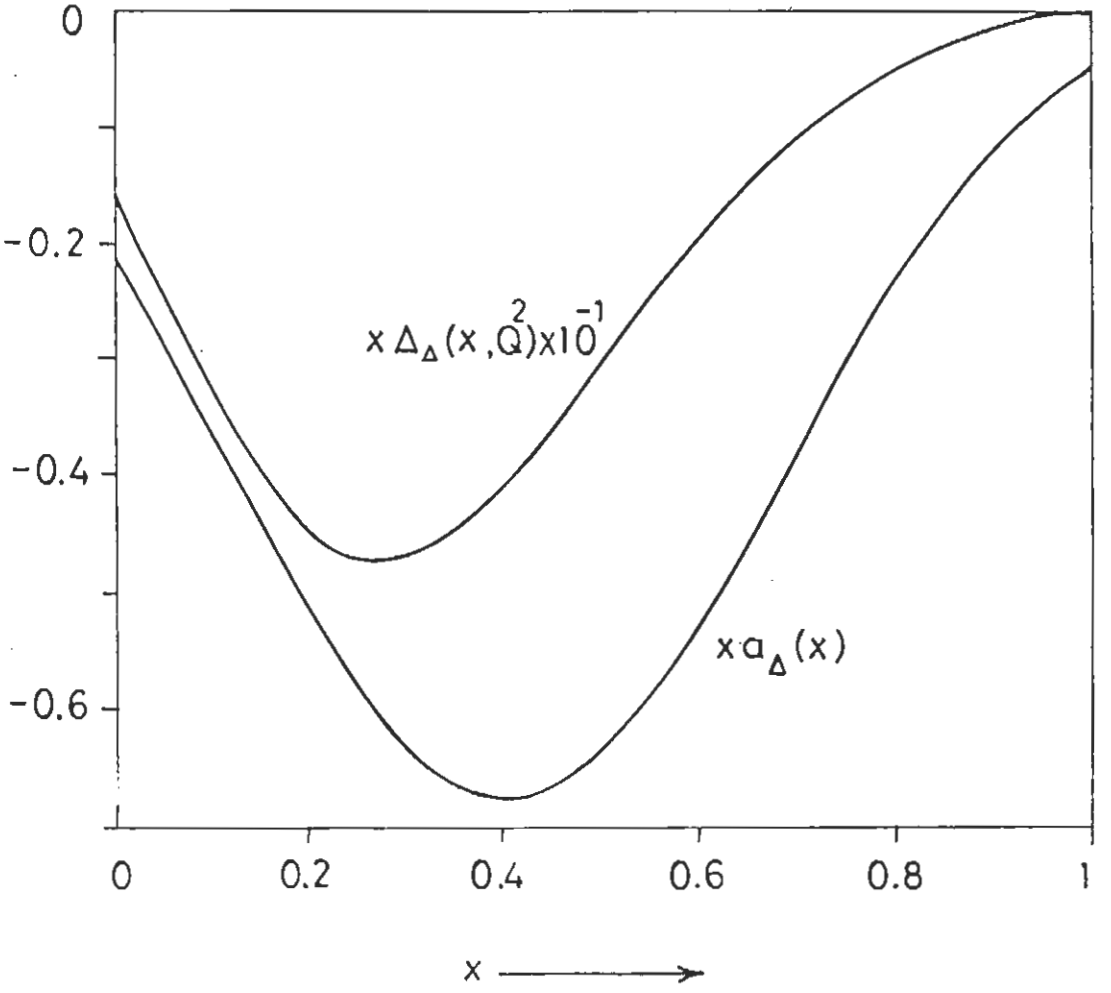

Figure 2.4: $xa_\Delta(x)$ and $x\Delta_\Delta(x,Q^2)$ for the Δ in the bag model.

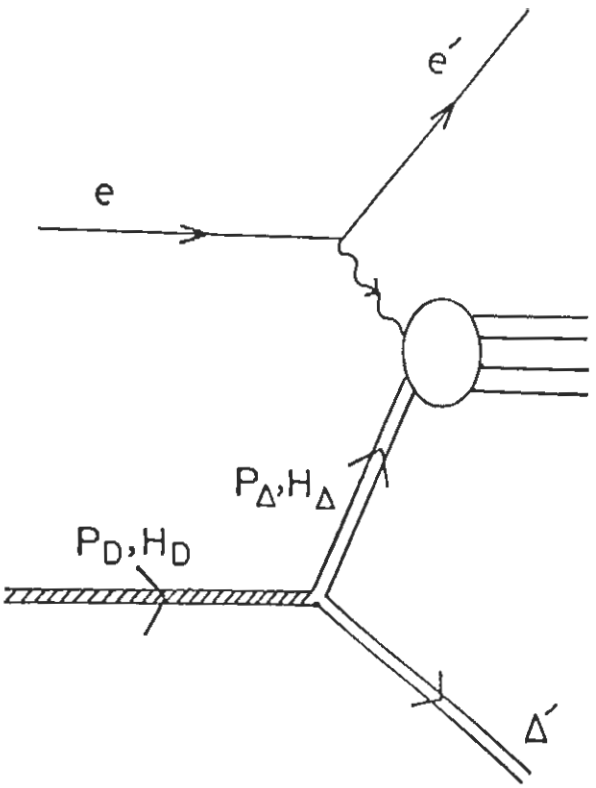

Figure 2.5: Scattering of an electron off the $\Delta - \Delta$ component of a deuteron target.

Under the assumption that probabilities can be convoluted we have,

$$\begin{aligned} g_i^{H_D}(x) &= \int dydz\delta(x-yz)\sum_{H_\Delta} h_{H_\Delta}^{H_D}(y) g_i^{H_\Delta}(x) \\ &\equiv h_{H_\Delta}^{H_D} \otimes g_i^{H_\Delta}, \end{aligned} \tag{2.50}$$

where $i = \hat{x}, \hat{y}$. In the above, $g_i^{H_D}(x)$ is the probability amplitude of finding a gluon of linear polarization i carrying fraction x of the deuteron's momentum when the deuteron has spin H_D in the $\hat{x}$-direction, $H_D = \pm 1, 0$. The quantity $g_i^{H_\Delta}(z)$ has a corresponding meaning. $h_{H_\Delta}^{H_D}(y)$ is the probability of finding the struck Δ with momentum fraction y for given H_D and H_Δ. It follows from parity and time reversal invariance that,

$$a_D^{H_D=1} = a_D^{H_D=-1} = -\frac{1}{2} a_D^{H_D=0} \equiv a_D, \tag{2.51}$$

and,

$$a_\Delta^{H_\Delta=\frac{3}{2}} = a_\Delta^{H_D=-3/2} = -a_\Delta^{H_\Delta=\frac{1}{2}} = -a_\Delta^{H_\Delta=-\frac{1}{2}} \equiv a_\Delta. \tag{2.52}$$

Here

$$a_D^{H_D} = g_{\hat{x}}^{H_D} - g_{\hat{y}}^{H_D},$$

and,

$$a_\Delta^{H_\Delta} = g_{\hat{x}}^{H_\Delta} - g_{\hat{x}}^{H_\Delta}.$$

Inserting these relations into Eq. (2.50), and using $h_{H_D}^{H_\Delta} = h_{-H_D}^{-H_\Delta}$ yields,

$$\begin{aligned} a_D(x) &= \Delta h \otimes a_\Delta \\ \Delta h(y) &= h_{\frac{3}{2}}^{1}(y) + h_{-\frac{3}{2}}^{1}(y) - h_{\frac{1}{2}}^{1}(y) - h_{-\frac{1}{2}}^{1}(y) \end{aligned} \tag{2.53}$$

Now we concentrate on estimating $\Delta h(y)$. For this, one must have as input the momentum space distribution of Δ's in a deuteron. Since a relativistic treatment is not available, we shall have to make do with the non-relativistic wave functions of Refs.[9-13], wherein

$$\begin{aligned} (P_\Delta\, | H_D\rangle &= \psi_{\Delta\Delta}^{H_D}(\mathbf{P}_\Delta) \\ &= \sum_{LS} \frac{u_{LS}(\mathbf{P}_\Delta)}{(2\pi)^{3/2}} C^{\frac{3}{2}\ \frac{3}{2}\ S}_{M_{S_1} M_{S_2} M_S} C^{S\ L\ 1}_{M_S M_L H_D} Y_{LM_L}(\hat{\mathbf{P}}_\Delta) \left|\frac{3}{2} M_{S_1}\right\rangle \left|\frac{3}{2} M_{S_2}\right\rangle . \end{aligned} \tag{2.54}$$

The wave function (probability amplitude) of a Δ with relative momentum P_Δ in a deuteron is then

$$\langle P_\Delta H_\Delta |\, H_D\rangle = \sum_{LS} \frac{u_{LS}(\mathbf{P}_\Delta)}{(2\pi)^{3/2}} C^{\frac{3}{2}\ \frac{3}{2}\ S}_{H_\Delta M_{S_2} M_S} C^{S\ L\ 1}_{M_S M_L H_D} Y_{LM_L}(\hat{P}_\Delta) \left|\frac{3}{2} M_{S_2}\right\rangle . \tag{2.55}$$

Symmetry considerations limit the values of (L,S) to (0,1), (2,1), (2,3) and (4,3). The radial wave functions are obtained as approximate solutions to the Schrodinger equation with $g_{N\Delta\pi}$ taken from the known $\Gamma_{\Delta\to N\pi}$ decay rate. The infinite momentum frame (IMF) momentum distribution $h_{H_\Delta}^{H_D}(y)$ is obtained from the laboratory frame distribution $h_{H_\Delta}^{H_D}(P_\Delta) \equiv |\langle P_\Delta H_\Delta |\, H_D\rangle|^2$ according to the

convolution model prescription [14],

$$h^{H_D}_{H_\Delta}(y) = \int d^3P_\Delta \delta\left(y - \frac{P^+_\Delta}{P^+_D}\right) h^{H_D}_{H_\Delta}(P_\Delta)\left(1 + \frac{P^3_\Delta}{M_\Delta}\right). \tag{2.56}$$

Here $P^+ = \frac{P^0+P^3}{\sqrt{2}}$. Performing the operation of projecting the isobar spin from Eq. (2.54), and then summing over all m quantum numbers, a convenient form for $\Delta h(y)$ can be written down

$$\begin{aligned}\Delta h(y) \;=\; & \sum_{LSL'S'l} Y(L'S'LSl) \int d^3P_\Delta \delta\left(y - \frac{P^+_\Delta}{P^+_D}\right)\left(1 + \frac{P^3_\Delta}{M_\Delta}\right) \\ & u^*_{L'S'}(\mathbf{P}_\Delta) u_{LS}(\mathbf{P}_\Delta) Y_{l0}(\hat{\mathbf{P}}_\Delta)\end{aligned} \tag{2.57}$$

where Y is composed of standard Wigner 3-j's, Racah W-coefficients, and 9-j symbols according to

$$\begin{aligned}Y(L'S'LSl) \;=\; & \sqrt{\frac{5}{\pi}}[J_D][L']^{1/2}[L]^{1/2}[S']^{1/2}[S]^{1/2}[l]^{1/2}(-1)^{L+S'} \begin{bmatrix} L' & L & l \\ 0 & 0 & 0 \end{bmatrix} \\ & W\left(\tfrac{3}{2}S', \tfrac{3}{2}S, \tfrac{3}{2}2\right) \sum_j [j] \begin{bmatrix} 1 & 1 & j \\ 1 & -1 & 0 \end{bmatrix} \begin{bmatrix} j & 2 & l \\ 0 & 0 & 0 \end{bmatrix} \\ & \begin{Bmatrix} l & j & 2 \\ L & 1 & S \\ L' & 1 & S' \end{Bmatrix}\end{aligned} \tag{2.58}$$

where $[J] = 2J + 1$

Eq. (2.57) is incomplete unless the energy of the Δ is specified inside the deuteron, which is at rest in the laboratory frame ($P^+_D = \frac{M_D}{\sqrt{2}}$). We assume non-relativistic kinematics: $P^0_\Delta = M_\Delta + \frac{P^2_\Delta}{2M_\Delta} - \epsilon$ with ϵ about equal to the Δ-N mass difference. Clearly the Δ is far off mass shell, and this treatment is valid only as a first estimate. The numerical evaluation of $\Delta h(y)$ is shown in Fig. 2.6. The wave functions $u_{LS}(\mathbf{P}_\Delta)$ have been taken from Nath and Weber[13] and are, perhaps, overly conservative in so far as the total $\Delta - \Delta$ probability is only .009 i.e.,

$$\sum_{H_\Delta} \int d^3P_\Delta h^{H_D}_{H_\Delta}(P_\Delta) = \sum_{LS} \int dP_\Delta P^2_\Delta \frac{|u_{LS}(\mathbf{P}_\Delta)|^2}{(2\pi)^3} \approx .009 \tag{2.59}$$

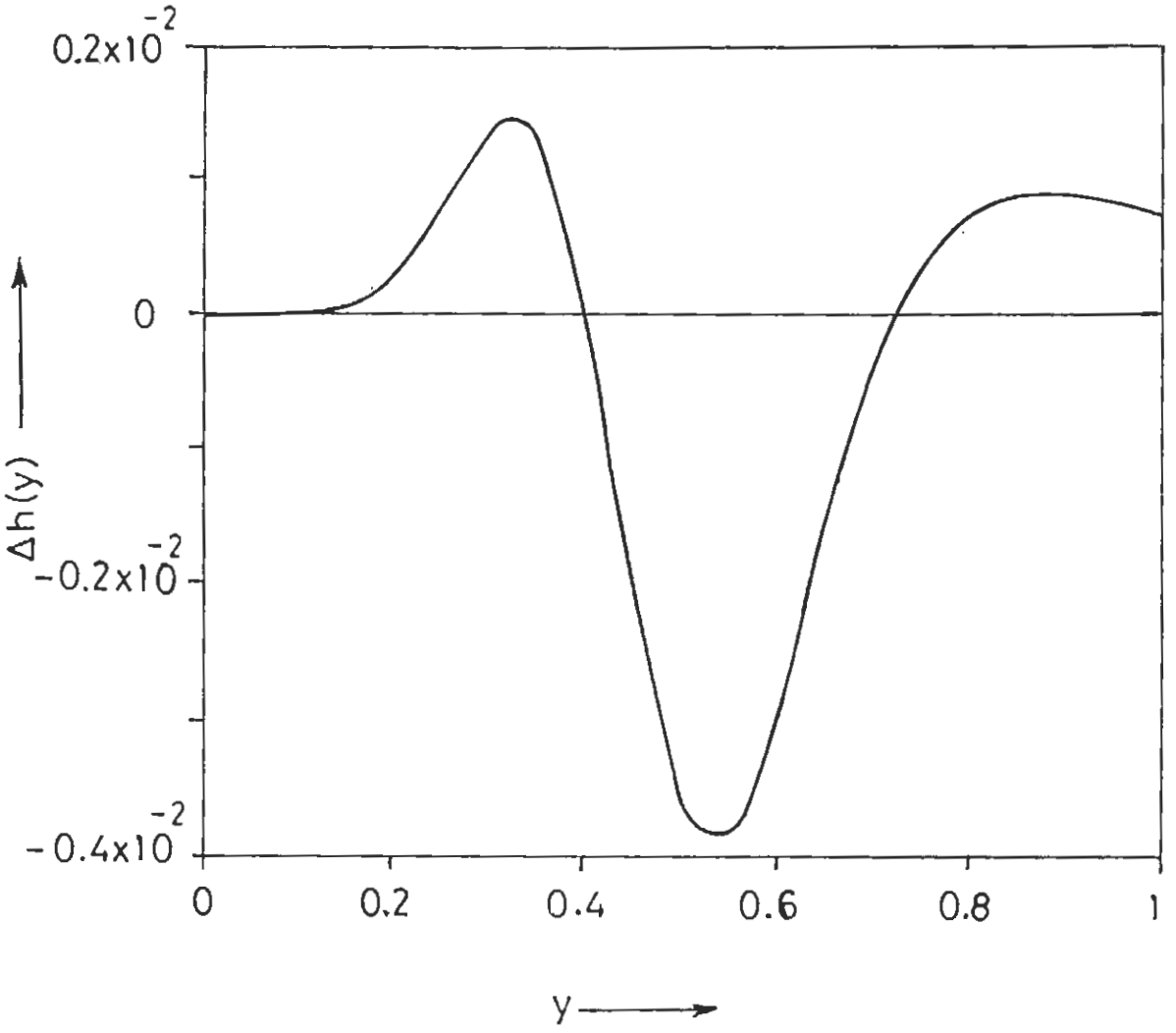

Figure 2.6: The difference of the deuteron's transversely polarized Δ probabilities $\Delta h(y)$, as defined in Eq. (2.57).

One would, therefore, reasonably expect that the scale of $\Delta h(y)$ could be larger by a factor of 2-3.

We may now combine a_Δ and Δh according to Eq. (2.53) to arrive at the deuteron distribution a_D. This is inputted into Eq. (2.24) and the results for $xa_D(x)$ and $x\Delta_D(x)$ are plotted in Fig. 2.7. By way of comparison, it is interesting to ask what the Δ contribution to the usual spin averaged structure function $F_1^D(x)$ would look like if a spectator Δ was detected in coincidence. This would be $F_{1\Delta}^D(x)$ itself. Thus to compare $\Delta_D(x)$ with $F_{1\Delta}^D(x)$ we estimate $F_{1\Delta}^D(x)$ as below.

Again assuming that probabilities can be convoluted, we have

$$q_f^D(x) = \int dydz\delta(x-yz)h(y)q_f^\Delta(z), \tag{2.60}$$

where $q_f^D(x)$ is the probability of finding a quark of flavor f carrying fraction x of the deuteron's momentum when the deuteron has $\Delta-\Delta$ configuration. $q_f^\Delta(z)$ has a corresponding meaning. $h(y)$ is the spin averaged probability of finding the struck Δ carrying fraction z of deuteron's momentum.

The spin averaged structure function $F_1(x)$ is defined as

$$F_1(x) = \frac{1}{2}\sum_f e_f^2 q_f(x). \tag{2.61}$$

Using Eqs. (2.60) and (2.61) we have,

$$F_{1\Delta}^D(x) = \int dydz\delta(x-yz)h(y)\frac{1}{4}\left[F_1^{\Delta^{++}}(x) + F_1^{\Delta^+}(x) + F_1^{\Delta^0}(x) + F_1^{\Delta^-}(x)\right] \tag{2.62}$$

Where we have used the fact that in a deuteron, Δ's come in pairs and both the pairs Δ^{++},Δ^- and Δ^+,Δ^0 are equally probable. Therefore, we have taken the average over all the four Δ's. In the above $h(y)$ is given by

$$h(y) = h_{3/2}^{H_D}(y) + h_{1/2}^{H_D}(y) + h_{-1/2}^{H_D}(y) + h_{-3/2}^{H_D}(y), \tag{2.63}$$

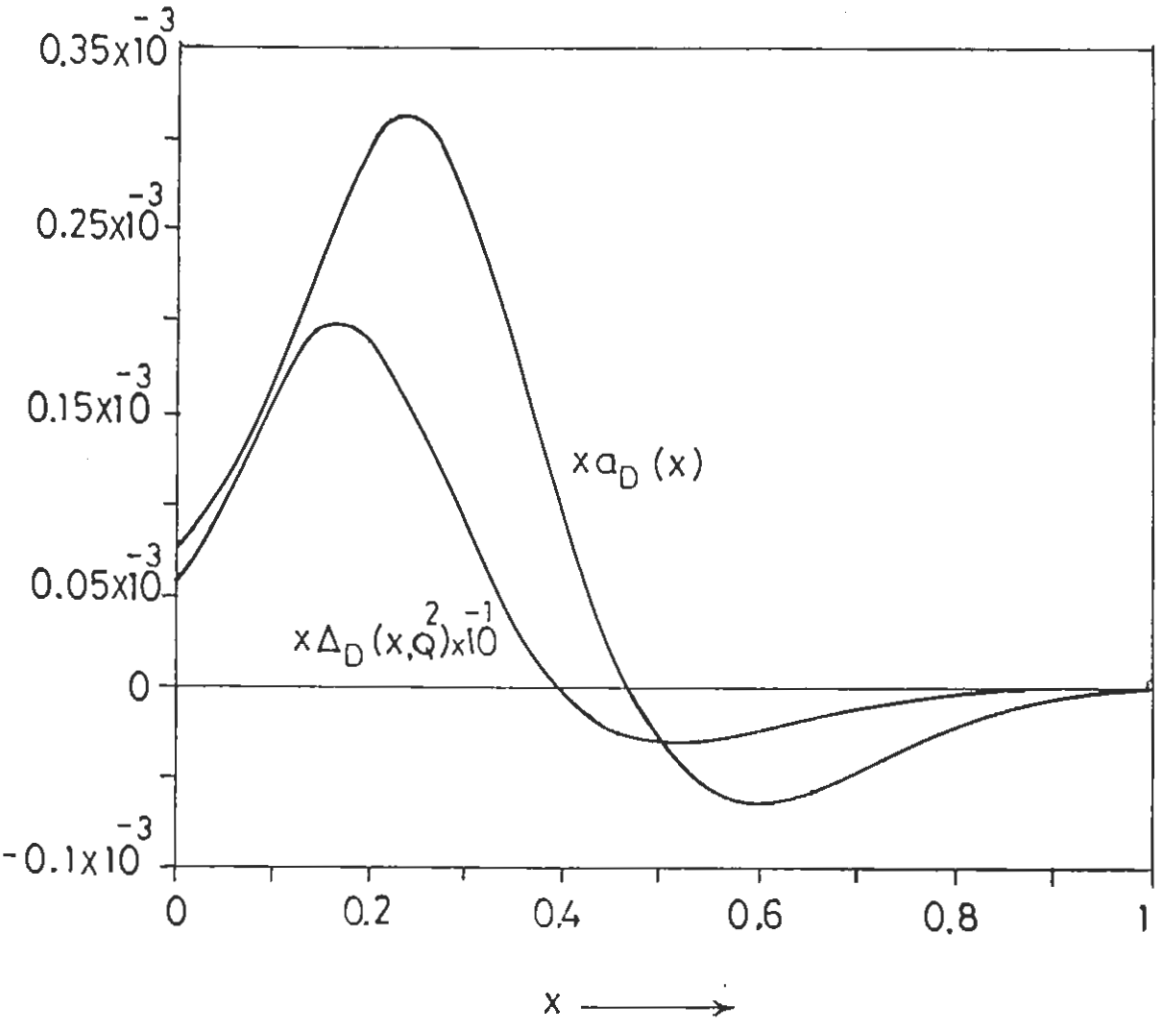

Figure 2.7: $xa_D(x)$ and $x\Delta_D(x, Q^2)$ for a deuteron.

where H_D may be 0, +1, -1 because $h(y)$ is the same for all the values of H_D. Now we estimate $F_1(x)$ for the Δ particle. The quark distribution function $q_f(x)$ is defined by the following light-cone correlation [15].

$$q_f(x) = \frac{1}{2}\int \frac{d\xi^-}{2\pi} e^{-ixP^+\xi^-} \left\langle P \left| \bar{\psi}_f(\xi^-)\gamma^+\psi(0) \right| P \right\rangle \tag{2.64}$$

To evaluate the matrix element in Eq. (2.64), we again use the MIT bag model for the Δ particle. A Δ, in the bag model, is represented by three massless quarks all in the lowest cavity mode. Repeating the steps which led from Eq. (2.34) to Eq. (2.40), and using the momentum space bag wave function of a quark in the lowest cavity mode

$$\psi_{M_S}(p) = \frac{N}{\sqrt{4\pi}} \begin{pmatrix} f_1(p)\ \chi_{M_S} \\ g_1(p)\sigma\cdot\hat{\mathrm{p}}\ \chi_{M_S} \end{pmatrix} \tag{2.65}$$

in Eq. (2.64), we arrive at the final expression for the quark distribution $q(x)$ in a bag,

$$q(x) = \frac{M_\Delta}{8\pi\omega^3(X-1)\sin^2 X}\int_{|p_{min}|}^{\infty} dp\, p\left[f_1^2(p) + g_1^2(p) + \frac{2p_{min}}{p} f_1(p)g_1(p)\right] \tag{2.66}$$

where $p_{min} = M_\Delta x - \omega$ and,

$$f_1(p) = \sqrt{\tfrac{2}{\pi}}\int_0^R dr r^2 j_0(pr) j_0(\omega r)$$
$$g_1(p) = \sqrt{\tfrac{2}{\pi}}\int_0^R dr r^2 j_1(pr)$$

From Eq. (2.61), we have

$$F_1^{\Delta^{++}}(x) = \tfrac{2}{3}q(x)$$
$$F_1^{\Delta^{+}}(x) = \tfrac{1}{2}q(x)$$
$$F_1^{\Delta^{0}}(x) = \tfrac{1}{3}q(x)$$
$$F_1^{\Delta^{-}}(x) = \tfrac{1}{6}q(x)$$

Thus Eq. (2.62) becomes

$$F_{1\Delta}^D(x) = \frac{5}{12}\int_0^1 dydz\delta(x-yz)h(y)q(z)$$

The results for $h(x)$, $F_1^{\Delta^{++}}(x)$ and $F_{1\Delta}^D(x)$ are plotted in Fig. 2.8. The ratio $\frac{\Delta p(x)}{F_{1\Delta}^D(x)}$ is shown in Fig. 2.9.

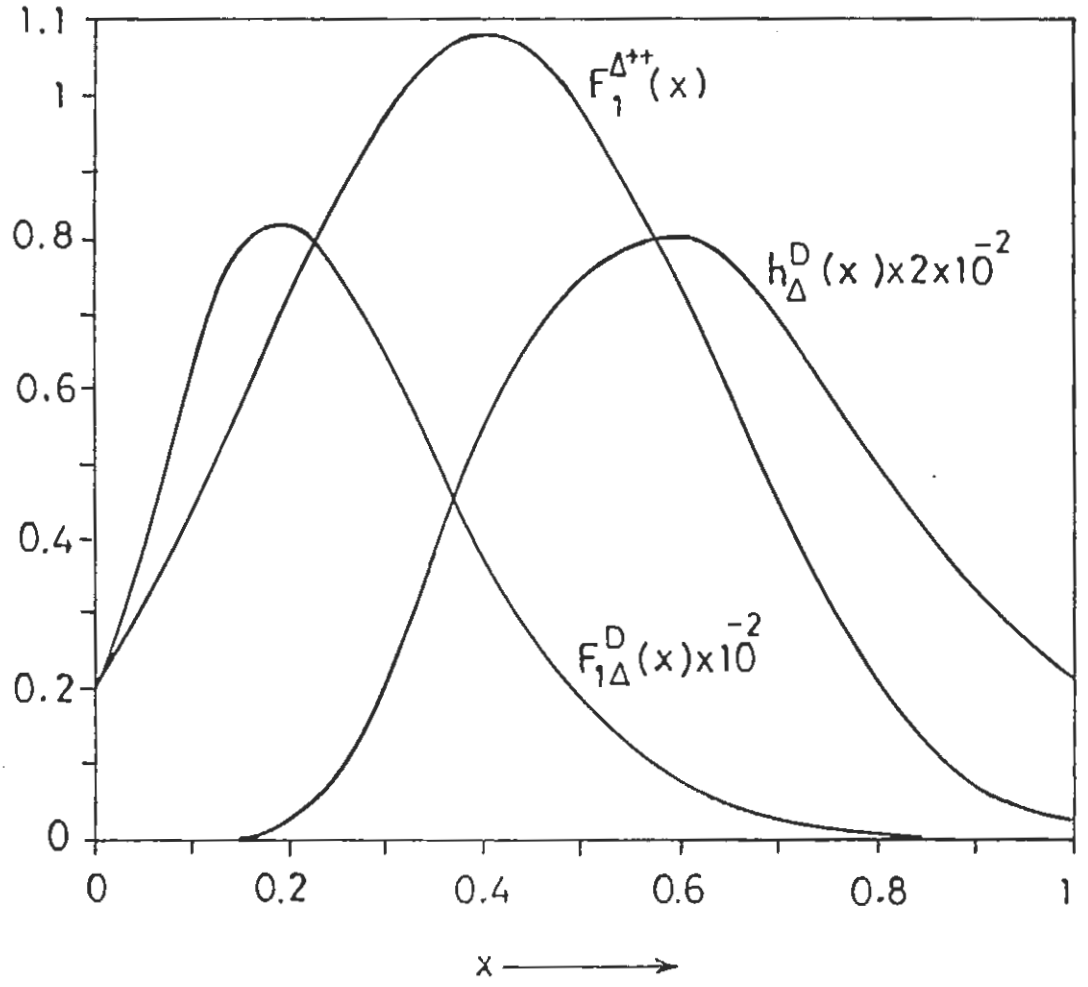

Figure 2.8: $F_1^{\Delta^{++}}(x)$ for a bag model Δ^{++} and $h_\Delta^D(x)$, the spin averaged probability of finding a Δ with momentum fraction x in a deuteron. Also plotted is $F_{1\Delta}^D(x)$, the Δ component contribution to $F_1(x)$ of the deuteron.

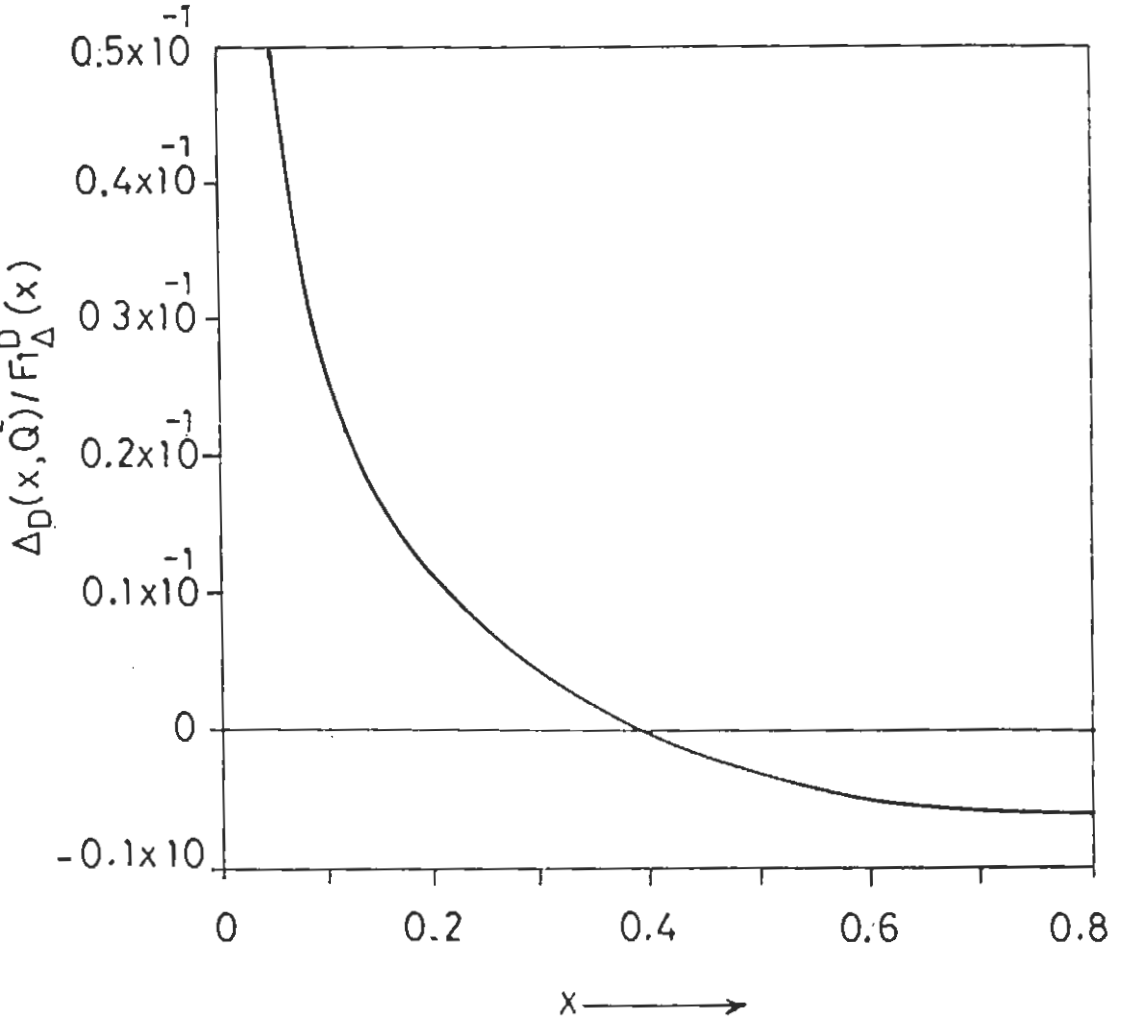

Figure 2.9: The calculated ratio of $\Delta_D(x, Q^2)$ to $F^D_{1\Delta}(x)$.

2.6 Discussion and conclusions

It is not easy to find precise probes of the quark and gluon substructure of the nucleus. The European Muon Collaboration (EMC) effect [16] and the higher spin structure functions discussed in Refs. [3] and [11] can receive contributions from the motion and binding of nucleons in the nucleus, as well as from familiar nuclear effects like pion exchange currents. The double helicity flip structure function $\Delta(x, Q^2)$ is free from these conventional sources. It receives no contributions from nucleons or pions bound in nuclei. This is obvious because neither nucleons nor pions can transfer two units of helicity to the nuclear target. The simplest "conventional" source would be from gluon distribution in ρ or Δ admixtures in the nuclear wave function. Generally, $\Delta(x, Q^2)$ receives contributions from gluons not associated with individual nucleons in the nucleus. We have calculated $\Delta(x, Q^2)$ for a deuteron which receives contributions from $\Delta - \Delta$ configuration of the deuteron. [The other source of contribution to $\Delta(x, Q^2)$ of a deuteron may be from quark and gluon exchange between nucleons. As the deuteron is a dilute nucleus therefore the quark and gluon exchange contribution to $\Delta(x, Q^2)$ is expected to be still smaller].

As can be seen from the Fig. 2.9, $\Delta_D(x, Q^2)$ is very small and may be difficult to measure. There are two independent reasons why $\Delta_D(x)$ is small: first the small probability of finding an isobar in the deuteron, and second, the smallness of $\Delta_\Delta(x)$ itself. The first can be dealt with to an extent by using a heavier nucleus, but the second is inescapable. Detecting the gluonic component of nuclei therefore seems to require an increase in precision of measuring deep inelastic scattering cross-sections by 2-3 order of magnitudes. Luckily, a measurement of $\Delta(x, Q^2)$ can be obtained for free in any experiment designed to measure $g_2(x)$ for a target with spin ≥ 1. From Eq. (2.11), we see that $\Delta(x, Q^2)$ is most readily extracted when scattering unpolarized electrons off a target which is polarized perpendicular to the beam- exactly the same target configuration as is needed

to measure $g_2(x)$. The HERMES collaboration at the DESY e-P collider HERA has proposed to use this fact to measure or set limits on $\Delta(x, Q^2)$ for a deuteron target[4].

Finally, we remark upon the validity of our calculations. First, we have assumed a convolution approach. This is quite well justified for weakly bound nucleons in a nucleus, although whether or not it explains EMC type effects, is still open to question. However, with Δ's it may not be equally justified because these are much more strongly bound (and thus quite relativistic). Whether bound Δ's and free Δ's have substantially the same structure functions is also open to question. Second we have relied upon the MIT bag model to calculate $\Delta_\Delta(x)$. But, as is well known, bag models have definite limitations of accuracy when used to calculate structure functions. This is reflected by non-vanishing support outside of the interval (0,1), and can be seen in our results as well (Fig. 2.4). While improved methods are available, for an exploratory calculation, the treatment in this chapter may be adequate.

References

[1] R.L. Jaffe and A. Manohar, Phys. Lett. **B223**, 218 (1989).

[2] Eric Sather and Carl Schmidt, Phys. Rev. **D42**, 1424 (1990).

[3] P. Hoodbhoy, R.L. Jaffe and A. Manohar, Nucl. Phys. **B312**, 571 (1989).

[4] The HERMES collaboration, 1990 (unpublished).

[5] A. Chodos, R.L. Jaffe, K. Johnson, C.B. Thorn, and V. Weisskopf, Phys. Rev. **D9**, 3471 (1974).

[6] A. Chodos, R.L. Jaffe, K. Johnson, and C.B. Thorn, Phys. Rev. **D10**, 2599 (1974).

[7] T. DeGrand. R.L. Jaffe, K. Johnson, and J. Kiskis, Phys. Rev. **D12**, 2060 (1975).

[8] F.E. Close and R.R. Horgan, Nucl. Phys. **B164**, 413 (1980).

[9] L.S. Kisslinger, Mesons in Nuclei, edited by Mannque Rho and Denys Wilkinson (North Holand, Amsterdam, 1979), Vol.1, p. 261.

[10] P. Hoodbhoy and R.L. Jaffe, Phys. Rev. **D35**, 113 (1987).

[11] R.L. Jaffe and A. Manohar, Nucl. Phys. **B321**, 343 (1989).

[12] D.A. Varshalovich, A.N. Moskalev, and V.K. Khersonskii, Quantum Theory of Angular Momentum (World Scientific, Singapore, 1988).

[13] N.R. Nath and H.J. Weber, Phys. Rev. **D6**, 1975 (1972).

[14] R.L. Jaffe, Relativistic Dynamics and Quark Nuclear Physics, (Wiley, New York 1986), and R.L. Jaffe, in Proc. of the XI. Int. Conf. on Particles and Nuclei (PANIC) (Kyoto, 1987).

[15] Charles J. Benesh and Gerald A. Miller, Phys. Rev. **D36**, 1344 (1987).

[16] J.J. Aubert, et al., Phys. Lett. **B123**, 275 (1983).

Chapter 3

Measuring nuclear gluon shadowing through 3-jet production in electron-nucleus collisions

3.1 Introduction

Deep inelastic electron scattering off a hadron target can be used as a probe of the parton distribution in the target. To a first approximation, it can be assumed that the parton (quarks and gluons) distribution in the nucleus is the sum of the parton distributions in the nucleons, corrected for the fact that the nucleons are in motion inside the nucleus (Fermi motion). Prior to the European Muon Collaboration(EMC) experiment [1] in 1983, little attention had been paid to the parton distribution in the nucleus. To the surprise of particle and nuclear theorists, the experimental data of deep inelastic scattering from an iron and a deuteron target showed nearly 15% difference in the region where the Fermi motion effects were

thought to be negligible. In other words, the parton distribution in the nucleus is not just a simple sum of the parton distributions inside the nucleons. This effect is known as the "EMC" effect [1]. This effect was confirmed by experiments at SLAC later [2]. For denser nuclei this effect is quite significant.

We may look at deep inelastic scattering off a nucleus in a frame where the nucleus is going very fast. The nucleons inside the nucleus are moving side by side. If P is the nuclear momentum and p the momentum per nucleon, p is approximately given by $p \approx P/A$, where A is the atomic weight of the nucleus. If M is the rest mass of the nucleon then $p^\mu = (\mathcal{P} + \frac{M^2}{2\mathcal{P}}, 0, 0, \mathcal{P})$ and the virtual photon four momentum is $q^\mu = (q_0, 0, 0, q_3)$. $\mathcal{P}$ is large and $Q^2 = -q^2$. In this standard infinite momentum frame, the virtual photon simply measures the parton number densities of the nucleus,

$$F_2^A(x, Q^2) = \sum_i e_i^2 x q_i^A(x, Q^2).$$

In the above e_i is the electric charge of the i-quark or antiquark and $q_i^A(x, Q^2)$ is the number density of the i-quarks in the nucleus. If the nucleons are independent then,

$$\begin{aligned} q_i^A(x, Q^2) &= Z q_i^{Proton}(x, Q^2) + (A - Z) q_i^{Neutron}(x, Q^2) \\ &\approx A q_i(x, Q^2) \quad (at\ small\ x). \end{aligned}$$

From above equation, the cross section for virtual photons off a nucleus should vary as A times the photon nucleon cross section. But in the energy regime $Q^2 \leq 2 \sim 3\ GeV^2$, the experimental data [3] shows A_{eff}/A is as small as 0.6 for a lead target. This implies that the nucleons inside the nucleus are not completely independent. This can be understood easily in the parton model as explained below.

In the nuclear infinite momentum frame, the nucleus occupies a longitudinal size $\Delta z_n \approx 2RM/p$, where R is the radius of the nucleus. The longitudinal size

of a sea quark or gluon of momentum k_z is $\Delta z \approx 1/k_z$.When $1/k_z > 2RM/p$ or $x = k_z/p < 1/2MR$, all sea quarks and gluons having such x values and having the same impact parameter overlap spatially. Such sea quarks and gluons are really a property of the nucleus rather than a property of the individual nucleons. If the number densities of sea quarks and gluons are large enough to have such overlapping, then sea quarks and gluons from different nucleons may interact with each other to reduce the number densities through annihilation which leads to an altered (or shadowed) nuclear parton distribution. We are interested in measuring the nuclear gluon shadowing. It is not easy to measure the contribution of gluons in deep inelastic scattering processes because the virtual photon has no direct coupling with gluons, and must perforce interact through a mechanism such as the box diagram. The contribution of this must be added on to the usual tree level $\gamma^* - q$ diagram and this makes isolation of the gluon component very difficult.

In principle the gluon contribution to deep inelastic scattering from a hadron target can be measured by classifying events according to the final state. Whereas $\gamma^* - q$ scattering leads to single-jet events, $\gamma^* - g$ scattering leads to two back-to-back jets in the center of mass system in the lowest order as shown in Fig. 3.1. This process has been the basis of a proposal for measuring the gluon content of a polarized proton by measuring the large transverse momentum jets [4]. Unfortunately, as pointed out by Manohar [5], this is not experimentally feasible for protons at rest in the laboratory. The problem is that, in the laboratory frame, for transverse momentum of order Q the angle θ between the jets, $\sin\theta \sim M/Q$, becomes small for large Q. For smaller values of the transverse momentum, $\sin\theta \sim M/k_\perp$. This too does not lead to a satisfactory situation because only events with $k_\perp \gg \langle k_\perp \rangle_{intrinsic}$ ought to be considered in order to avoid contamination with the proton's intrinsic transverse momentum. Thus, for a target at rest, two-jet events are difficult to separate from the dominant one-jet events.

A possible way out has been suggested by Manohar [5], who considers an

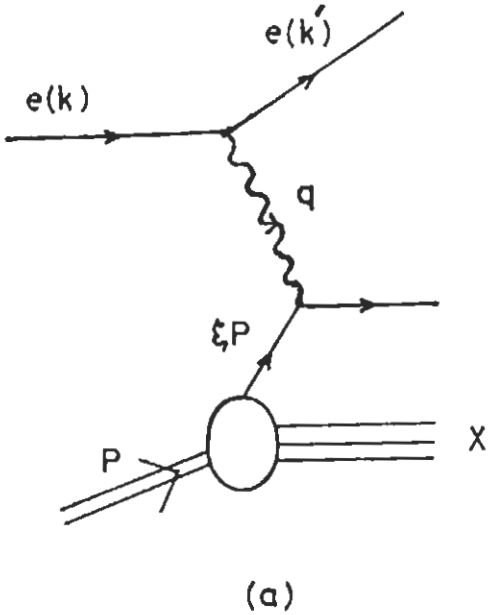

(a)

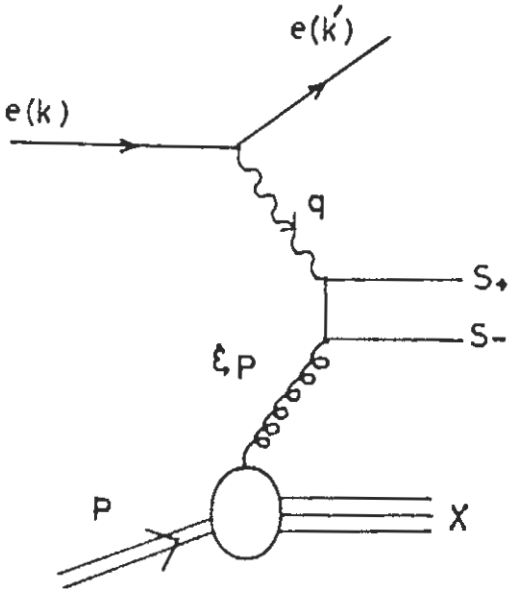

(b)

Figure 3.1: (a) Scattering of a photon from a quark carrying momentum ξ of the hadron target. (b) Scattering of a photon from a gluon carrying momentum fraction ξ of the hadron target.

experimental situation in which both the electron and the polarized proton are highly relativistic in the laboratory frame, an arrangement which may be possible at colliders such as HERA. The kinematics for this process suggest that the three jets (the third being the proton debris) will be distinguishable, provided that the opening angle between any two jets exceeds a certain minimum value δ, and the transverse-jet momentum fraction is large enough,

$$\lambda^2 \geq (1 - cos\delta)\frac{E_{min}^2/E_P^2}{2x(x + E_l/E_P)}$$

Here $\lambda^2 = k_\perp^2/Q^2$, E_l is the lepton energy, E_P is the proton energy, and E_{min} is the minimum energy of a jet which should be large compared to Λ_{QCD}. It additionally obeys the restriction $E_{min} \leq (\xi - x)E_P$, where ξ is the longitudinal momentum fraction carried by the struck gluon. The requirement that perturbative QCD hold, $Q^2 \geq Q_{min}^2$, translates into the condition that $x \geq x_{min}$ for measureable 3-jet events, where $x_{min} = Q_{min}^2/4E_P E_l$.

We consider adapting the discussion of Ref. [5] for the purpose of measuring the unpolarized gluon distribution in a hadron. The leading order contribution from gluons is given by the Feynman diagram in Fig. 3.1(b). Working in parallel with Ref. [5], we calculate the 3-jet contribution to $F_1(x)$ (spin averaged structure function of the target) arising from a gluon distribution $g(\xi)$.

To estimate the size of the 3-jet contribution, we use a simple model for gluon distribution in a nucleon, as well as in a nucleus, proposed by Qiu [6]. As a result of our calculations we find that the 3-jet contribution to $F_1(x)$ of the target has a measureable value if the energy of the target is sufficiently high. Also 3-jet events could discriminate between different nuclear gluon distributions. It thus appears that a clean measurement of gluon shadowing is possible, provided that a colliding beam of leptons and nuclei, rather than a fixed nuclear target, can be arranged.

3.2 The kinematics of 3-jet production

Consider the photon-gluon scattering diagram as shown in Fig. 3.1(b). The gluon carries momentum fraction ξ of the momentum P of the hadron target and q is the momentum of the virtual photon. The final state partons then have momentum S and $\xi P + q - S$. It is convenient to write

$$S^\mu = \alpha P^\mu + \beta q^\mu + \lambda \gamma^\mu, \tag{3.1}$$

where γ is a vector in the transverse momentum direction and is normalised so that it satisfies the equations,

$$\gamma.P = 0$$

$$\gamma.q = 0$$

$$\gamma^2 = -Q^2.$$

The transverse momentum of the final state quarks is $k_\perp^2 = \lambda^2 Q^2$. The massless quarks are on shell, so that

$$S^2 = (\xi P + q - S)^2 = 0$$

which determines α and β,

$$\alpha_\pm = \frac{1}{2}\xi \pm (x - \frac{1}{2}\xi)\sqrt{1 - \frac{4x\lambda^2}{\xi - x}} \tag{3.2}$$

$$\beta_\pm = \frac{1}{2}\left(1 \pm \sqrt{1 - \frac{4x\lambda^2}{\xi - x}}\right) \tag{3.3}$$

There are two possible signs for the square root, which correspond to exchanging the momenta, $S \leftrightarrow \xi P + q - S$ of the quark and antiquark if we also let $\lambda \rightarrow -\lambda$. We will therefore refer to the two momenta as $S_\pm$ and quantities referring to the partons will be denoted by the subscripts $\pm$. The target fragment has momentum $(1 - \xi)P$ and will be referred to using the subscript T. These three fragments hadronize to form jets.

3.2.1 When the target is at rest

In the rest frame of the target, $P = (M, 0, 0, 0)$, where M is the mass of the target. Using the definition of x

$$x = \frac{Q^2}{2P.q},$$

We have

$$q^0 = \frac{Q^2}{2Mx},$$

and so,

$$\begin{aligned} S_\pm^0 &= \alpha_\pm M + \beta_\pm q^0 \\ S_\pm^\perp &= \pm \lambda Q. \end{aligned} \tag{3.4}$$

The 3-axis has been chosen along the direction of the virtual photon momentum, and is parallel to the lepton beam direction in the deep inelastic limit. The two partons produce jets with angles $\theta_\pm$ with respect to the virtual photon direction, where,

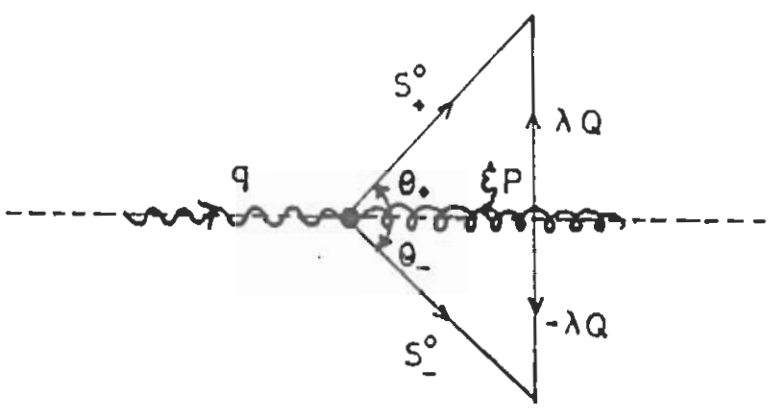

$$\sin\theta_\pm = \frac{S_\pm^\perp}{S_\pm^0} = \pm\frac{\lambda Q}{S_\pm^0}. \tag{3.5}$$

For transverse momentum of order Q, λ and hence $\beta_\pm$ are of order 1, S^0 is of order $Q^2/2Mx$, and

$$\sin\theta_\pm \sim \pm\frac{\lambda Mx}{Q} \to 0 \tag{3.6}$$

in the deep inelastic limit. Thus $\theta_{\pm} \rightarrow 0$. For small transverse momentum ($\lambda \rightarrow 0$), β_+ is of order 1 and hence $\theta_+ \rightarrow 0$ as before. For θ_-, we need to expand β_- to first order in λ^2,

$$\beta_- \rightarrow \frac{x\lambda^2}{\xi - x}. \tag{3.7}$$

Hence,

$$\sin\theta_- = -\frac{\lambda Q}{S^0_-} = \frac{Q(\xi - x)}{\lambda x q^0} = \frac{2M(\xi - x)}{k_\perp} << 1 \tag{3.8}$$

and thus $\theta_- \rightarrow 0$. We require $k_\perp >> M$ to avoid contamination by intrinsic transverse momentum in the hadron wave function. Thus for $k_\perp/Q$ small, but $k_\perp$ large compared with Λ_{QCD}, the two parton jets are collinear even though they may have large transverse momentum. Therefore one cannot separate out the photon-gluon graph by looking at two-jet events.

3.2.2 When both the target and the lepton beam are relativistic

In this case, $P = (E_P, 0, 0, -E_P)$, where $E_P >> M$ is the energy of the target beam. Let E_l be the energy of the lepton beam and

$$y = \frac{E_l - E'_l}{E_l} = \frac{q_0}{E_l} \tag{3.9}$$

be the fractional energy loss of the lepton. Then by using the relation

$$k_i.k_j = E_i E_j(1 - cos\theta_{ij}),$$

the angles θ_{+T}, θ_{-T} and θ_{+-} between the parton fragments are,

$$E_+E_-(1 - cos\theta_{+-}) = \frac{Q^2(\xi - x)}{2x} \tag{3.10}$$

$$E_\pm E_P(1 - cos\theta_{\pm T}) = \frac{Q^2}{4x}\left[1 \pm \sqrt{1 - \frac{4x\lambda^2}{\xi - x}}\right]. \tag{3.11}$$

The parton energies are,

$$E_{\pm} = \alpha_{\pm} E_P + \beta_{\pm} q^0 \tag{3.12}$$

$$E_T = (1-\xi)E_P \tag{3.13}$$

Depending on the values of x and λ, the final state will have two or three jets (including the target jet).

Now we determine the kinematic region in the $x-\lambda$ plane which corresponds to three-jet events and would be used to compute the gluon contribution to F_1 of the target. All three jets must have some minimum energy, E_{min}, which is large compared to Λ_{QCD}, but can be chosen to be much smaller than Q. This gives the restrictions (for small λ),

$$E_+ = \frac{Q^2}{4xE_P} = xE_P + yE_l \geq E_{min} \tag{3.14}$$

$$E_- = (\xi - x)E_P \geq E_{min} \tag{3.15}$$

$$E_T = (1-\xi)E_P \geq E_{min}. \tag{3.16}$$

Recall that for small λ, $\beta_+ \to 1$, $\beta_- \to x\lambda^2/\xi - x$. If the opening angle between the jets is too small, they cannot be distinguished experimentally. If δ is the minimum opening angle required to reliably separate jets, then we require that

$$1 - cos\theta_{ij} \geq 1 - cos\delta, \tag{3.17}$$

For large $k_\perp^2$, the jets are well separated from each other. However, as $k_\perp \to 0$, or equivalently $\lambda \to 0$), it can be seen from Eq. (3.11) that

$$E_- E_P(1 - cos\theta_{-T}) \longrightarrow 0.$$

From this $\theta_{-T} \to 0$, while Eqs. (3.10) and (3.11) give $\theta_{+-}, \theta_{+T} \longrightarrow \pi$. Thus one of the quark jets becomes collinear with the target jet. From equations (3.11) and (3.15), the limiting value of θ_{-T} for small λ is given by

$$1 - cos\theta_{-T} \to \frac{Q^2\lambda^2}{2(\xi - x)^2 E_P^2}. \tag{3.18}$$

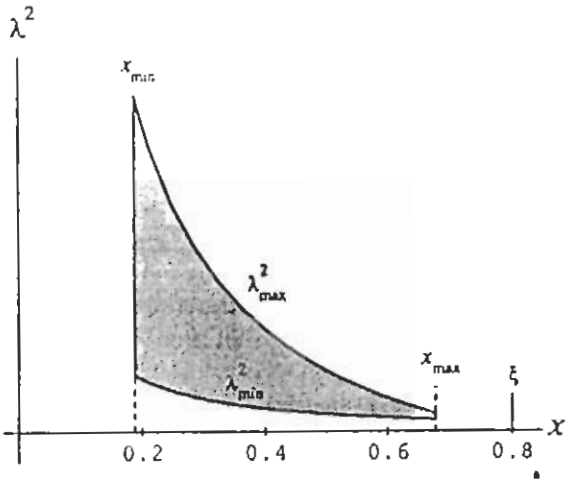

Figure 3.2: The region in the $\lambda^2 - x$ plane where the photon-gluon scattering graph leads to experimentally measurable three-jet events. The values of x_{min} and $\xi - x_{max}$ have been exaggerated for clarity. In the deep inelastic limit, both quantities approach zero.

Eq. (3.14) yields

$$Q^2 = 4xE_P(xE_P + yE_l), \tag{3.19}$$

so that our requirement Eq. (3.17) becomes

$$\begin{aligned} \lambda^2 &\geq (1 - cos\delta)\frac{(\xi - x)^2}{2x(x + yE_l/E_P)} \\ &\geq (1 - cos\delta)\frac{(\xi - x)^2}{2x(x + E_l/E_P)}. \end{aligned} \tag{3.20}$$

The last line above follows because $0 \leq y \leq 1$. Combining this with the energy constraint Eq. (3.15) gives,

$$\lambda^2 \geq (1 - cos\delta)\frac{E^2_{min}/E^2_P}{2x(x + E_l/E_P)} \tag{3.21}$$

In addition, to remain in the domain of validity of perturbative QCD, and to avoid higher twist effects, we also require $Q^2 \geq Q^2_{min}$, which implies that

$$x \geq x_{min} = \frac{Q^2_{min}}{4E_PE_l}. \tag{3.22}$$

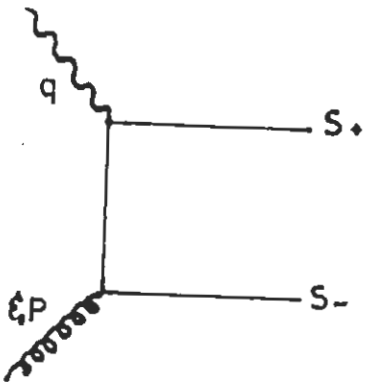

Figure 3.3: The photon-gluon scattering graph.

The combined region which is allowed by (3.20) and (3.22) is shown in Fig. 3.2. Thus we can determine the contribution of a gluon with momentum fraction ξ to the experimentally measured three-jet events by using the allowed values of x and λ^2 given by Eqs. (3.21) and (3.22).

3.3 Three-jet contribution to $F_1(x)$

We now calculate the three-jet contribution to $F_1(x)$ of the hadron for the purpose of measuring the unpolarized gluon distribution. The leading order contribution from gluons is given by the Feynman diagram in Fig. 3.3. The photon-gluon scattering graph has been computed in Ref. [4] and its contribution to the spin averaged structure function $F_1(x)$ is,

$$F_1^{\gamma g}(z) = \frac{\alpha_s N_f}{8\pi} \int_{\epsilon(z)}^{\frac{1-z}{4z}} \frac{d\lambda^2}{\sqrt{1-\frac{4z\lambda^2}{1-z}}} \left[\frac{1-2z+2z^2}{\lambda^2} + \frac{2z(1+2z-2z^2)}{1-z} \right]. \quad (3.23)$$

In the above $z = x/\xi$ is the effective value of x for the parton-parton subprocess, and

$$\epsilon(z) = \frac{E_{min}^2(1-\cos\delta)}{2xE_P(xE_P+E_l)} \ll 1, \quad (3.24)$$

is the lower transverse momentum cut off. Doing the integration in Eq. (3.23), we get

$$F_1^{\gamma g}(z) = \frac{\alpha_s N_f}{8\pi}\left[(1-2z+2z^2)\ln\left(\frac{1-z}{z\epsilon(z)}\right)+(1+2z-2z^2)\right]. \qquad (3.25)$$

If $g(\xi)$ is the probability of finding a gluon with momentum fraction ξ in the target (i.e., the unpolarised gluon distribution in the target), then the 3-jet part of the structure function $F_1(x)$ of the target is

$$\begin{aligned} F_1^{3-jet}(x) &= \int_0^1 d\xi\, dz\, \delta(x-\xi z)\, g(\xi)\, F_1^{\gamma g}(z) \\ &= \frac{\alpha_s N_f}{8\pi}\int_{\xi_{min}}^{\xi_{max}} \frac{d\xi}{\xi}\, g(\xi)\, F(x,\xi) \end{aligned} \qquad (3.26)$$

The limits of integration are

$$\begin{aligned} \xi_{min} &= x + \tfrac{E_{min}}{E_P} \\ \xi_{max} &= 1 - \tfrac{E_{min}}{E_P} \end{aligned} \qquad (3.27)$$

instead of x and 1 because for minimum value of the opening angle required to reliably separate jets, we have from equations (3.15) and (3.16)

$$\xi \geq x + \frac{E_{min}}{E_P},$$

and

$$\xi \leq 1 - \frac{E_{min}}{E_P}.$$

The kernel $F(x,\xi)$, with $z = x/\xi$ is

$$F(x,\xi) = [z^2+(1-z)^2]\log\left(\frac{1-z}{z\epsilon(z)}\right) + 2\left[\frac{1}{z}+z(1-z)\right].$$

Thus the gluon distribution $g(\xi)$ in the target can be determined (in principle) by measuring the 3-jet contribution to F_1 using the relation (3.26) between F_1^{3-jet} and $g(\xi)$.

3.4 Results and discussion

To estimate the size of the 3-jet contribution, we use a simple model for gluon distribution in the nucleon given by Qiu [6],

$$\left.\begin{aligned} \xi\, g(\xi) &= 1.4(1-\xi)^6\,(1+9\xi) && \xi \geq 0.1 \\ &= \tfrac{0.173}{\sqrt{\xi}} + 0.868 && 0.001 < \xi < 0.1 \end{aligned}\right\}, \tag{3.28}$$

at $Q^2 = 4GeV^2$. We consider 35 GeV electrons, available at HERA, in collision with a proton beam with various energies at a fixed value $Q^2 = 4GeV^2$. Each jet is assumed to have an energy in excess of 1GeV. The angular size of the cone formed around a fast quark is approximately $\theta =< k_T > /P_q \approx 0.3$ radians at $Q^2 = 4GeV^2$ [7]. Thus the minimum opening angle δ, which is needed to identify individual jets, must exceed 0.6 radians. In Fig. 3.4, numerical values for $xF_1^{3-jet}(x)$ for a nucleon with nucleon energy $E_P = 50GeV$, $200GeV$ and $300GeV$ are displayed.

The results (3.23)-(3.28) have immediate application to the nuclear gluon distribution provided that colliding beams of electrons and relativistic ions can be arranged. Nuclear gluons at small x are of particular interest since, for $x \leq 1/2MR$, partons are no longer confined to individual nucleons. Instead, they extend over the entire nucleus in the longitudinal direction as a consequence of which they undergo recombination. This nuclear effect leads to an altered (or shadowed) gluon distribution. To observe this would be very interesting. It is the purpose of the present calculation to see whether 3-jet production offers a realistic possibility for this.

A simple model has been proposed by Qiu [6], building upon earlier work by Mueller and Qiu [8], which models the gluon distribution in a nucleus as

$$\frac{1}{A}\, g^A\left(\xi, Q_0^2\right) = g\left(\xi, Q_0^2\right)\, R_g\left(\xi, Q_0^2, A\right). \tag{3.29}$$

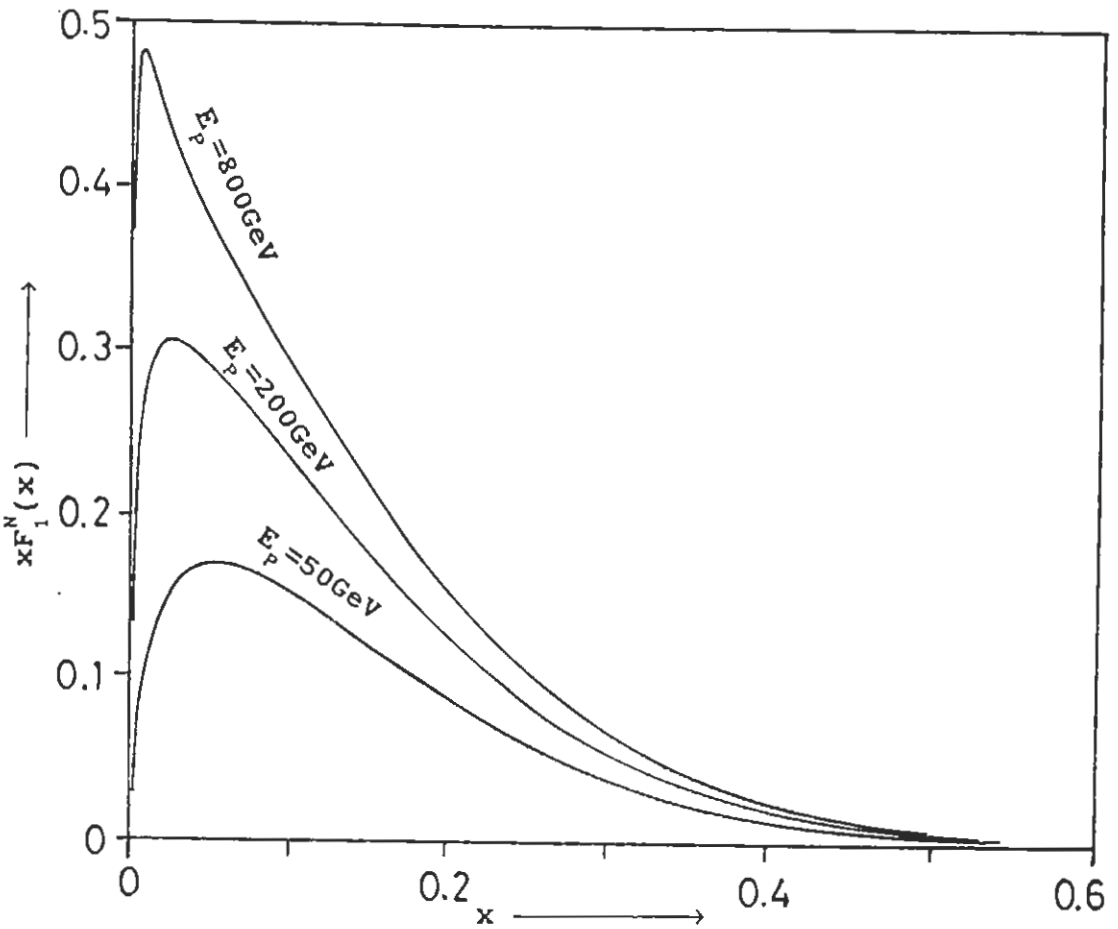

Figure 3.4: Three jet contribution to $xF_1(x)$ for a nucleon with nucleon energy E_P = 50 GeV, 200 GeV, and 800 GeV, and with other parameters as discussed in the text.

At a fixed value of $Q^2 = Q_0^2$, the gluon shadowing factor is

$$R_g(\xi, Q_0^2) = \begin{cases} 1 & x_n < \xi < 1 \\ 1 - K_g(A^{1/3} - 1)\frac{1/\xi - 1/x_n}{1/x_A - 1/x_n} & x_A \leq \xi \leq x_n \\ 1 - K_g(A^{1/3} - 1) & 0.001 < \xi < x_A. \end{cases} \tag{3.30}$$

The parameters x_n and x_A for the nucleon and the nucleus respectively, are $x_n = 1/2rM$ and $x_A = 1/2RM$, where r is the radius of the nucleon and R is the nuclear radius ($R = 1.2\,A^{1/3} fm$). The constant K is essentially unknown and has somewhat arbitrarily been chosen to lie between 0.02 and 0.1 in Ref. [6] at a reference value of $Q_0^2 \approx 4GeV^2$. To estimate the extent to which 3-jet events could discriminate between different nuclear gluon distributions, we consider ^{32}S ions in collision with electrons with all parameters identical to the single nucleon case discussed above. Figures (3.5)-(3.7) show the relative shadowing for 50 GeV/nucleon, 200 GeV/nucleon and 800 GeV/nucleon ions for $K = 0.02$, 0.05 and 0.10. Increasing the ion energy much further leads to relatively little increase in the relative shadowing, which is fairly substantial even at the values shown.

It thus appears that the use of a relativistic nuclear target in deep inelastic scattering could enable the measurement of gluon shadowing. This method is, in principle, superior to using charmonium production from gluon fusion processes because final state quark interactions are unimportant for jet measurement. In contrast, the heavy quark system undergoes complicated A-dependent interactions as it makes its way out of the nucleus.

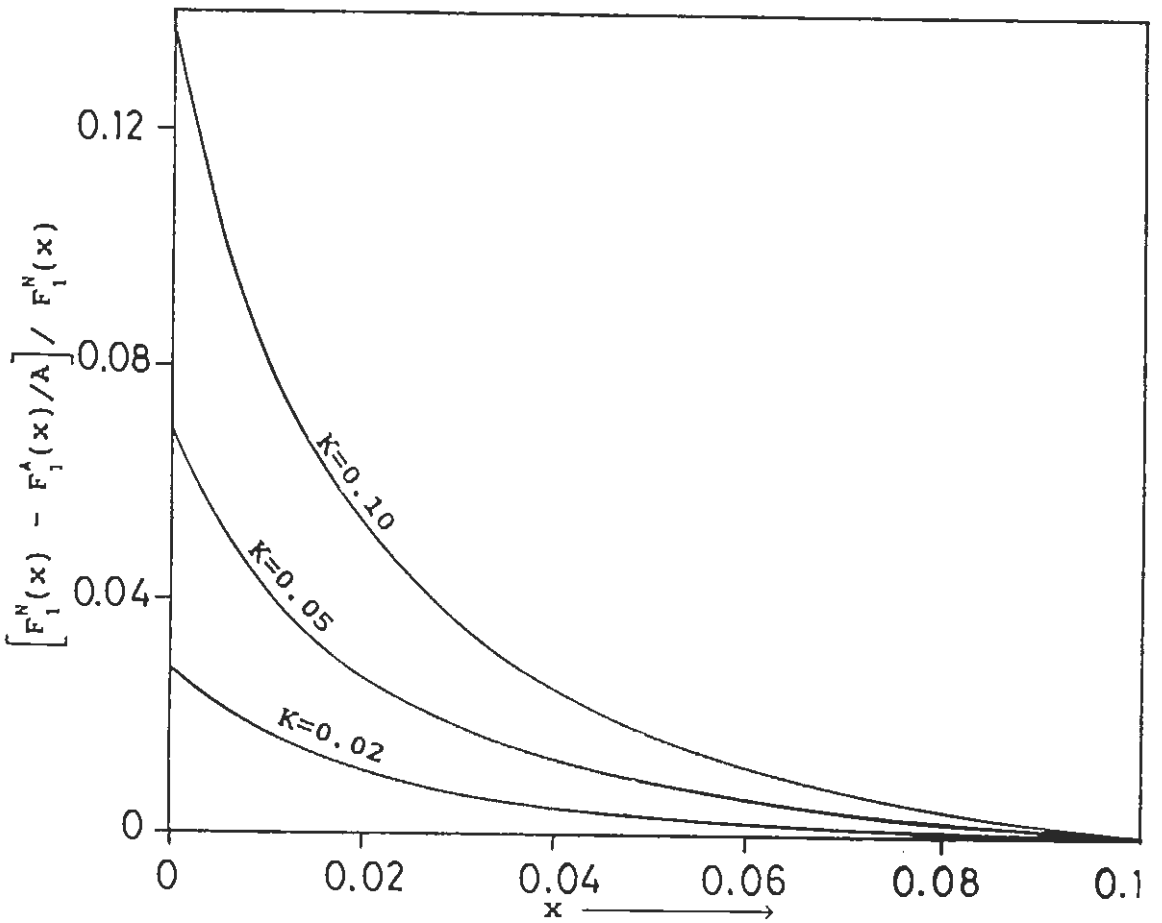

Figure 3.5: Relative shadowing for $E_P = 50$ GeV/nucleon ^{32}S ions for shadowing factor $K = 0.02, 0.05, 0.1$ and other parameters as discussed in the text.

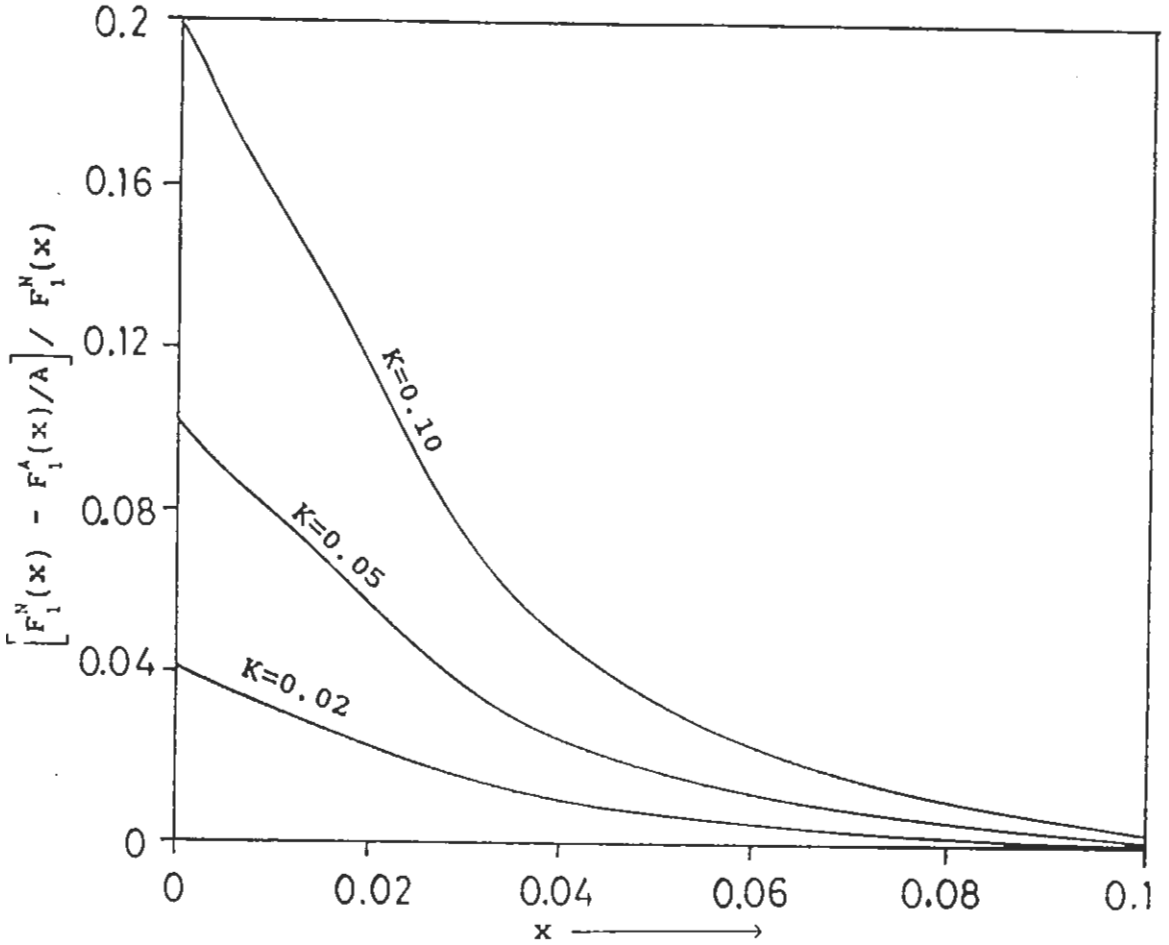

Figure 3.6: Relative shadowing for $E_P = 200$ GeV/nucleon ^{32}S ions for shadowing factor $K = 0.02, 0.05, 0.1$ and other parameters as discussed in the text.

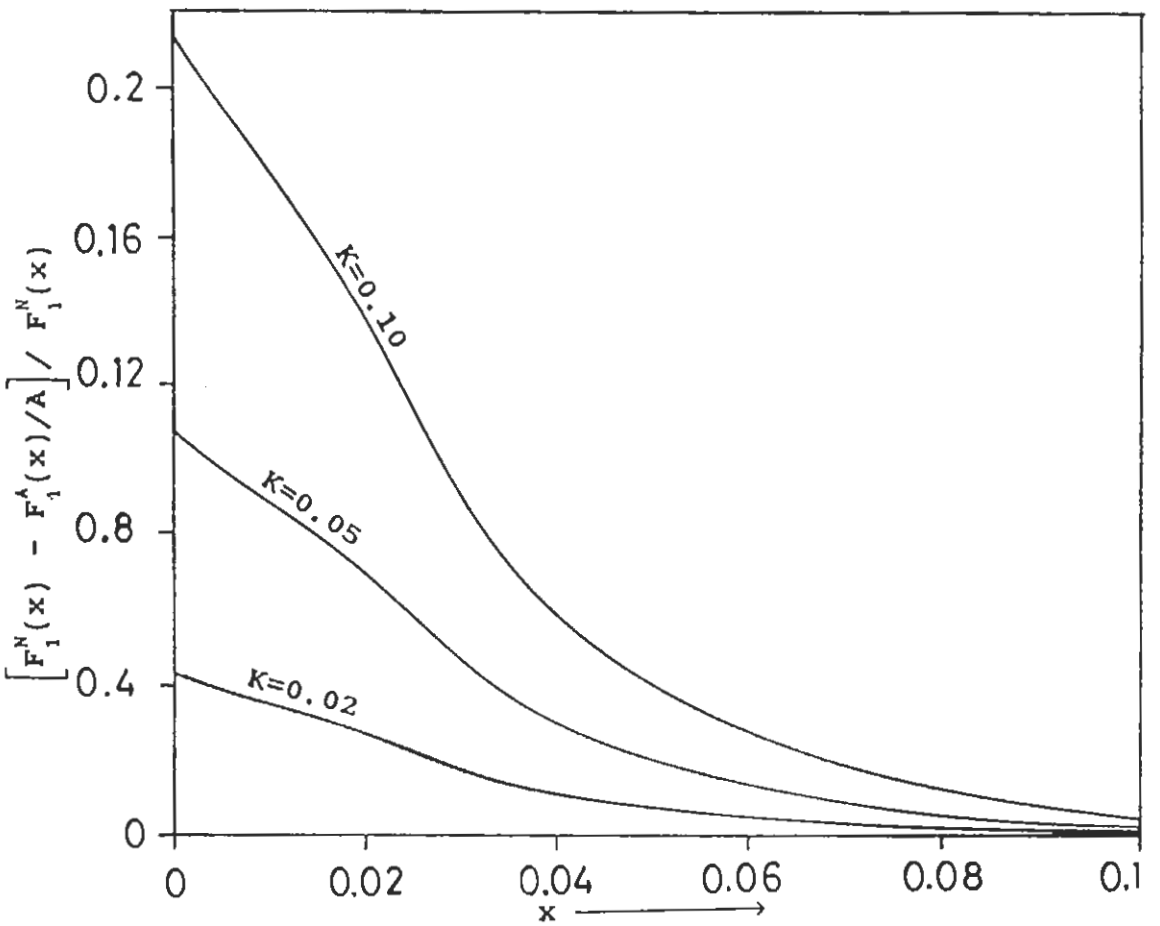

Figure 3.7: Relative shadowing for $E_P = 800$ GeV/nucleon ^{32}S ions for shadowing factor $K = 0.02, 0.05, 0.1$ and other parameters as discussed in the text.

References

[1] J.J. Aubert, et al., Phys. Lett. **B123**, 275 (1983).

[2] R.G. Arnold, et al., Phys. Rev. Lett. **52**, 727 (1984).

[3] M.S. Goodman, et al., Phys. Rev. Lett. **47**, 293 (1981).

[4] R.D. Carlitz, J.C. Collins and A.H. Mueller, Phys. Lett. **B214**, 224 (1988).

[5] A.V. Manohar, Phys. Lett. **B255**, 579 (1991).

[6] J. Qiu, Nucl. Phys. **B291**, 746 (1987).

[7] F. Halzen and Alan D. Martin, Quarks and Leptons, (John Wiley and Sons 1984), p. 242.

[8] A.H. Mueller and J. Qiu, Nucl. Phys. **B268**, 427 (1986).

Chapter 4

Quark fragmentation functions in a diquark model for proton and Λ hyperon production

4.1 Introduction

Fragmentation of partons produced in a high-energy process into definite hadronic states is a problem in QCD of considerable current interest. Parton fragmentation, in a sense, is dual to the process of uncovering hadron structure using high momentum probes. This duality has recently been emphasized by Jaffe and Ji [1-2]. These authors have made a detailed exploration of the spin, chirality, and twist structures of fragmentation using the fact that parton fragmentation functions can be expressed in QCD as matrix elements of quark and gluon field operators at light-cone separations. Indeed, a one-to-one correspondence between fragmentation functions and parton distribution functions can be established. While this is a useful step towards understanding the nature of the hadronization process, it certainly does not solve the problem —– the calculation of distribution func-

tions belongs to the realm of non-perturbative QCD and therefore can only be modeled. Fragmentation functions are even harder to model theoretically, and existing models using strings and shower algorithms etc.[3] are complicated and involve many parameters. In this chapter we explore an alternate, and much simpler, description for the conversion of a fast quark into specific hadrons– we calculate the quark fragmentation functions for proton and Λ hyperon production in a quark-diquark model of the baryon. The diquark model is a popular way of approximating nucleon structure functions. Several authors have recently emphasized this [4-7] and have calculated the leading twist contributions to the nucleon structure functions at the low energy hadronic scale. A discussion of the flavour and spin dependance of quark distributions is presented in the work of Close and Thomas[8]. They also discuss the influence of the one gluon exchange mechanism (which is also responsible for the N-Δ splitting) in the spectrum of intermediate states in deep inelastic scattering. The one gluon exchange mechanism causes a significant energy difference between the spin $S = 0$ and spin S=1 configurations for the two spectator quarks (i.e., diquark) that remain after the virtual photon knocks out one quark, thus explaining the dominance of the spin $S = 0$ and isospin $I = 0$ state at large x values. Meyer and Mulders [4] have investigated the flavour and spin dependance of the structure functions in deep-inelastic scattering in a field-theoretical description. The input in the calculation is the structure of the quark-diquark-nucleon vertex. In principle, this is a matrix in Dirac space which is expanded in standard Dirac matrices multiplying form factors that determine the flavour and spin structure of the nucleon. They use just the unit Dirac matrix with one form factor, treating the spin dependence by using the symmetric flavour spin wave function for the nucleon ground state. In this way an ordinary spin$\otimes$isospin wave function is combined with a relativistic calculation for the matrix elements as well as the kinematics.

The approach towards fragmentation functions taken in this work will be a very simple, naive one. We shall assume that a quark fragments entirely into a

baryon and an antidiquark. The baryon is represented by a 3 quark wavefunction with parameters fixed from other inputs. The emerging diquark can be either scalar or vector. This calculation models the lowest twist result at the typical low energy scale and is to be considered as the non-perturbative model input. The results at an appropriate high energy scale are obtained by doing a perturbative QCD evolution with the Altarelli-Parisi equations [9]. When evolved from the initial to the final Q^2 scale, the calculated fragmentation functions are in remarkable agreement (for $z > 0.4$) with those extracted from partially inclusive $e - P$ and e^+e^- experiments at high energies. Predictions are made, using no additional parameters, for longitudinally and transversally polarized quarks to fragment into P and Λ.

4.2 Unpolarized quark distribution $f_1(x)$ in a quark-diquark model for the nucleon

In high energy processes the structure of hadrons is described by light-cone parton distributions or, in broader sense, parton correlations. These processes in turn provide a unique channel to access to these distributions experimentally and thereby help us to learn the non-perturbative QCD physics of hadrons. One of the distributions which characterize the state of quarks in the nucleon in leading order high energy processes is defined by the following light-cone correlation

$$f_1(x) = \frac{1}{2P^+}\int \frac{d\lambda}{2\pi} e^{i\lambda x} \left\langle PS \left| \bar{\psi}(0)\gamma^+\psi(\lambda n) \right| PS \right\rangle , \tag{4.1}$$

where p^μ and n^μ are null vectors with $p^2 = n^2 = p^- = n^+ = 0$ and $p.n = 1$. For a target moving in the $\hat{z}$- direction, we choose $p = \frac{1}{\sqrt{2}}(\mathcal{P}, 0, 0, \mathcal{P})$, $n = \frac{1}{\sqrt{2}}(\frac{1}{\mathcal{P}}, 0, 0, -\frac{1}{\mathcal{P}})$, where $\mathcal{P}$ is a parameter specifying the coordinate system. In terms of these, the four momentum of the target is $P^\mu = p^\mu + \frac{1}{2}M^2 n^\mu$. The normalization for $f_1(x)$ is chosen such that, $F_1^{eN}(x) = \frac{1}{2}\sum_a e_a^2 f_1^a(x)$, where $F_1^{eN}(x)$ is

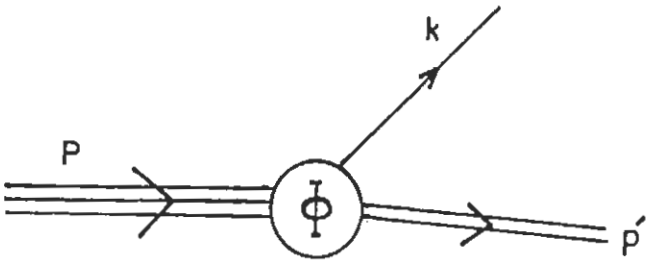

Figure 4.1: Quark-diquark picture of the nucleon.

the standard electroproduction structure function and the sum is over quarks and anti-quarks of different flavours. The distribution $f_1(x)$, represents the light-cone quark density with momentum $k^+ = xp^+$.

In order to calculate the quark distribution $f_1(x)$, a model is needed that describes the quark structure of the nucleon. We use the quark-diquark model i.e., we suppose that the nucleon is a bound state of a quark and a diquark. Thus in the quark-diquark model, Eq. (4.1) becomes (see Fig. 4.1)

$$f_1(x) = \frac{1}{2P^+} \int \frac{d\lambda}{2\pi} e^{i\lambda x} [dp'] \left\langle PS \left| \bar{\psi}(0) \right| p' \right\rangle \gamma^+ \left\langle p' \left| \psi(\lambda n) \right| PS \right\rangle , \qquad (4.2)$$

where,

$$[dp'] = \frac{d^2 p'_\perp dp'^+}{(2\pi)^3 2p'^+}. \qquad (4.3)$$

In the above $k = P - p'$ is the four momentum of the quark, which is off-mass shell whereas the spectator diquark is on shell. Considering only scalar diquarks, the matrix element $\langle p' | \psi(\lambda n) | PS \rangle$ then becomes

$$\langle p' | \psi(\lambda n) | PS \rangle = \frac{i}{\not{k} - m} \Phi u(PS) e^{-i\lambda k \cdot n}. \qquad (4.4)$$

Φ is the vertex that connects the quark with the diquark and nucleon. It connects the spin spaces of these particles and depends upon their momenta and isospins. It can also depend on the polarization vector of the nucleon, but this dependence is not present for a spherically symmetric distribution. As in Ref. [4], we consider

the case where the vertex Φ is approximated by,

$$\Phi = \phi(P^2, p'^2, k^2)\mathcal{I}. \tag{4.5}$$

$\mathcal{I}$ is the unit matrix in Dirac space and ϕ is a scalar function. We note that in principle the most general vertex coupling to spin zero and spin one diquarks can be considered within the same formalism. However for simplicity we shall only consider scalar diquarks as spectators. For vector diquarks, the spin and space-time structure cannot be decoupled. In the approximation used, the spin and isospin dependence will then be assumed to be given by the $SU(6)$ wavefunction of the nucleon. With the assumption (4.5), Eq. (4.2) becomes,

$$f_1(x) = \frac{1}{4(1-x)} \int_0^\infty \frac{dp_\perp'^2}{(2\pi)^2} \frac{x^2M^2 + p_\perp'^2}{(k^2 - m^2)^2} |\phi|^2. \tag{4.6}$$

We have neglected the quark mass m in the numerator. The off-shell quark has its k^2 given by

$$k^2 = xM^2 - \frac{xm_d^2 + p_\perp'^2}{1-x},$$

where m_d is the mass of the diquark and M is the mass of the nucleon. The integral in Eq. (4.6) is logarithmically divergent and needs to be damped by a suitable form factor. As in Ref. [4] we choose ϕ to be,

$$\phi(k^2) = N \frac{k^2 - m^2}{(k^2 - \Lambda^2)^2}. \tag{4.7}$$

Here Λ is a mass parameter whose choice will be decided upon latter and N is a normalization constant. For the spin isospin structure of the nucleon, we use the symmetric $SU(6)$ wave function for the nucleon - for a spin up proton this is

$$|P\uparrow\rangle = \frac{1}{\sqrt{2}} \left[P_S^P \chi(M_S) + P_A^P \chi(M_A) \right],$$

where

$$P_S^P = \frac{1}{\sqrt{6}} \left[(ud + du)u - 2uud \right],$$

$$P_A^P = \frac{1}{\sqrt{2}} (ud - du)u,$$

$$\chi(M_S) = \frac{1}{\sqrt{6}}[(\uparrow\downarrow + \downarrow\uparrow)\uparrow - 2\uparrow\uparrow\downarrow],$$

$$\chi(M_A) = \frac{1}{\sqrt{2}}(\uparrow\downarrow - \downarrow\uparrow)\uparrow .$$

$|P\uparrow\rangle$ can also be written in terms of quarks and diquarks degrees of freedom as

$$|P\uparrow\rangle = \frac{1}{\sqrt{2}} {}^{\uparrow}u\, S_0^0 + \frac{1}{\sqrt{18}} {}^{\uparrow}u\, T_0^0 - \frac{1}{3} {}^{\downarrow}u\, T_0^1 - \frac{1}{3} {}^{\uparrow}d\, T_1^0 - \sqrt{\frac{2}{9}} {}^{\downarrow}d\, T_1^1. \qquad (4.8)$$

S indicates the diquark combination with spin and isospin zero,

$$S_o^o = \frac{1}{2}\left({}^{\uparrow\downarrow}ud - {}^{\uparrow\downarrow}du - {}^{\downarrow\uparrow}ud + {}^{\downarrow\uparrow}du\right),$$

and T indicates the diquark combination with spin and isospin one,

$$T_1^1 = {}^{\uparrow\uparrow}uu,$$

$$T_o^1 = \frac{1}{\sqrt{2}}\left({}^{\uparrow\uparrow}ud + {}^{\uparrow\uparrow}du\right),$$

$$T_1^o = \frac{1}{\sqrt{2}}\left({}^{\uparrow\downarrow}uu + {}^{\downarrow\uparrow}uu\right),$$

$$T_o^o = \frac{1}{2}\left({}^{\uparrow\downarrow}ud + {}^{\uparrow\downarrow}du + {}^{\downarrow\uparrow}ud + {}^{\downarrow\uparrow}du\right).$$

Assuming that all quarks are in s-waves, these are the only possibilities allowed by the Pauli principle.

For the masses of the scalar and vector diquarks, m_S and m_V, the only information available to us is that from low energy models, such as the bag model or the non-relativistic quark model. There, at a (Q^2)-scale of order of a few hundred MeV^2, the diquark masses are expected to be somewhere within the range of 600 MeV to 1100 MeV [8,10]. Furthermore, just as the nucleon and delta baryons are split by the one-gluon exchange color magnetic spin-spin interaction, the S and T diquarks are also split by this interaction. Using the $N - \Delta$ mass difference as input, we anticipate that m_V would be some 200 MeV larger than m_S.

$$4\frac{\hat{h}_1(z)}{z}S_\perp p^+ = \int \frac{d\lambda}{2\pi} e^{-i\lambda/z} Tr < 0 \mid \gamma^+\gamma^\perp\gamma_5\psi(0) \mid PS_\perp X >< PS_\perp X \mid \bar{\psi}(\lambda n) \mid 0 > . \tag{4.14}$$

In the above, p^μ and n^μ are null vectors with $p^2 = n^2 = p^- = n^+ = 0$ and $p.n = 1$. In terms of these, the four momentum of the produced hadron, whose rest frame we shall take as our reference frame, is $P^\mu = p^\mu + \frac{1}{2}M^2 n^\mu$. The spin vector of the produced spin- $\frac{1}{2}$ hadron is $S^\mu = S.np^\mu + S.pn^\mu + MS_\perp^\mu$, and $\gamma^+ = 1/\sqrt{2}\,(\gamma^0 + \gamma^3)$. A summation over X is implicit and covers all possible states which can be populated by quark fragmentation. The quark operators are at equal $x_\perp$ and x^+ but are separated by a variable light-cone distance $x^- = \lambda n^-$. To interpret $\hat{f}_1(z)$ physically, define a composite operator $C^\dagger(P)$ which creates a hadron of a specific type and momentum from the vacuum, $\mid P >= C^\dagger(P) \mid 0 >$. Using completeness of X it is easy to show that,

$$\hat{f}_1(z) = \int [dk]\delta\left(\frac{k^+}{P^+} - \frac{1}{z}\right) \frac{< k \mid C^\dagger(P)C(P) \mid k >}{< k \mid k >}. \tag{4.15}$$

This shows that $\hat{f}_1(z)$ is the probability of finding a given hadron with fixed z in a quark, irrespective of the transverse quark momentum.

4.4 Quark fragmentation functions in a diquark model

The matrix elements in Eqs. (4.12–4.14) need to be modeled as they cannot be calculated ab-initio. Perhaps the simplest assumption is that the quark fragments into a baryon and anti-diquark (Fig. 4.2(b)). This may be reasonable provided that z is not too far from 1, i.e., the produced hadron carries away most of the momentum of the quark. The amplitude for the process is,

$$< PS \mid \bar{\psi} \mid 0 >= \bar{u}(PS)\Phi\frac{i}{\not k - m} \tag{4.16}$$

where Φ is the vertex that connects the quark with the two outgoing particles. Φ is a matrix in Dirac space, and its most general form is rather complicated

since it involves several unknown form factors. Instead, we shall be guided by the investigations of Meyer and Mulders[4], and Melnitchouk, Schreiber, and Thomas[5], who have calculated nucleon structure functions in the diquark model and obtained rather good fits to deep inelastic scattering at all data except small x. Following Ref.[4], we take

$$\Phi = \phi(P^2, p'^2, k^2)\, \mathcal{I}, \tag{4.17}$$

where $\mathcal{I}$ is the unit matrix and only scalar diquarks (actually antidiquarks) are included in the vertex. Inserting Eqs. (4.16) and (4.17) into Eqs. (4.12-4.14) and neglecting the quark mass m in the numerator yields

$$\hat{f}_1(z) = \frac{1}{4(1-z)} \int_0^\infty \frac{dk_\perp^2}{(2\pi)^2} \frac{M^2 + z^2 k_\perp^2}{(k^2 - m^2)^2} |\phi|^2, \tag{4.18}$$

$$\hat{g}_1(z) = \frac{1}{8(1-z)} \int_0^\infty \frac{dk_\perp^2}{(2\pi)^2} \frac{M^2 - z^2 k_\perp^2}{(k^2 - m^2)^2} |\phi|^2, \tag{4.19}$$

$$\hat{h}_1(z) = \frac{1}{8(1-z)} \int_0^\infty \frac{dk_\perp^2}{(2\pi)^2} \frac{M^2}{(k^2 - m^2)^2} |\phi|^2. \tag{4.20}$$

The fragmenting quark, which is highly off-shell, has its k^2 given by

$$k^2 = \frac{M^2}{z} + \frac{m_d^2 + z k_\perp^2}{1-z}. \tag{4.21}$$

To calculate the fragmentation functions , we use the same k^2 dependence of the vertex functions ϕ as modeled in Refs.[4] and [5]. We now concentrate on the spin-isospin structure of the produced baryon.

4.4.1 Proton production

The SU(6) wavefunction for a spin-up proton in terms of quarks and diquarks is given by Eq. (4.8). There is, of course, no explicit coupling to vector diquarks in the vertex Eq. (4.17) although, at the expense of some complication, it could be put in. We follow instead the easy route suggested by the calculations of Ref.[4] wherein it was assumed that the S(x) and T(x) distribution functions

are of identical form but differ because the S and T diquarks have somewhat different masses m_S and m_V, as well as mass parameters Λ_S and Λ_V. Following a similar logic, define $\hat{S}(z)$ and $\hat{T}(z)$ to be fragmentation functions where the emitted anti-diquark is repectively S and T,

$$\begin{aligned} \hat{S}(z) &= \hat{f}_1(z) \;\; with \;\; m_d = m_S, \; \Lambda = \Lambda_S, \\ \hat{T}(z) &= \hat{f}_1(z) \;\; with \;\; m_d = m_V, \; \Lambda = \Lambda_V. \end{aligned} \tag{4.22}$$

The polarized quantities $\Delta\hat{S}(z)$, $\Delta\hat{T}(z)$ are defined similarly with $\hat{f}_1(z)$ replaced by $\hat{g}_1(z)$ and $\Delta_1\hat{S}(z)$, $\Delta_1\hat{T}(z)$ are defined with $\hat{f}_1(z)$ replaced by $\hat{h}_1(z)$ in the above. From the SU(6) wavefunction in Eq. (4.8) the u and d fragmentation functions are readily seen to be

$$\begin{aligned} \hat{f}_{1u}^P(z) &= \frac{1}{2}\hat{S}(z) + \frac{1}{6}\hat{T}(z), \\ \hat{f}_{1d}^P(z) &= \frac{1}{3}\hat{T}(z), \\ \hat{g}_{1u}^P(z) &= \frac{1}{2}\Delta\hat{S}(z) - \frac{1}{18}\Delta\hat{T}(z), \\ \hat{g}_{1d}^P(z) &= -\frac{1}{9}\Delta\hat{T}(z), \\ \hat{h}_{1u}^P(z) &= \frac{1}{2}\Delta_1\hat{S}(z) - \frac{1}{18}\Delta_1\hat{T}(z), \\ \hat{h}_{1d}^P(z) &= -\frac{1}{9}\Delta_1\hat{T}(z). \end{aligned} \tag{4.23, 4.24}$$

4.4.2 Λ hyperon production

To find the effects of parton fragmentation (or to measure the spin dependent fragmentation functions) in a hard scattering, we have to measure the polarization of the produced baryon. This can be done for an unstable hyperon by measuring the angular distribution of the decay products. We follow the same approach for the production of a Λ hyperon from u, d, or s quarks as for proton production. The quark model wave function for a Λ (uds) hyperon with spin up is

$$|\Lambda\uparrow\rangle = \frac{1}{\sqrt{2}}\left[P_S^\Lambda\chi(M_S) + P_A^\Lambda\chi(M_A)\right],$$

with

$$P_S^\Lambda = \frac{1}{\sqrt{2}}\left[\frac{(ds+sd)u}{\sqrt{2}} - \frac{(us+su)d}{\sqrt{2}}\right],$$

and

$$P_A^\Lambda = \frac{1}{\sqrt{6}}\left[\frac{(sd-ds)u}{\sqrt{2}} + \frac{(us-su)d}{\sqrt{2}} - 2\frac{(du-ud)s}{\sqrt{2}}\right].$$

$\chi(M_S)$ and $\chi(M_A)$ have been already defined in section 4.2, and the Λ state in terms of quarks and diquarks is,

$$|\Lambda\uparrow> = \frac{1}{\sqrt{12}}\left(\overset{1}{u}\,T^0 - \overset{1}{d}\,T^0 - \sqrt{2}\,\overset{1}{u}\,T^1 + \sqrt{2}\,\overset{1}{d}\,T^1 + \overset{1}{u}\,\mathcal{S}^0 + \overset{1}{d}\,\mathcal{S}^0 - 2\,\overset{1}{s}\,S^0\right). \tag{4.25}$$

Here $\mathcal{S}$ (T) is a scalar (vector) diquark with one s and either a u or d quark, while S is a ud system as before. Define new fragmentation functions,

$$\begin{aligned}
\hat{\mathcal{S}}(z) &= \hat{f}_1(z) \;\; with \;\; m_d = m_{\mathcal{S}},\; \Lambda = \Lambda_{\mathcal{S}},\\
\hat{\mathcal{T}}(z) &= \hat{f}_1(z) \;\; with \;\; m_d = m_{\mathcal{T}},\; \Lambda = \Lambda_V,\\
\hat{S}(z) &= \hat{f}_1(z) \;\; with \;\; m_d = m_S,\; \Lambda = \Lambda_S.
\end{aligned} \tag{4.26}$$

The quantities $\Delta\hat{\mathcal{S}}(z)$, $\Delta\hat{\mathcal{T}}(z)$, $\Delta\hat{S}(z)$ are defined similarly with $\hat{f}_1(z)$ replaced by $\hat{g}_1(z)$. $\Delta_1\hat{\mathcal{S}}(z)$, $\Delta_1\hat{\mathcal{T}}(z)$, $\Delta_1\hat{S}(z)$ are defined with $\hat{f}_1(z)$ replaced by $\hat{h}_1(z)$. In terms of these, the fragmentation of u, d, and s into Λ is given by,

$$\begin{aligned}
\hat{f}_{1u}^\Lambda(z) = \hat{f}_{1d}^\Lambda(z) &= \frac{1}{4}\hat{\mathcal{T}}(z) + \frac{1}{12}\hat{\mathcal{S}}(z),\\
\hat{f}_{1s}^\Lambda(z) &= \frac{1}{3}\hat{S}(z).
\end{aligned} \tag{4.27}$$

For the polarized quantities,

$$\begin{aligned}
\hat{g}_{1u}^\Lambda(z) = \hat{g}_{1d}^\Lambda(z) &= \frac{1}{12}\left[\Delta\hat{\mathcal{S}}(z) - \Delta\hat{\mathcal{T}}(z)\right],\\
\hat{g}_{1s}^\Lambda(z) &= \frac{1}{3}\Delta\hat{S}(z),\\
\hat{h}_{1u}^\Lambda(z) = \hat{h}_{1d}^\Lambda(z) &= \frac{1}{12}\left[\Delta_1\hat{\mathcal{S}}(z) - \Delta_1\hat{\mathcal{T}}(z)\right],\\
\hat{h}_{1s}^\Lambda(z) &= \frac{1}{3}\Delta_1\hat{S}(z).
\end{aligned} \tag{4.28}$$

4.5 Results and discussion

We now turn to a discussion of numerical results and comparisons with fragmentation data, where available. The diquark model for fragmentation of u, d quarks to protons needs, as input, the scalar and vector diquark masses m_S, m_V as well as the cut-offs Λ_S, Λ_V. Consistent with the conclusions of Melnitchouk et al., [5], we can choose the values of the parameters m_S, m_V, Λ_S and Λ_V to fit not only the experimental nucleon distributions but also the u quark fragmentation function for proton production. We find the best fit to the experimental valence quark distribution $u_V(x) + d_V(x)$ in the proton [15,16] at $Q^2 = 4GeV^2$ [1] for masses $m_S = 900MeV$, $m_V = 1100MeV$, and cut-offs $\Lambda_S = 840MeV$, $\Lambda_V = 925MeV$. For each choice of the parameter Λ, the normalization constant N in Eq. (4.7) can be found by using the Eq. (4.11). The fit to the valence quark distribution $u_V(x) + d_V(x)$ in the proton is shown in Fig. 4.3. It should be noted that the magnitude of the fragmentation functions is very sensitive to the values of the cut-offs Λ_S and Λ_V but the normalized structure functions are not. In choosing the values of Λ_S and Λ_V, we used the Eqs. (4.23) and the following experimental result [17]: $\hat{f}^P_{1u}(z)$ and $\hat{f}^P_{1d}(z)$ are about equal for $z < 0.4$ but at larger z the ratio $\hat{f}^P_{1u}(z)/\hat{f}^P_{1d}(z)$ increases, becoming about 2 for $0.4 < z < 0.6$, and greater than 2 for $0.6 < z < 0.8$. For these measurements $\mu = Q^2 = 80GeV^2$, where Q is the four momentum of the fragmenting quark. This fixes all the parameters needed for the model, and one may now use it for calculating fragmentation rates into the protons. Fig. 4.4 shows $\hat{f}^p_{1u}(z)$ and $\hat{f}^p_{1d}(z)$ calculated using Eqs. (4.7) and (4.18). Since these are scale dependent quantities, one must specify the scale as well. It appears reasonable to take the initial scale to be $m_d + M_P$, where M_P is the proton mass. This, of course, is the minimum off-shell mass of the fragmenting quark. Evolution of the fragmentation functions to the experimental

[1] The curve is evolved from $Q_0^2 = 0.15GeV^2$ using leading order QCD evolution, with $\Lambda_{QCD} = 200MeV$.

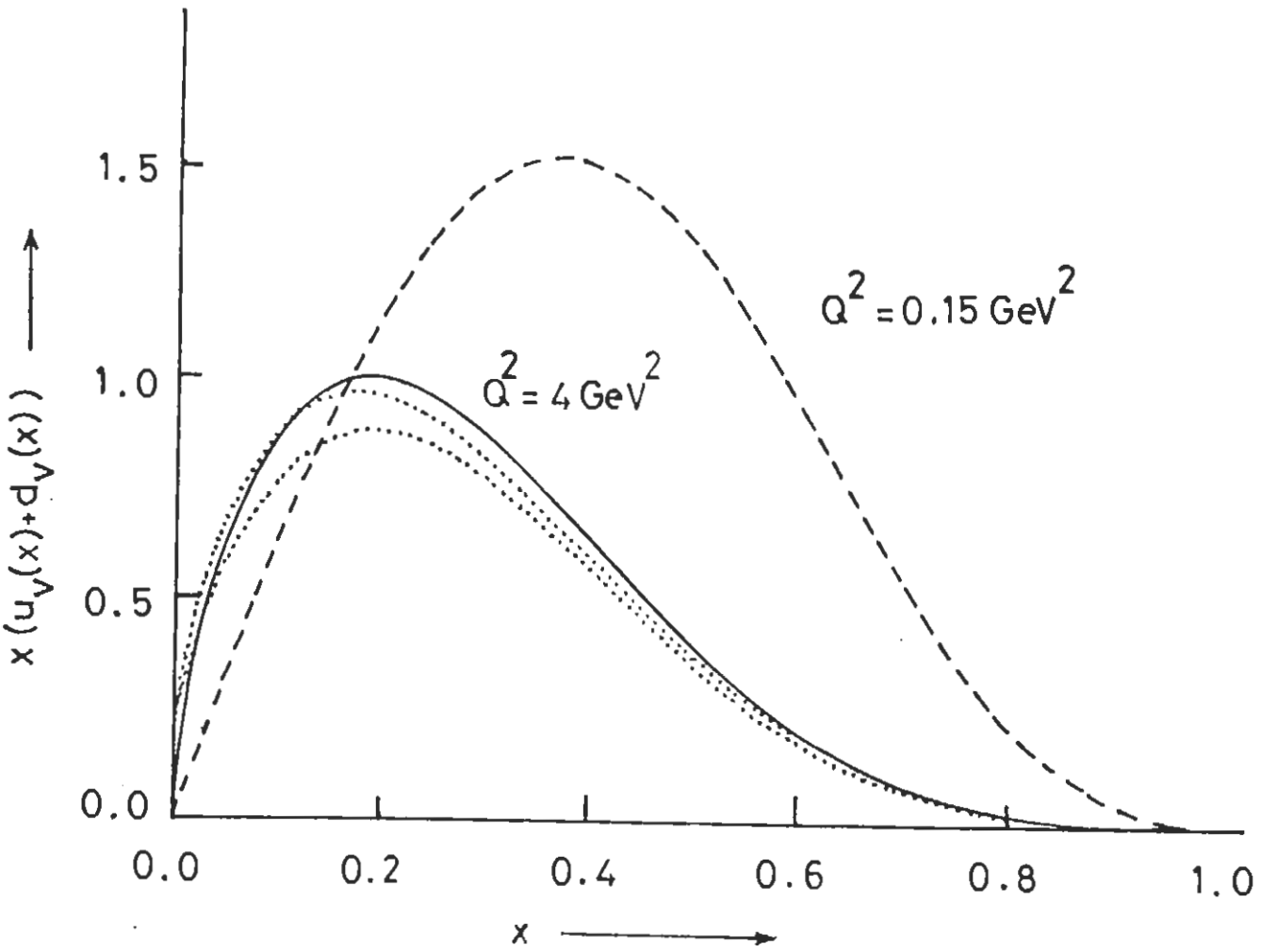

Figure 4.3: Valence quark distribution $u_V(x) + d_V(x)$ in the proton, evolved from $Q_0^2 = 0.15 GeV^2$ (dashed curve) to $Q^2 = 4 GeV^2$ (solid curve), and compared against parameterisations (dotted curves) of world data [15,16].

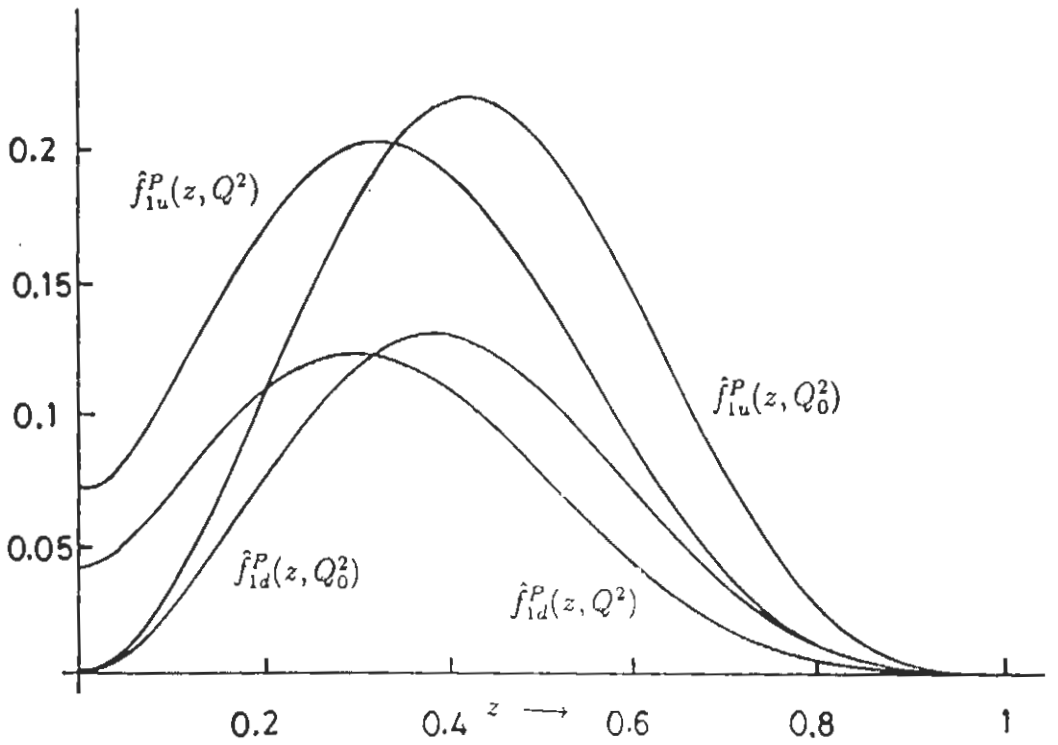

Figure 4.4: Fragmentation functions for u and d quarks to go into a proton, calculated in the diquark model, evolved from the initial scale $Q_0^2 = (m_d + m_P)^2$ to $Q^2 = 80GeV^2$.

scale can be performed exactly as for quark distribution functions [9],

$$\mu\frac{\partial}{\partial\mu}f_i^P(z,\mu)=\sum_j\int_z^1\frac{dy}{y}P_{i\to j}\left(\frac{z}{y},\mu\right)f_j^P(y,\mu), \tag{4.29}$$

where $P_{i\to j}(x,\mu)$ is the Altarelli-Parisi function for the splitting of the parton of type i into a parton of type j with longitudinal momentum fraction x. In principle the sum in Eq. (4.29) extends over gluons and anti-quarks as well. At large z these terms are hopefully small and so we ignore them, including only $P_{u\to u}(x,\mu)$ and $P_{d\to d}(x,\mu)$, where

$$P_{u\to u}(x,\mu)=\frac{2\alpha_s(\mu)}{3\pi}\left(\frac{1+x^2}{1-x}\right)_+. \tag{4.30}$$

The + function is defined in usual way:

$$f(x)_+=f(x)-\delta(1-x)\int_0^1 dx'\,f(x'). \tag{4.31}$$

The evolved fragmentation function $\hat{f}_u^P(z,Q^2)$ [2] is compared in Fig. 4.5 with the European Muon Collaboration (EMC) data [6] extracted from $\mu-P$ and $\mu-D$ scattering. The agreement is fairly good even down to rather small values of z, where model has no obvious reason to be valid. Without changing the parameters, predictions for $\hat{g}_1$ and $\hat{h}_1$ are shown in Figs. 4.6 and 4.7, respectively.

The calculation of u, d, s quark fragmentation into Λ hyperons proceeds identically with the sole change of increasing the diquark mass by $M_\Lambda - M_P = 176MeV$ if the outgoing antidiquark contains a strange quark. The SU(6) wave-functions then determine the relative magnitudes of $\hat{f}_1$, $\hat{g}_1$, and $\hat{h}_1$, which are plotted, respectively, in Figs. 4.8-4.10. That the produced Λ carries the spin of the fragmenting s-quark is apparent from Fig. 4.9. The transverse fragmentation function $\hat{h}_1$ for $u,\ d,\ s\to\Lambda$, if measured, would be a good tool for uncovering the transverse distribution function $h_1(x)$ [1,18] of the proton. While no experimental spin data exists, data from e^+e^- collisions at large center of mass (c.m.)

[2] The evolution has been performed to a final scale of $Q^2 = 80GeV^2$, which is the average value of Q^2 for the given data.

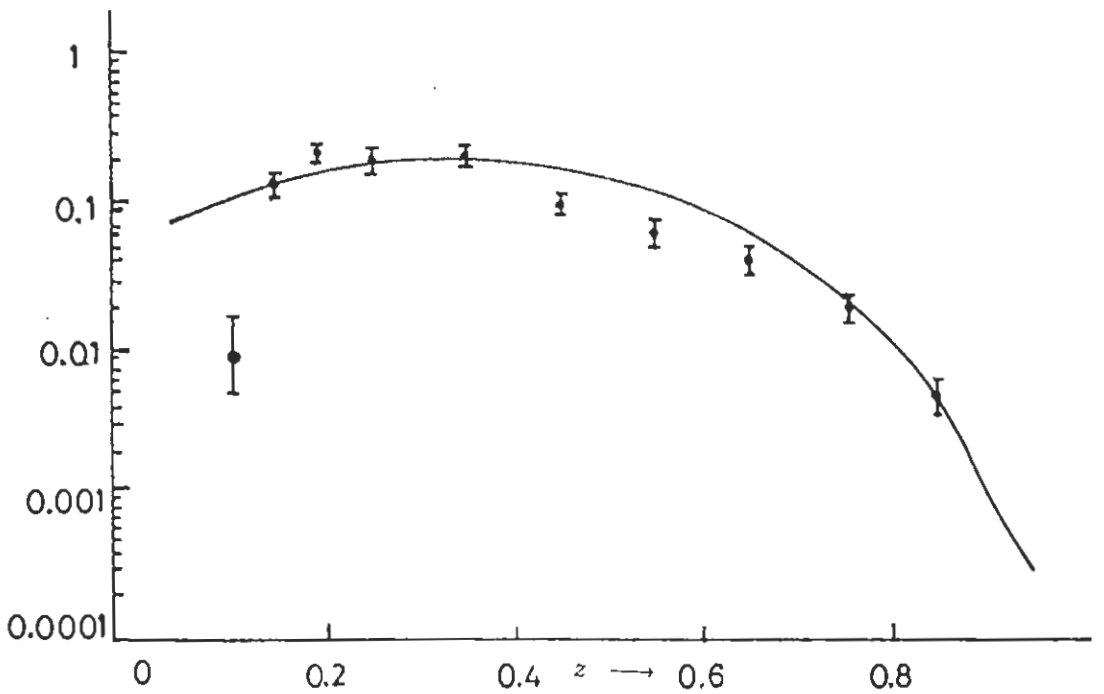

Figure 4.5: Evolved diquark model fragmentation function $\hat{f}_u^P(z, Q^2)$ compared against EMC [6] data extracted from $\mu - P$ and $\mu - D$ scattering.

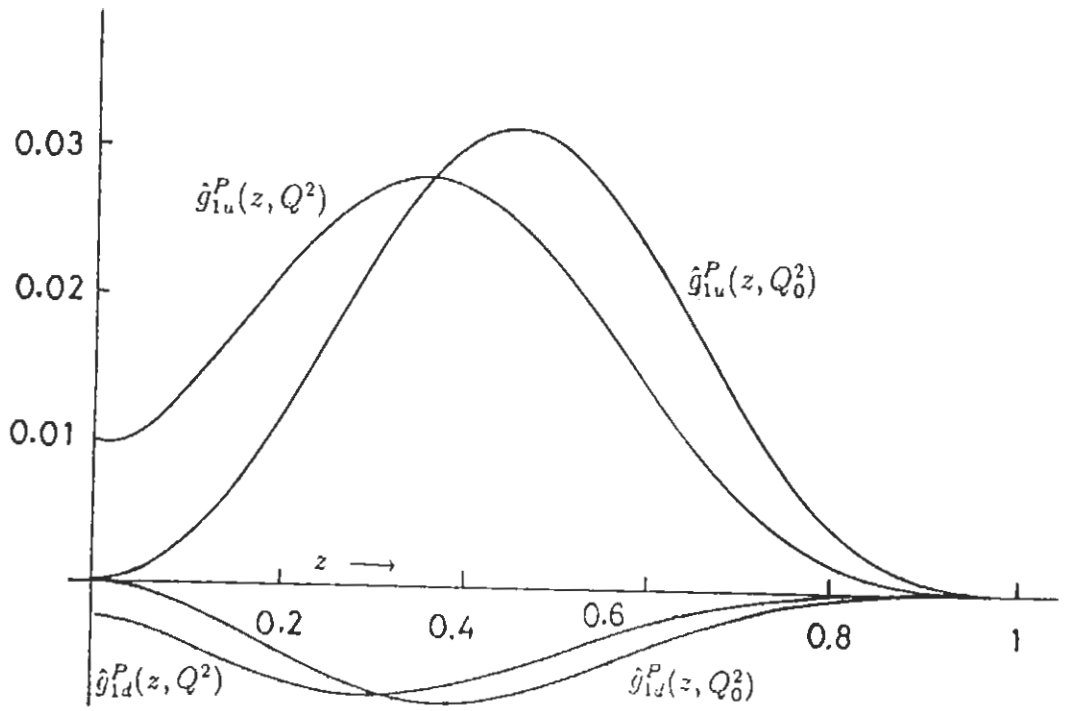

Figure 4.6: Fragmentation functions $\hat{g}_1$ for u and d quarks to go into a proton, calculated in the diquark model, evolved from the initial scale $Q_0^2 = (m_d + m_P)^2$ to $Q^2 = 80GeV^2$.

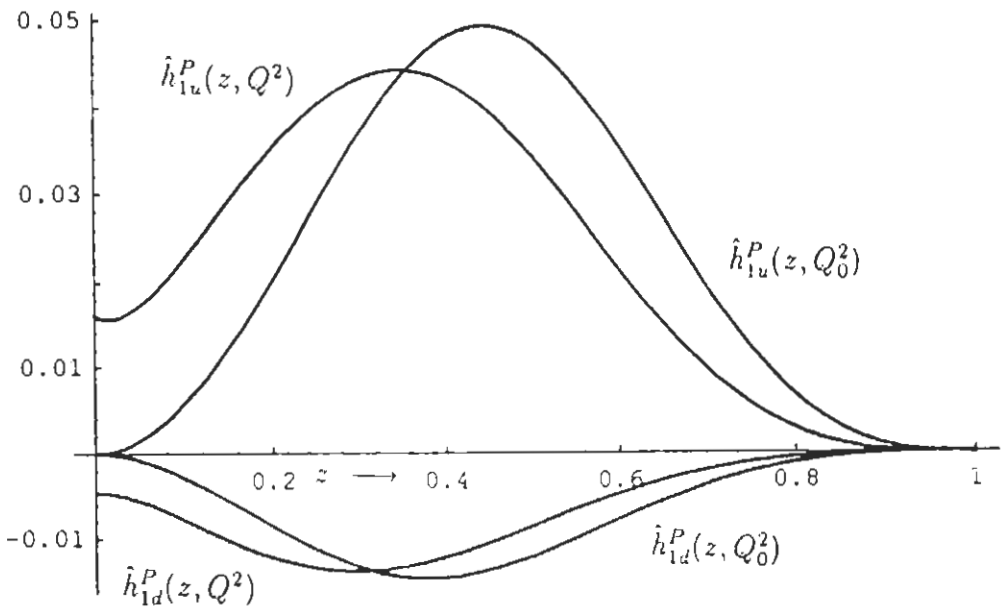

Figure 4.7: Fragmentation functions $\hat{h}_1$ for u and d quarks to go into a proton, calculated in the diquark model, evolved from the initial scale $Q_0^2 = (m_d + m_P)^2$ to $Q^2 = 80GeV^2$.

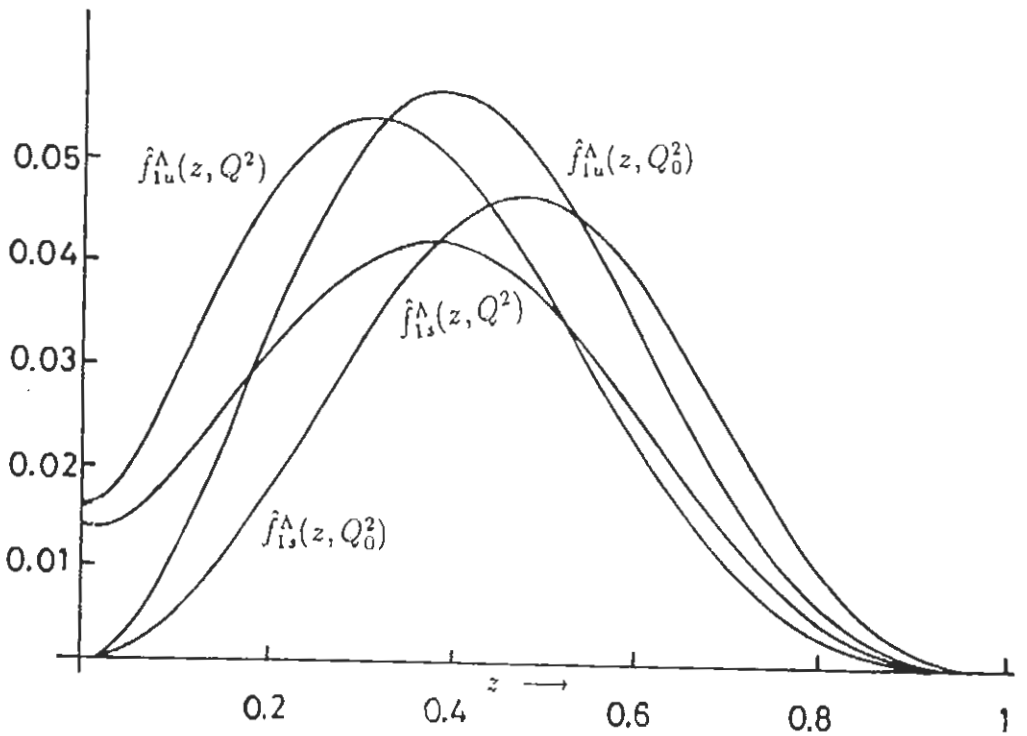

Figure 4.8: Fragmentation functions $\hat{f}_1$ for u, d and s quarks to go into a Λ hyperon, calculated in the diquark model, evolved from the initial scale $Q_0^2 = (m_d + m_\Lambda)^2$ to $Q^2 = 80GeV^2$.

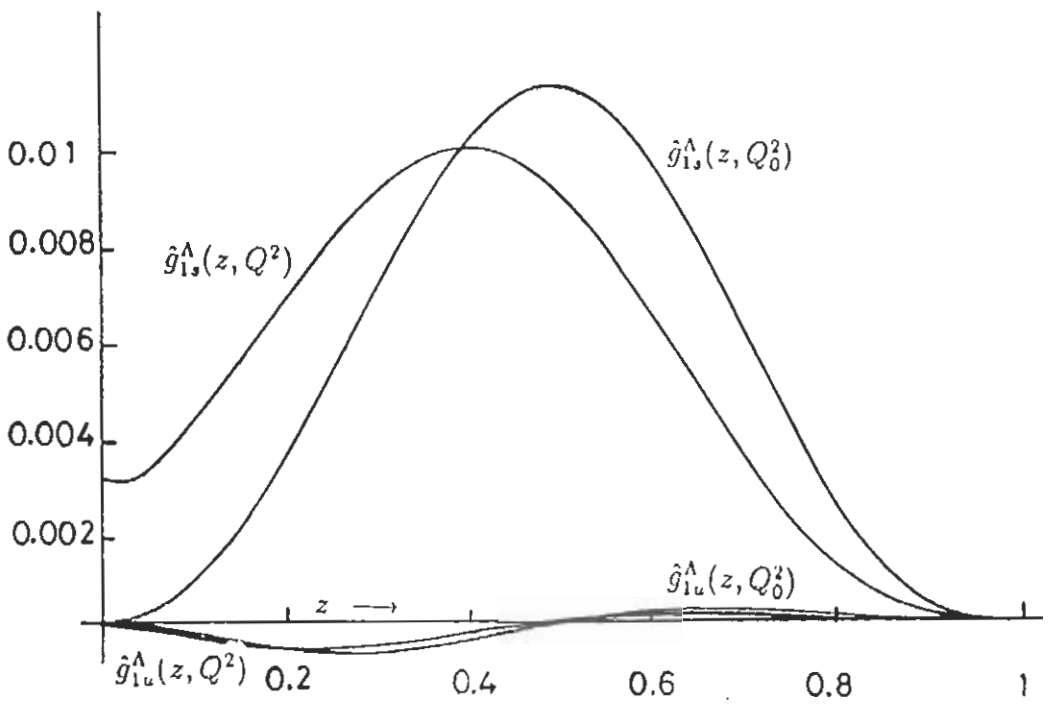

Figure 4.9: Fragmentation functions $\hat{g}_1$ for u, d and s quarks to go into a Λ hyperon, calculated in the diquark model, evolved from the initial scale $Q_0^2 = (m_d + m_\Lambda)^2$ to $Q^2 = 80GeV^2$.

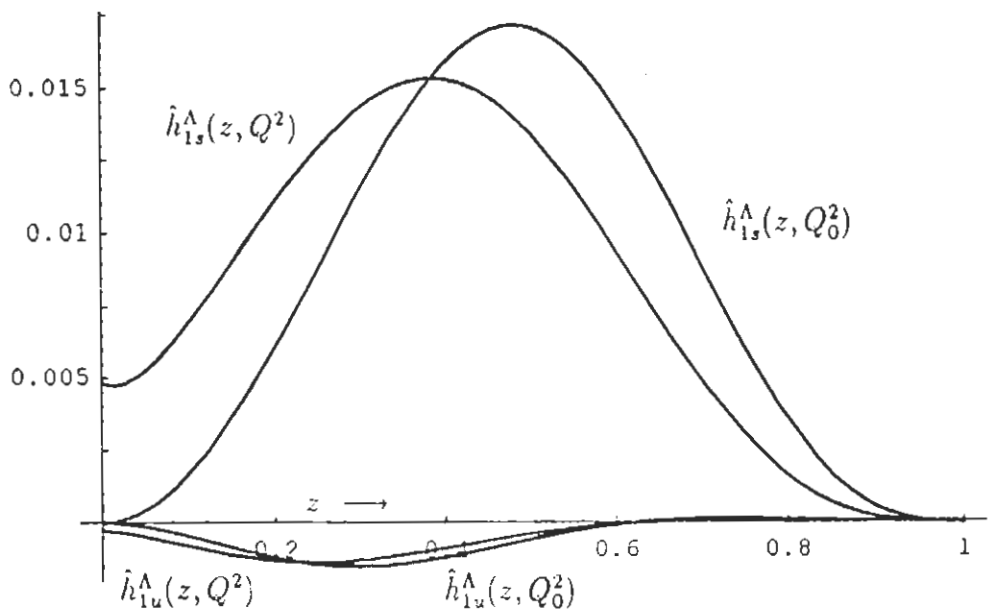

Figure 4.10: Fragmentation functions $\hat{h}_1$ for u, d and s quarks to go into a Λ hyperon, calculated in the diquark model, evolved from the initial scale $Q_0^2 = (m_d + m_\Lambda)^2$ to $Q^2 = 80GeV^2$.

energies can be compared with predictions of the present model. For large c.m. energies, the fraction of hadrons from fragmentation becomes important and one could expect an approximate scaling in $\frac{1}{\sigma}\frac{d\sigma}{dz}$ [19] (z is the energy fraction carried by the final state particle) i.e.,

$$\frac{1}{\sigma}\frac{d\sigma}{dz}(e^+e^- \to h + X) = \frac{\sum_i e_i^2 \left[\hat{f}_i^h(z) + \hat{f}_{\bar{i}}^h(z)\right]}{\sum_i e_i^2} \tag{4.32}$$

Note here that the photon produces a quark-antiquark pair, either of which could have produced the observed hadron. Hence the $\hat{f}_i^h$ *and* $\hat{f}_{\bar{i}}^h$ appear. In our model only u, d quarks lead to proton production, and only u, d, s quarks lead to Λ production. Therefore,

$$\frac{1}{\sigma}\frac{d\sigma}{dz}(e^+e^- \to P + X) = \frac{\frac{4}{9}\hat{f}_u^P(z) + \frac{1}{9}\hat{f}_d^P(z)}{\sum_i e_i^2}, \tag{4.33}$$

and

$$\frac{1}{\sigma}\frac{d\sigma}{dz}(e^+e^- \to \Lambda + X) = \frac{\frac{4}{9}\hat{f}_u^\Lambda(z) + \frac{1}{9}\hat{f}_d^\Lambda(z) + \frac{1}{9}\hat{f}_s^\Lambda(z)}{\sum_i e_i^2}. \tag{4.34}$$

A comparison of scaled P and Λ production cross-section in e^+e^- experiment [20-22] at c.m. energy 30 GeV is shown in Fig. 4.11. At this energy, only five quarks can be produced in e^+e^- collisions and $\sum_i e_i^2 = \frac{11}{9}$. Again the evolution has been performed to a final scale of $Q^2 = 80\,GeV^2$[3]. Fig. 4.11 shows that the data compares very well with our theoretical predictions for large z because antiquarks and gluons cannot fragment into observed baryons with large z. The maximum possibility for the production of P and Λ with large z is through valence quark fragmentation. At small z, the contribution of gluons and antiquarks for the production of P and Λ becomes significant and one does not expect the model used here to be valid.

[3]For c.m. energy of about 30 GeV the average value of Q^2 for fragmentating quark is $\approx 80\,GeV^2$.

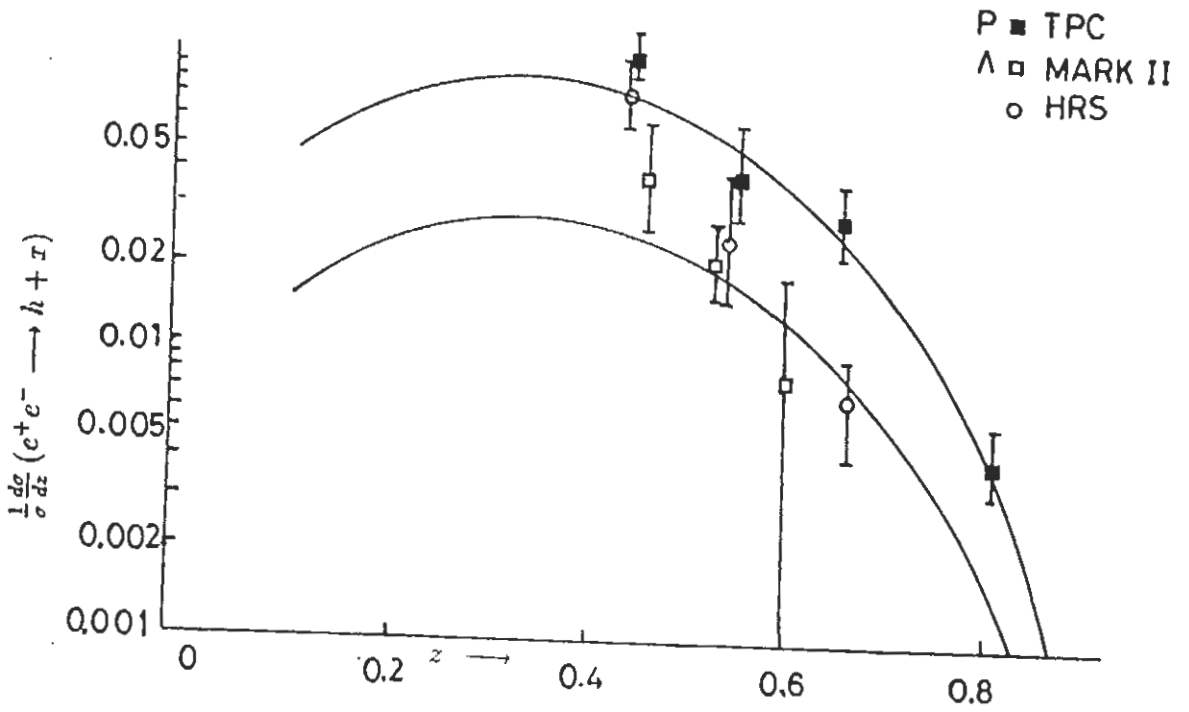

Figure 4.11: Production of protons and hyperons in e^+e^- collisions at c.m. energy of about 30 GeV. The solid curves are predictions of the diquark fragmentation model, and the data is from TPC [20], HRS [21], and MARK II [22] collaborations.

4.6 Conclusion

To conclude, we have investigated a simple fragmentation model for a quark to go into a P, Λ and the appropriate anti-diquark, using a vertex with a suitable form-factor determined by fitting to deep inelastic data. The good agreement with experiment, even down to rather small z values where this agreement is surely fortuitous, suggests that one is perhaps using the right effective degrees of freedom for P, Λ production from quarks. At the same time, it is obvious that one is far from a complete description of fragmentation; the model gives zero chance for anti-proton production from a quark. Neverthelesss, it has good predictive power, and we have calculated the spin-fragmentation functions $\hat{g}_1$ and $\hat{h}_1$ for P, Λ production. It will be interesting to see how well these are eventually borne out by experiment.

References

[1] R.L. Jaffe and X. Ji, Phys. Rev. Lett. **71**, 2547 (1993).

[2] X. Ji, Phys. Rev. **D49**, 114 (1994).

[3] See, for example, V.D. Barger and R.J.N. Phillips, Collider Physics, (Addison-Wesley, Reading, MA, 1987).

[4] H. Meyer and P.J. Mulders, Nucl. Phys. **A528**, 589 (1991).

[5] W. Melnitchouk, A.W. Schreiber, and A.W. Thomas, Phys. Rev. **D49**, 1183 (1994).

[6] M. Anselmino, F. Caruso, E. Leader and J. Soares, preprint; CBPF-NF-024/90.

[7] Katsuhiko Suzuki, Takayuki Shigetani and Heroshi Toki, preprint; hep-ph/9310266, Nucl. Phys. A.

[8] F.E. Close, and A.W. Thomas, Phys. Lett. **B212**, 227 (1988).

[9] G. Altarelli and G. Parisi, Nucl. Phys. **B126**, 298 (1977).

[10] A.W. Schreiber, A.I. Signal and A.W. Thomas, Phys. Rev. **D44**, 2653 (1991).

[11] V.N. Gribov and L.N. Lipatov, Sov. J. Nucl. Phys. **15**, 438, 675 (1972).

[12] R.P. Feynman, Photon-Hadron Interactions (Benjamin, Reading, MA, 1972).

[13] J.C. Collins and D. Soper, Nucl. Phys. **B194**, 445 (1982).

[14] R.L. Jaffe and X. Ji, MIT CTP preprint, October 1992.

[15] J.G. Morfin and W.K. Tung, Z. Phys. **C52**, 13 (1991).

[16] J.F. Owens, Phys. Lett. **B266**, 126 (1991).

[17] M. Arneodo et al., Nucl. Phys. **B321**, 541 (1989).

[18] X. Artru and M. Mekhfi, Z. Phys. **C45**, 669 (1990).

[19] F.E. Close, An Introduction to Quarks and Partons, (Academic Press, London, 1979).

[20] TPC, H. Aihara et al., Phys. Rev. Lett. **53**, 2378 (1984).

[21] HRS, M. Derrick et al., Phys. Rev. **D35**, 2639 (1987).

[22] Mark II, C. de la Vaissiere et al., Phys. Rev. Lett. **54**, 2071 (1985).